Natural and Anthropogenic Underwater Ambient Sound in the Baltic Sea

MIRKO MUSTONEN

**TAL
TECH**
PRESS

TALLINN UNIVERSITY OF TECHNOLOGY
School of Engineering
Department of Civil Engineering and Architecture

The dissertation was accepted for the defence of the degree of Doctor of Philosophy (Water and Environmental Engineering) on 20 July 2020

Supervisor: Professor Aleksander Klauson
Department of Civil Engineering and Architecture
Tallinn University of Technology
Tallinn, Estonia

Opponents: Professor Zygmunt Klusek
Marine Ecology Department
Polish Academy of Sciences
Warsaw, Poland

Professor Ari Poikonen
Finnish Naval Academy
Helsinki, Finland

Defence of the thesis: 24 August 2020, Tallinn

Declaration:
Hereby I declare that this doctoral thesis, my original investigation and achievement, submitted for the doctoral degree at Tallinn University of Technology, has not been submitted for any academic degree elsewhere.

Mirko Mustonen

_____
signature

Läänemere looduslik ja inimtekkeline veealune ümbrusheli

MIRKO MUSTONEN

Contents

List of Publications

Publication I: Mirko Mustonen, Aleksander Klauson, Janek Laanearu, Madis Ratassepp, Thomas Folegot, and Dominique Clorennec. Passenger ship source level determination in shallow water environment. *Proceedings of Meetings on Acoustics 4ENAL*, 27:070015, 2016

Publication II: Aleksander Klauson and Mirko Mustonen. Ship source strength estimation in shallow water. *Proceedings of Meetings on Acoustics 174ASA*, 31(1):070004, 2017

Publication III: Mirko Mustonen, Aleksander Klauson, Julia Berdnikova, and Mihkel Tommingas. Assessment of the proportion of anthropogenic underwater noise levels in passive acoustic monitoring. *Proceedings of Meetings on Acoustics 174ASA*, 31:070003, 2017

Publication IV: Mirko Mustonen, Aleksander Klauson, Mathias Andersson, Dominique Clorennec, Thomas Folegot, Radomił Koza, Jukka Pajala, Leif Persson, Jarosław Tegowski, and Jakob Tougaard. Spatial and Temporal Variability of Ambient Underwater Sound in the Baltic Sea. *Scientific Reports*, 9(1):1–13, 2019. Publisher: Nature Publishing Group

Publication V: Mirko Mustonen, Aleksander Klauson, Thomas Folégot, and Dominique Clorennec. Natural sound estimation in shallow water near shipping lanes. *The Journal of the Acoustical Society of America*, 147(2):EL177–EL183, 2020. Publisher: Acoustical Society of America

Author's Contributions to the Publications

I In Publication I, I participated in conceiving of the manuscript and co-wrote the main text. I also prepared the table and all the figures except the figures 4 and 5.

II In Publication II, I contributed to the writing and revising the main manuscript text. I prepared the figure 6.

III In Publication III, I prepared all the figures and tables, participated in conceiving of the manuscript and co-wrote the main manuscript text. I revised and reimplemented the threshold selection process of the detectors chosen and implemented by Mihkel Tomingas and Julia Berdnikova.

IV In Publication IV, I prepared all the figures and tables, participated in conceiving of the manuscript and co-wrote the main manuscript text.

V In Publication V, I prepared all the figures and tables, participated in conceiving of the manuscript and co-wrote the main manuscript text.

Introduction and objectives

The man-made underwater sound and its impacts on marine species have been recognised as an environmental protection challenge that needs the cooperation of scientists, legislators, ship owners and the offshore industry in order to be solved. The essential role of the scientists is to provide the other counterparts reliable information and propose effective solutions. There are various knowledge gaps regarding the assessment of the negative impacts of underwater anthropogenic sound. The most important among them concerns the quantification and mapping of the man-made sound in the seas and oceans. Consequently, the objective of the thesis is to suggest and demonstrate several methods that aid in the quantification of the anthropogenic underwater sound.

Measurement is the first step in the assessment of the levels of anthropogenic underwater sound in marine habitats. In the frame of the BIAS-project an unprecedented amount of Baltic Sea sound monitoring data covering 36 different locations spanning one whole year was collected. In the BIAS project the data was primarily used for validating the soundscape modeling. However, the measured levels hold value by themselves and are worthy of being made available for wider scientific community as they serve as a baseline against which any future measurements can be compared. Also the associated analysis of these levels with emphasis on their temporal and the spatial variability and their relation to ship traffic intensity and environmental factors are an invaluable source for any specialist within the field of underwater sound monitoring.

In the measured sound the natural and anthropogenic components exist often simultaneously. Therefore, the key question for quantifying the prevalence of anthropogenic sound is to estimate its excess over the underlying natural levels. One approach is to detect times when the measured sound is anthropogenic and assume that the remaining sound is natural. More effective solution is to find the natural sound level's dependence on environmental factors. This dependence enables the estimation of levels that would exist in a location naturally and compare them with the measured sound levels. Their difference could serve as a metric for assessing the environmental pressure posed by the anthropogenic sound. Having methods for extracting times of the natural and anthropogenic sound is also useful for validating the modeling of these two components of the soundscape.

The most widespread underwater anthropogenic sound is created by the maritime traffic. Measuring the characteristics of the sound radiated by individual ships of the ever changing merchant fleets is essential for the modeling and mitigation efforts. At the same time cost effective measurement methods suitable for shallow water are lacking. For that reason providing a method that makes use of the abundant sound monitoring data is also of key interest in attaining quieter seas and oceans and their sustainable use in the future.

Therefore the objectives of the thesis are to:

1. quantify the spatial and temporal variability of underwater sound in the Baltic Sea;

2. suggest and demonstrate a method that estimates the excess of anthropogenic sound over the underlying natural levels;

3. provide a method that enables using the abundant sound monitoring data for characterising ships as sources of underwater sound.

Abbreviations

ADC	Analogue-to-digital converter
AIS	Automatic identification system
BIAS	Baltic Sea Information on the Acoustic Soundscape
BSN	Below self-noise
COG	Course over ground
CPA	Closest point of approach
D11	Descriptor 11
DFT	Discrete Fourier transform
GES	Good Environmental Status
GM	Geometric mean
HELCOM	The Baltic Marine Environment Protection Commission (Helsinki Commission)
JOMOPANS	Joint Monitoring Programme for Ambient Noise North Sea
MSFD	Marine Strategy Framework Directive
NFFT	Numerical Fourier transform
PDF	Probability density function
PL	Propagation loss
RAM	Range-dependent acoustic model
RL	Received level
SL	Source level
SOG	Speed over ground
SPL	Sound pressure level
TSG Noise	Technical Sub-Group on Underwater Noise
QA	Quality assurance

1 Underwater sound

Underwater acoustics is the science of sound in water and mostly in natural water bodies like oceans, seas, lakes and rivers. The underwater realm accounts for more than 70 % of our globe's surface and this realm is mostly inaccessible to electromagnetic waves. The favourable conditions for acoustic wave propagation inside the seas and oceans have made the marine organisms more adapted to using sounds for communication, prey locating, predator avoidance than their land or air based relatives. The more favourable conditions are exemplified by the speed of sound in air being over four times slower than in water. Also the distance sound travels in air is not usually more than a few kilometers, whereas in the ocean sound can travel distances reaching thousands of kilometers. Therefore, the field of underwater acoustics is of key importance for the exploration, understanding and in the end preservation of the Blue Marble in a condition suitable for human life.

1.1 History of developments

One of the first quantitative underwater sound measurements is attributed to Daniel Colladon and Charles Strum who in 1826 measured the speed of sound in the Lake of Geneva [1]. The striking of an underwater bell with simultaneous flash of gunpowder enabled the observer at a distance to measure the time difference between the flash and the arrival of sound. Strum and Colladon reported the sound speed at temperature of 8° C to be 1435 m/s. This is only about 3 m/s less than the values accepted today in similar conditions [2].

The first practical application of underwater sound was also connected to submarine bells. It was around the end of the 19th century when bells were started to be placed under lightships or near lighthouses. The aim was to serve as navigational aid that is a cheaper and more reliable option replacing lighthouse sirens, horns, and whistles [2]. Onboard ships the underwater sound was received by carbon button microphones encased in water proof enclosures. According to Karlik [3] this type of system was also installed in the Eastern Baltic Sea. In 1910 they were added for the Nekmangrund lightship on Hiiu Shoal and near Oviši (Lyser Ort) lighthouse. During the early 1900s navies also increased radically their use of submarines and the underwater warfare became a major driving force for the development of underwater acoustics. An evidence of the increase in the use of submarines can be considered the establishment of the Noblessner Yard in 1912 by Emanuel Nobel ja Gustav Lessner in Tallinn. The aim of this company was to build Bars-class submarines for the Imperial Russian Navy [4].

Among the first profound scientific publications regarding underwater acoustics was published by a German physicist Hugo Lichte after the First World War in 1919 [5]. In this paper Lichte correctly deduced from measurements conducted before the war the effects of temperature, salinity, and depth on sound velocity. He also concluded that the range sound propagates underwater should be longer in winter than in summer due to refraction. This type of quality research, in turn, lead to further advances in sonar technology. The level of the equipment available at the end of the interwar period can be characterised by the specifications of the hydroacoustic devices onboard the Kalev-class mine-laying submarines of the Estonian Navy. According to Arto Oll [6] the submarines were equipped with Atlas Werke AG 500 W underwater telegraph transmitters with range of 5-7 nautical miles, hydrophones (passive listening for detection and target locating) with operating range of 2-2.5 nautical miles and an echo sounder capable of measuring water depths in ranges of 0-100 m and 0-500 m.

The Second World War saw a multiplication of research efforts in large part due to the

successes of the U-boats. The amount of scientists hired in the field during the war started to transform the "pragmatic art" of underwater acoustics into a developing science. At this time underwater ambient sound and its sources were started to be measured and studied systematically in the United States [2] as it is essential for predicting the underwater sound measuring equipment's signal-to-noise ratios. A notable pioneering study summarising some of these wartime efforts was published by Knudsen, Alford and Emling in 1948 [7]. This paper lists as main sources of ambient noise the motion of water, marine life, and the ships as man-made sources. There is also shown corresponding spectral characteristics in frequencies from 100 Hz to 25 kHz. Also the paper lists a number of different soniferous marine species and shows the spectra produced by the snapping shrimp, croakers, sea robins, porpoises and bastard trout.

According to Poikonen [8] long term monitoring (surveillance) of underwater sound took place during The Second World War in the Gulf of Finland. For this purpose two coastal variants of the GHC apparatus produced by Atlas Werke were used. The systems consisted of circular hydrophone arrays near the islands of Kallbådan, Gogland (Suursaar) and Vaindloo. Therefore, the ambient sound has probably been measured in the various parts of the Baltic Sea for a long time. Simultaneously, the list of published studies is not numerous. One of the first articles being published only as late as 1984 [9] and reported levels from a single location in Eastern Gotland Basin.

The advent of the Cold War brought about the continuation in research as all counterparts wanted to reach a technological superiority in underwater warfare. For these and other purposes at the end of the 1950s the Soviet Navy constructed their test range in the Hara Bay. For the measurement of noise from and reflectivity of surface ships and submarines three seafloor platforms of five hydrophones with preamplifiers, underwater cables and onshore equipment were installed. This system named Altair was commissioned from the Morfizpribor Central Research Institute [10].

Significant contributions about the underwater ambient sound were included in classic paper by Wenz [11]. Wenz expanded and systematised the ambient sound spectra by Knudsen [7] and provided a composite schematic spectra where the noise levels are connected to impacts from the different prevalent sources of underwater sound. The source mechanisms are also described in more detail than previously.

1.2 Underwater sound as pollution

In parallel to the advances in the applications of underwater acoustics to marine seismology, naval warfare, fish detection and navigation there have been a growth of knowledge about the use of sounds by marine life. It was only natural that the quantification of the potential harm proposed by man-made (anthropogenic) underwater sound would emerge as a separate research subject. Serious concerns regarding anthropogenic underwater sound can be traced back to at least as far as the 1970s [12].

Among all anthropogenic sound sources a growing international concern has been related to the sound produced by ships. This has been related to the fact that within the last twenty years seaborne trade in the World has more than doubled [13]. Both the number of merchant ships and their size have grown significantly [14]. Ship propulsion systems have long been revealed to be a dominant source of radiated underwater sound at frequencies < 200 Hz [15]. Therefore, it is only natural that the rise in intensity of ship traffic has in various studies been shown to be related to the increase in the oceanic low-frequency ambient noise [16, 17]. The increasing continuous levels introduced by ships could pose considerable risks for the overall health of our seas. One of the long-term detrimental effects on marine ecosystems is the reduction of communication range [18, 19]. The reduction of

communication range means that animals have to be closer to each other in order to communicate [20]. Among other effects are the increase in stress levels [21] and perturbation of development of marine species [22]. Special focus has often been on marine mammals (whales, dolphins, seals, sea lions, sea cows) that use the sound both actively and passively to communicate and sense their environment, covering frequencies from 2 Hz to 100 kHz depending on species [23]. At the same time, the list of marine animals known to be sensitive to sound has been ever extending. Now it is ranging from marine mammals and fish to crustaceans and invertebrates [22]. There are also additional continuous anthropogenic sound sources besides ships being introduced to the marine environment. Examples are offshore wind farms and various emerging marine energy installations.

An example of a the Baltic Sea fish species that could be affected by increasing underwater sound level is the Baltic Sea cod. Cod is known to perceive sounds generated within a frequency range of 100 - 1000 Hz and display a heightened cortisol plasma level with potential negative impacts on their spawning performance [21]. Another recent study has demonstrated loud ship noise to reduce foraging in harbour porpoises [24]. Besides these species the Baltic Sea pinnipeds - grey seal, harbour seal, and ringed seal along with fish species Baltic Herring and European Sprat could be affected as well.

1.3 The MSFD and the BIAS project

The concerns regarding potential negative effects of anthropogenic underwater sound have been recognised in existing European legislation. EU's Marine Strategy Framework Directive (MSFD) was adopted in June 2008 with the aim to achieve the Good Environmental Status (GES) for maintaining the marine biodiversity of European marine habitats by the year 2020 [25]. This directive sets qualitative descriptors for GES. Among these, Descriptor 11 (D11) concerns the energy introduced into the marine environment, including underwater sound, which should be at levels that do not adversely affect the marine environment. The Technical Sub-Group on Underwater Noise (TSG Noise) issued a set of recommendations [26] and monitoring guidance specifications [27] concerning this descriptor. In regards to the criterion for the continuous low-frequency underwater sound, it is stated that it should be monitored in two one-third octave bands (here and after base 2) with the center frequencies of 63 Hz and 125 Hz [28]. The sound pressure level (SPL) of these frequency bands has been chosen due to being a good proxy for the abundance of the continuous low-frequency anthropogenic sound, mostly generated by commercial vessels.

In 2012 an international cross-bordering effort with the aim of assessing the levels of underwater sound in the Baltic Sea in the form of a Life+ project called "Baltic Sea Information on the Acoustic Soundscape" (BIAS) was launched [29]. Scientists from six Baltic Sea countries - Sweden, Denmark, Germany, Poland, Estonia, and Finland led an extensive sound monitoring programme covering 36 different sound monitoring locations around the Baltic Sea. The conjugate use of monitoring and modeling enabled mapping the soundscape of the whole sea. Within this project the monitored sound data was mainly used for the calibration and validation of the sound propagation modeling. Additionally a planning tool for using the sound maps was developed [30] for easy access and use by beneficiaries.

2 Measurement of sound in the Baltic Sea

Sound is defined in acoustics as the alteration in pressure, stress or material displacement that is propagated via the action of an elastic medium [31]. When characterising an acoustic field the quantity most commonly measured is the alteration in pressure *i.e.* the sound pressure. The transducer used for measuring the alterations of pressure in water is called a hydrophone. Hydrophones convert the pressure changes into electrical signals and most commonly by the use of piezoelectric materials. This electrical signal goes through amplifiers and filters before storage or real time use. Nowadays the signal is often converted by an analogue-to-digital converter (ADC) into a digital audio format for ease of analysis with a computer. Although cabled systems have long existed and are becoming more popular for the long term sound monitoring, a more widespread option has been to deploy an autonomous system to record for a relatively long period of time. Underwater sound measurement system that records digital audio autonomously and consists of hydrophones, amplifiers, filters, ADC with storage is called a digital autonomous acoustic recorder [32]. In the BIAS-project, two different digital autonomous acoustic recorders were used: the DSG Ocean by Loggerhead Instruments [33] and the SM2M by Wildlife Acoustics [34]. The measurement equipment specifications and data processing overview is presented in Appendix B of the thesis.
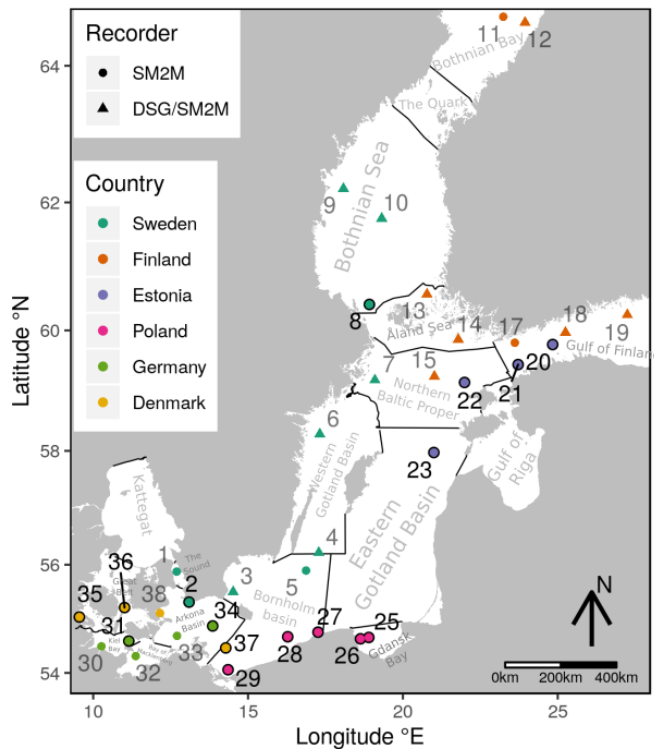
Figure 1: Underwater sound monitoring locations of the BIAS-project within the HELCOM subbasins. The locations where SM2M marine submersible recorder was used throughout the sound monitoring are depicted with a circular marker and locations with alternate deployments of the DSG Ocean recorder with triangular markers. The numbers of the monitoring locations analysed are highlighted with a darker colour. This figure without the subbasin borders and names is shown in [Publication IV].

2.1 Sound monitoring locations

The BIAS project stands out for its longevity and spatial coverage in shallow watered seas and specifically in the Baltic Sea. This can be confirmed by looking at the overview of published sound monitoring efforts prior to BIAS in the thesis by Poikonen [8]. Figure 1 shows all of the 36 sound monitoring locations of the BIAS-project along with the HELCOM sub-basin names. The locations were chosen to cover different depths, seabed substrates and ship traffic intensities. As seen in Fig. 1 the numbering of the monitoring locations follows mostly a clockwise direction around the coast of the Baltic Sea. The numbering starts in The Sound subbasin near the coast of southern Sweden and follows the Swedish coast up to the Bothnian Sea where locations 9 and 10 are located. The under ice recordings presented in [Publication IV] and subsection 5.2 is performed in Bothnian Bay location 11. The numbering continues on the Finnish coast of the Åland Sea and the Gulf of Finland. Two of the Estonian positions 20 and 21 are also located in the Gulf of Finland. From there the numbering continues clockwise down to the Gulf of Gdansk and Bornholm Basin. The German locations 30-34 are numbered anticlockwise moving from the Bay of Kiel to the Bay of Mecklenburg and Arkona Basin. The Danish measurement locations 35-38 are in the Great Belt subbasin, location 37 is in the Bornholm basin and the last of the locations number 38 is in the Arkona Basin (Faxe Bay).

The BIAS project sound monitoring spanned the whole year of 2014 in duration. Since the end of the BIAS project monitoring has continued in some selected BIAS locations. The Estonian position that has been serviced with minor interruptions until the present day is location 20. In [Publication IV] the monitoring results from a subset of the total BIAS locations were analysed. The coordinates of the subset and corresponding HELCOM subbasin names are listed in Table 1. It must be noted that in each monitoring location a number of deployments were made and the coordinates listed in Table 1 changed from one deployment to another.

Table 1: The subbasin names, location names and coordinates of the selected monitoring locations from the BIAS-project. The asterisk behind location 8 is to point out significantly lower data coverage (May to December 2014, coverage 64% against 88-100% for the other locations). List of coordinates taken from [Publication IV].

No	Country	Loc. Name	Helcom subbasin	Lat. °N	Long. °E
2	SWE	Trelleborg	Arkona Basin	55.3210	13.0950
8*	SWE	Sea of Åland	Bothnian Bay	60.4158	18.9183
20	EST	Tallinn	Gulf of Finland	59.7715	24.8397
21	EST	Paldiski	Gulf of Finland	59.4416	23.7276
22	EST	Hiiumaa	North. Baltic Proper	59.1499	21.9901
23	EST	Saaremaa	East. Gotland Basin	57.9689	21.0035
25	POL	Gulf of Gdansk	Gdansk Bay	54.6665	18.9001
26	POL	Puck Bay	Gdansk Bay	54.6413	18.6310
27	POL	Łeba & Rowy	Bornholm Basin	54.7649	17.2589
28	POL	Darłowo-Ustka	Bornholm Basin	54.6793	16.2813
29	POL	Świnoujście	Bornholm Basin	54.0602	14.3549
31	GER	Fehmarn Belt	Kiel Bay	54.5997	11.1497
34	GER	Arkona Basin	Arkona Basin	54.8803	13.8574
35	DNK	Little Belt	Great Belt	55.0755	9.92133
36	DNK	Great Belt	Great Belt	55.3672	11.0193
37	DNK	Rønne Banke	Bornholm Basin	54.7853	14.4673

2.2 Sound pressure level

The sound monitoring creates a large amount of data in the form of digital audio files. This data has to be processed before analysis. The processing was performed following the data processing standards developed in the BIAS project [35]. There are numerous different quantities that can be calculated from the measured sound pressure values. The aim of the monitoring in the Baltic Sea has mostly been the characterisation of the long-term soundscapes *i.e.* statistical representation of sounds that can be considered continuous. The Good Practice Guide for Underwater Noise Measurement [36] states that: "The metric most suitable for quantifying the continuous sounds, is the Sound Pressure Level (SPL)". The SPL is the level of the acoustical power quantity mean-square sound pressure defined among other entities in the ISO standard [31] in formula form as

$$L_p = 10 \log_{10} \frac{\widehat{p^2}}{p_0^2} \qquad (1)$$

where p_0 is the reference value for sound pressure which in water is $p_0 = 1\ \mu\text{Pa}$. The $\widehat{p^2}$ is the mean-square sound pressure that in formula form is defined as

$$\widehat{p^2} = \frac{1}{t_2 - t_1} \int_{t_1}^{t_2} p^2(t)\, dt \qquad (2)$$

where $p(t)$ is the sound pressure, and t_1 and t_2 are the start and end times, respectively. As this definition indicates, instead of being instantaneous, the SPL characterises the sound pressure values recorded over some time period.

Besides varying time periods the SPL can be calculated for different frequency bands. If the band spans a wide range of frequencies *e.g.* 10 - 10 000 Hz it is called a broadband. Other narrower bands that are widely used in acoustics are decades and octaves but also their subdivision into thirds of octaves and tenths of decades. The bands spanning third of an octave and tenth of decade are practically the same width. In the underwater acoustics terminology standard they are both named "one-third octave band" [31]. The use of the tenth of a decade requires the addition of the specified base and the corresponding term should be called "one-third octave band (base 10)". Due to the ambiguity in the use of the term **"one-third octave band" in the thesis and associated publications the "one-third octave band (base 2)" is used and not "one-third octave band (base 10)" *i.e.* decidecade**.

In the BIAS project the 63 Hz and 125 Hz one-third octave band SPL values were monitored as these are required by the MSFD indicator D11 criterion for continuous low frequency sound [28]. Besides, two bands were decided to be monitored additionally. The 2 kHz one-third octave band SPL was chosen, as the hearing of marine mammals is known to be more sensitive within this band. Also a broadband (10-10 000 Hz) SPL representing a wider range of frequencies was chosen in the BIAS project. Therefore, the BIAS project limited itself to only 4 different frequency bands. In the project JOMOPANS (Joint Monitoring Programme for Ambient Noise in the North Sea) that has followed BIAS the sound is monitored in one-third octave bands (base 10), with centre frequencies between 10 Hz and 20 kHz [37].

3 Oceanography of the Baltic Sea

The Baltic Sea is an intracontinental sea in northeast Europe. In this section a description of this sea is given through the viewpoint of the underwater acoustics. A brief overview starting from the lower boundary – the sea bottom – will be followed by description of the characteristics of the waterbody and the sea surface. The characteristics of the main sources of underwater sound can be found in the section 4 of the thesis.
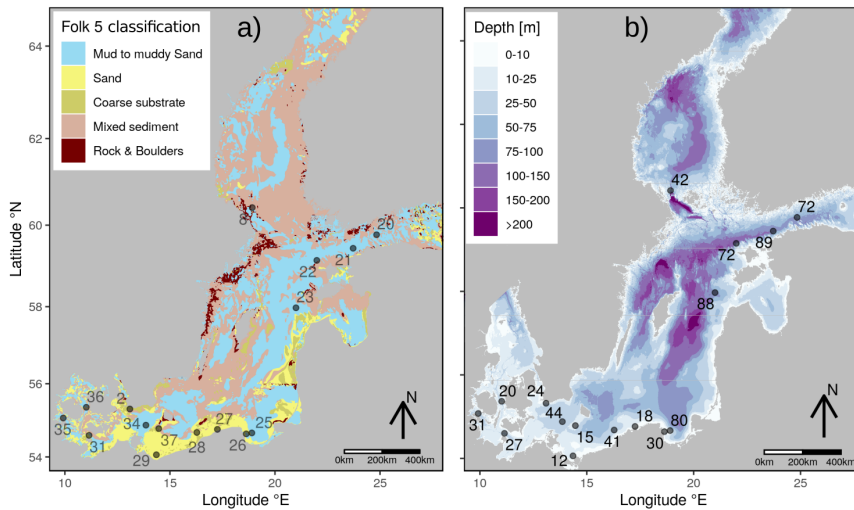

Figure 2: *a) Mapped seabed substrates data of the Baltic Sea from EMODnet (http://www.emodnet-geology.eu/). The substrates shown are classified according to Folk 5-class classification. The black dots mark the sound monitoring locations along with their ID numbers. b) Bathymetry data of the Baltic Sea from the Baltic Sea Bathymetry Database (BSDB - http://data.bshc.pro/). The black dots mark the sound monitoring locations along with the depths in meters at the monitoring locations.*

3.1 The sea floor

The defining feature of shallow water acoustics is that the low-frequency sound interacts strongly with the sea bottom. The Baltic Sea is a shallow sea with average depth of 54 m. The sea fills a complex and old depression in the East European Craton forming distinct subbasins depicted in Fig. 1. The morphology of the present-day sea floor of the Baltic Sea has been affected by [38]: 1) pre-glacial bedrock surface; 2) glacial erosion and deposition; 3) post glacial sedimentary processes. According to Winterhalter [39] the properties and stratigraphic characteristics of the post glacial sediments have been affected by:

- The regional bedrock of the sea floor and surrounding land areas. The southern and central Baltic Sea have predominantly sedimentary bedrock and the northern parts are exposed to crystalline basement. Both have influenced the sedimentation and the resulting sea floor morphology.

- Variations in the salinity and other physicochemical parameters together with the actual source of sedimentary material has affected the grain size and mineralogical composition of the deposited material including organic components.

- Bathymetry and sea floor topography in relation to prevailing barometric (air pres-

sure) and wind fetch conditions together with factors like depth to wave base and the existence of near bottom currents govern the balance between erosion, non-deposition and sedimentation.

- Biological factors including bioturbation caused by bottom burrowing animals and decomposition of deposited organic matter.

All this has made the sea bottom of the Baltic Sea a diverse and multilayered boundary. The properties of this boundary effect the reflection, attenuation and scattering of the interacting sound waves. In order to understand the acoustics at a given site one would need to know the local sediment types and their variation with depth down to a depth broadly 2-3 acoustic wavelengths into the sediment [40]. For a 63 Hz acoustic wave this would amount to knowing the seabed composition to a depth around 50 m. In most locations in the Baltic Sea this data is not readily available. With a varying spatial resolution the seabed substrate data can be found in the EMODnet (http://www.emodnet-geology.eu/). The EMODnet seabed substrates according to the Folk 5-class classification scheme are shown in Fig 2-a) along with the mapped selected sound monitoring locations of the BIAS project. Table 2 lists the seabed substrate types at the selected monitoring locations according to the Folk 5-class and Folk 7-class substrate classification schemes. The Folk classification schemes used in EMODnet are described in the following article [41]. The difference between the Folk 5-class and Folk 7-class classification is the further subdivision of mud to muddy sand into mud, sandy mud and muddy sand.

Table 2: Seabed substrate types, sea depths, and distances to land in the selected BIAS sound monitoring locations. An indication of the unevenness of the sea bottom near the monitoring locations is given by the standard deviation of depths in 5 km radius from the locations.

No.	Folk 5-class	Folk 7-class	Depth [m]	Land [km]
2	Coarse substrate	Coarse substrate	24 ($\pm$ 8)	5
8	Mixed sediment	Mixed sediment	42 ($\pm$ 28)	19
20	Mud to muddy sand	Sandy mud	72 ($\pm$ 7)	16
21	Mud to muddy sand	Mud	89 ($\pm$ 4)	16
22	Mud to muddy sand	No data at this level	72 ($\pm$ 31)	>20
23	Mud to muddy sand	No data at this level	88 ($\pm$ 2)	>20
25	Mud to muddy sand	Muddy sand	80 ($\pm$ 9)	7
26	Mud to muddy sand	Mud	30 ($\pm$ 4)	6
27	Sand	Sand	18 ($\pm$ 5)	3
28	Sand	Sand	41 ($\pm$ 3)	>20
29	Sand	Sand	12 ($\pm$ 2)	14
31	Sand	Sand	27 ($\pm$ 3)	8
34	Mud to muddy sand	Mud	44 ($\pm$ 1)	>20
35	Mud to muddy sand	Muddy sand	31 ($\pm$ 10)	5
36	Mixed/M. to m. sand	Mixed/Muddy sand	20 ($\pm$ 5)	5
37	Mixed/Sand	Mixed/Sand	15 ($\pm$ 2)	>20

The shape of the sea bottom *i.e.* bathymetry is shown in Fig. 2-b) along with the sea depths at each selected sound monitoring location. Table 2 lists along with the depths at each location additional data about the variability of the bathymetry within 5 km radius from the sound monitoring locations. According to this data the seabed is most uneven in locations 22 and 8, where the standard deviation of the depth within 5 km is 31 and 28 metres accordingly. The seabed is the flattest in location 34, where the standard de-

viation within 5 km from the monitoring location is only around 1 m. Table 2 also lists the approximate distances to land in km from each of the sound monitoring locations. As listed in Tab. 2 several of the locations (2, 25, 26, 27, 31, 35, 36) are close to land with the location 27 being only 3 km from the shoreline. The closeness of land indicates the possibility of surf noise in the location. There have been shown that long beaches parallel to the direction of approaching wave fronts may generate surf noise that propagates many kilometers seaward [42]. According to Bardyshev the surf-generated underwater sound near pebble-type coasts is higher than the noise of the open sea at a distance of 10 km from the coast [43].

3.2 The water body

The thermodynamic state of the seawater is commonly characterised by salinity, temperature, and density. The Baltic Sea is brackish with mean salinity about 7 ‰ (1/5 the salinity of normal ocean waters) [44]. The surface salinity is maximal in Danish Straits 32 ‰ and minimal in the Bothnian bay 2.5 ‰ as well as in the mouth of the river Neva in the Finnish Bay < 2.0 ‰ [45]. Salinity is higher in the bottom of the sea and there exists a halocline (salinity gradient) at depths of 60-80 m [46]. It is well established that changes in the water temperature and salinity can both affect the bubble density and size [47]. Bubble size distribution affects the sound radiation by bubbles as the major source of underwater ambient sound that may be linked to the level of the wind-driven ambient sound [48].
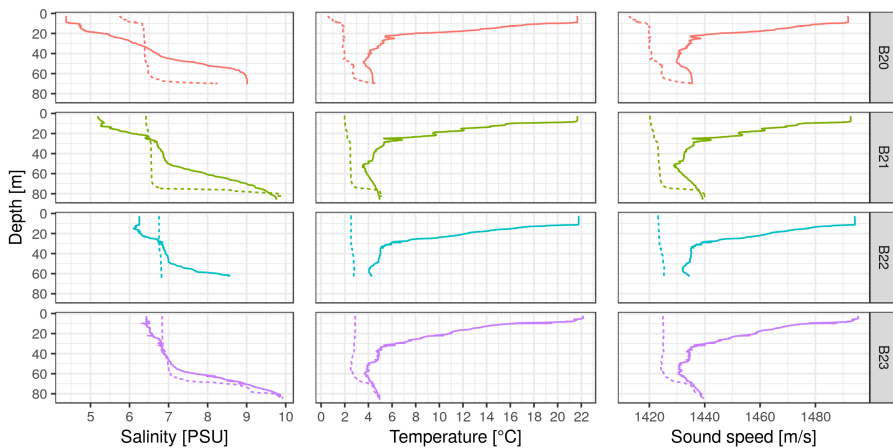

Figure 3: Measured salinity and temperature profiles along with calculated sound speed profile in four Estonian BIAS-project sound monitoring locations on 5 February (dashed lines) and 12 August 2014 (solid lines).

Firstly, the temperature follows the two layer structure determined by salinity. Secondly, every year the upper layer temperature forms a warm surface layer and a thermocline in the summer months [44]. Figure 3 shows the measured salinities and temperature profiles for four different sound monitoring locations and two different times of the year in 2014. The measurements were performed by Fred Buschmann with IDRONAUT Ocean Seven 320 Plus WOCE-CTD multiparameter probe. The salinity profiles during February show a simple two layered structure in locations 21, 22, 23 with additional lower salinity surface layer in location 20. Expectedly, the salinity decreases from the southernmost location 23 in the Eastern Gotland basin towards the locations 20 in the Gulf of Finland.

Temperature profiles in Fig. 3 all show similar thermoclines at depths of 10-30 m in August. It is known that in shallow water the temperature variability is a good first order proxy for sound-speed variability [40]. This is exemplified by the calculated sound speed profiles in Fig. 3 that closely resemble the shapes of the temperature profiles.

Over most of the Baltic Sea the tidal amplitudes are 2 - 5 cm [44] and tidal currents can be considered almost negligible [49]. There exist surface currents with weak long-term mean speeds around 5 cm/s, but during storms the wind drift surface currents can reach 50 cm/s. Besides surface currents there have been observed an intra-halocline current with speeds over 20 cm/s [50] and eddies at different depths with highest velocities more than 30 cm/s [51]. The circulation in the western Baltic Sea is dominated by the exchange of water masses with the North Sea through the Belts and the Sound. In some locations in the Fehmarnbelt the current speeds can reach maximums over 200 cm/s [49]. When recording sound in locations with high current speeds the flowing water around the measurement rig can cause acoustic self-noise. For example, the fluctuations related to turbulence around a hydrophone creates a pseudo-noise in the recordings that is known to contribute significantly at lower frequencies (< 500 Hz) increasing with decreasing frequency [52]. Flow induced acoustic self-noise has usually been detected in locations with high tidal currents [53, 52]. For tidal currents the periodicity makes the detection of the flow noise easier when compared to aperiodic currents. According to Basset the current velocities have to be > 30 cm/s for the acoustic signature consistent with flow-noise to begin dominating low-frequency measurements. Although it must be noted that the flow noise characteristics are dependent on the hydrophone geometry. It is reasonable to assume that flow induced acoustic self-noise can be significant in the Baltic Sea and it is most likely significant in the Belts.

3.3 The sea surface

The characterisation of the sea-surface in underwater acoustics is important as it is both a reflector and a scatterer of sound [54]. The wind driven sea-surface agitation is also a major source of underwater ambient sound that will be further discussed in the subsection 4.1 of the thesis.

Wind speed is usually considered a good first order descriptor for the characterisation of the complicated sea-surface interaction zone [57]. Over the Baltic Sea the most frequent wind directions are southwest and west because of prevailing westerly upper and surface level air flow [49]. More than 50 % of winds in the Baltic Sea have speeds of 5-9 m/s. The share of winds with speeds > 17 m/s is less than 5 %. Share of winds with speeds < 3 m/s is around 15 % [44]. The wind speeds near the selected BIAS sound monitoring locations were obtained from the SMHI mesoscale analysis system MESAN [56]. Figure 4-b) shows the boxplots composed from 2014 MESAN model wind speeds extracted from the model nodes closest to each monitoring location. The node locations are mapped in Fig. 4-c). According to this data 50 % of the wind speeds in the sound monitoring locations are between 4-8 m/s. This is also apparent from Fig. 4-b), where box edges representing the first and third quartiles also mostly fall within this range. The median wind speeds are shown with black lines within the boxes in Fig. 4-b). According to MESAN data the lowest median wind speed 4.7 m/s was near the sound monitoring location 26 and the highest 7.1 m/s in location 34. There also exists a seasonal cycle in the wind speeds, which mirrors an analogous cycle in cyclone generation over the North Atlantic with higher wind speeds during the winter months and lower wind speeds in the summer months. This was also apparent from the MESAN wind speed data near all the monitoring locations where the median wind speed during January was 8.0 m/s and June 4.7 m/s.
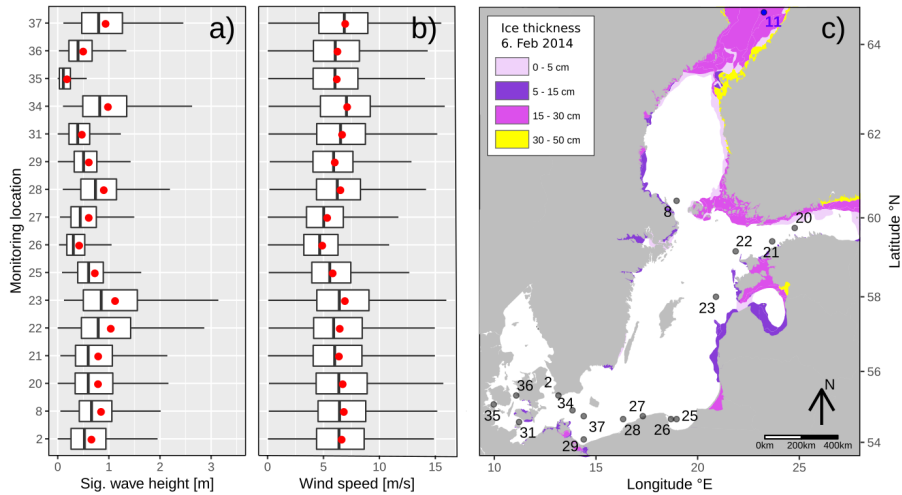
Figure 4: **a)** *Boxplots of significant wave heights in the selected sound monitoring locations. The red dots mark the arithmetic mean. The wave height data originates from the SMHI SWAN forecast model [55], extracted from the closest model node to each monitoring location.* **b)** *Boxplots of wind speeds in the selected sound monitoring locations. Wind data originates from the SMHI MESAN model [56], extracted from the model node closest to each monitoring location.* **c)** *Mapped selected BIAS sound monitoring locations along with ice thicknesses during 2014 peak extent of ice in 6 February. The ice chart originated from the Federal Maritime and Hydrographic Agency of Germany.*

An attempt of a more precise characterisation of the sea-surface interaction zone should also consider the wave field. The Baltic Sea wave fields show large spatio-temporal variations. Seasonally the wave activity follows a similar variation that appears in the wind speed. Higher wave heights appear mostly during winter months and lower during summer. The significant wave height near the selected BIAS sound monitoring locations were obtained from the SMHI numerical wave model SWAN [55]. According to the 2014 SWAN data near the monitoring locations the significant wave height during December was 0.9 m and 0.4 m during July. The Baltic Sea areas where the waves are highest should be located in the eastern parts of the Bothnian Sea and northern Baltic Proper, south of Gotland, and in the Arkona Basin [58]. The boxplots in Fig. 4-a) show the SWAN 2014 significant wave heights. The 2014 median significant wave height was highest 0.9 m in location 23 and lowest 0.1 m in location 35.

During winter seasons sea ice forms in the Baltic Sea and reaches its largest extent usually between February and March. Depending on the air temperatures ice can reach a cover of 10 - 100 % of the sea [59]. The regions where ice usually forms first are the Bay of Bothnia and the eastern part of the Gulf of Finland. From there the usual extent reaches to cover the Bothnian Sea, the Archipelago Sea, the Gulfs of Finland and Riga as well as the northern part of the Baltic Proper [59]. The soundscape of the sea when covered with ice is expected to be very different when compared to the period when the sea is open [60]. During 2014 the ice reached its maximum extent in 7. February when it covered approximately 38 % of its surface [61, 62]. The thickness of ice during this time along with the MESAN model nodes closest to each monitoring location are shown in Fig. 4-c). The ice chart in Fig. 4-c) shows that none of the selected sound monitoring locations was covered by ice during 2014.

4 Sources of underwater ambient sound

The types of sources contributing to sound fields in seas, oceans, rivers and lakes can be categorised broadly as anthropogenic or natural. The anthropogenic sources are sometimes subdivided between sources that make sound intentionally, and others that produce sound as an unintended by-product of other activities [63]. The natural sources are also subdivided into biological as by non-human animals and non-biological. The sounds resulting from these sources are themselves named as the anthropophony, geophony, and biophony that make up a soundscape in a location. The underwater sound source categories with examples that are more relevant to the Baltic Sea are listed in table 3.

Table 3: An incomplete list of categorised underwater sound sources.

Natural sources		Anthropogenic sources	
Non-biologic	Biologic (Baltic)	Non-intentional	Intentional
Sea-surf. agitation	Mammals	Vessel traffic	Acoustic deterrents
• L-H mechanism	• Harb. porpoise	Fishing	Active sonars
• Turbulent flow	• Harbour seal	Offshore ind.	Echo sounders
• Bubble clouds	• Grey seal	• Wind turbines	Fish finders
• Ind. bubbles	• Ringed seal	• Oil drilling	Sidescan sonars
• Spray and splash	Fish	Offshore const.	Sub-bottom profilers
Rain (+ hail & snow)	• Atlantic cod	• Dredging	UW. communication
Ice noise	• Atlantic herring	• Pile driving	Acoustic positioning
Sediment transport		Explosions	Seismic exploration
Lightning			

By the duration of the emitted sounds the sources are divided and defined as impulsive and non-impulsive. Sources that create sounds usually lasting < 1 second are said to be impulsive. The created impulsive sounds are relatively broadband with high peak sound pressure characterised by rapid rise and decay times [64]. In table 3 the examples of impulsive sources are for example explosions, seismic exploration (in case of air guns), and some ice related processes. The non-impulsive sources can create sounds that can have varied frequency bands, being broadband, narrowband or tonal. Heavy rain, sea surface agitation are two examples of relatively broadband sources. An example of tonal sound source is a badly maintained or designed ship propeller that can create sounds with very strong tonal components. The duration of sounds by non-impulsive sources can also be different and vary from brief to prolonged or intermittent to continuous.

4.1 Natural sound sources

The most omnipresent and continuous non-biological natural sound comes from the sea-surface agitation. Wenz reported that in absence of other sources the sound level in frequency band roughly between 50 Hz and 20 kHz changes along with the sea state [11]. Since the time of Wenz, studies have widened this band showing dependence to as low frequency as 0.05 Hz [65]. In the lower frequencies from 0.8 - 80 Hz one of the sound generating mechanisms is said to be nonlinear surface wave interactions [66, 67, 68] also called the Longuet-Higgins mechanism [65]. Turbulent flows containing microbubbles are also known to produce sound that is a significant contributor at frequencies below 10 Hz [69, 70]. In turbulent flows the microbubbles provide the compressibility and turbulence provide the mechanical energy. The different frequency bands of the sound source mechanisms are visualised on Fig. 5 along with the resulting spectral curves by various authors.
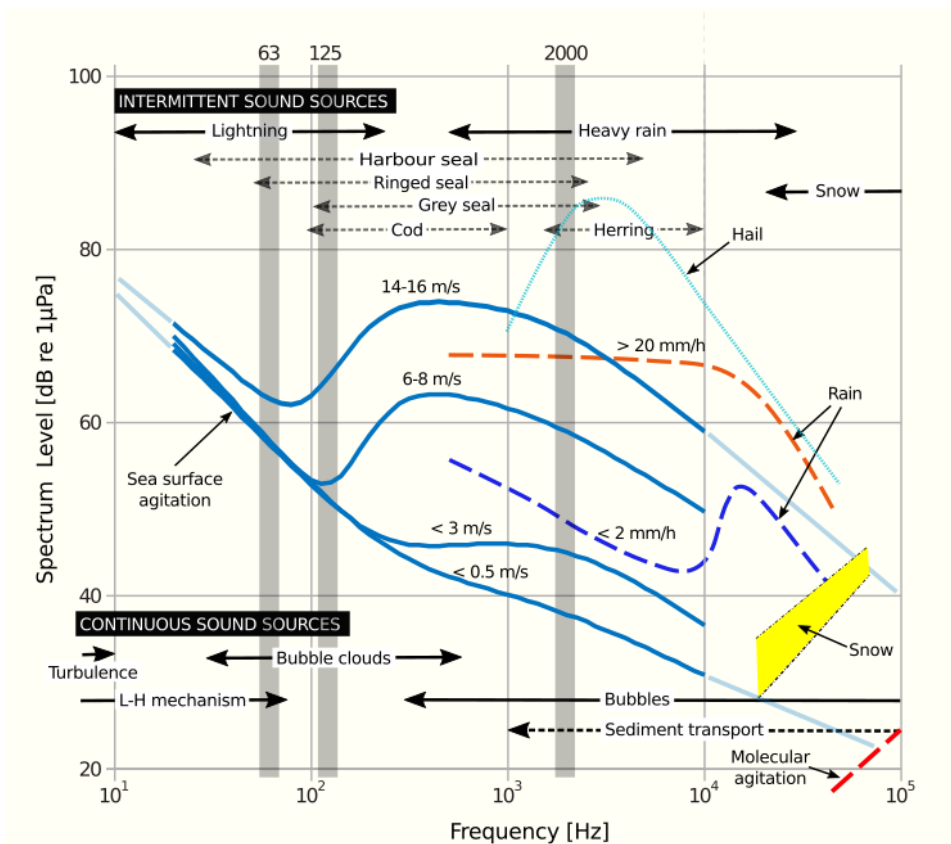
Figure 5: Intermittent and continuous natural sound sources and the resulting spectral curves excluding ice noise. Wind dependent sea surface agitation curves are adapted from [8], rain rate dependence curves from [71], hail and snow curves from [72]. With arrows are shown the preeminent frequency bands where the continuous and intermittent sources are important. The sediment transport is marked with a dashed line, as it is important only in areas with high flow at the bottom. With grey background colour are marked the two MSFD one-third octave bands (63 Hz, 125 Hz) and the additional 2 kHz one-third octave band chosen in the BIAS-project.

As shown in Fig. 5 within a wide frequency range the wind dependent sound has been attributed to the oscillation of air bubbles in water. One of the first studies about air bubbles oscillations in water was published by Minnaert already in 1933 [73]. Since the time of Minnaert there has been found that in the lower frequencies of 30 Hz to 200 Hz the sound is generated not by oscillation of individual air bubbles but by oscillating bubble plumes and clouds [74, 57]. In frequencies 200 - 500 Hz the dependence is said to be due to both the bubble clouds and individual bubbles and only above 500 Hz mainly due to volume pulsation of individual bubbles [57]. The bubbles are produced by entrainment of air underwater in case of breaking waves, spray and splash. Prior to visible wave breaking there have been suggestions that hydrodynamic surface instabilities or microbreaking might be responsible for the air entrainment [75]. The spray and splash create also sounds in higher frequencies via drop impact that creates a sudden change of momentum at the sea surface.

An intermittent natural underwater sound is introduced by the appearance of rain at

sea [76]. During rain the sound generation mechanism is similar to the sounds from spray and splash. There is a sudden change in momentum when the water droplet hits the sea surface [77] and formation of underwater air bubbles that oscillate afterwards [78]. The sound produced by rain has been found to be dependent on the rain rate but also the wind speed [71]. The adapted spectras presented by Ma [71] are shown in Figure 5. In case of heavy rains Ma noted the sound having a white noise like spectra in frequency range between 0.5 kHz and 20 kHz. When the rain is light and the raindrops are small in size 0.8 mm - 1.2 mm Ma noted a spectral peak between frequencies 13 - 25 kHz. In the Baltic Sea region the precipitation usually amounts to 20 - 100 mm/month and heavy rains with rates greater than 10 mm/h are not very common.

Besides rain there have been measurements of sound produced by hail and snow. While the hail noise can be relatively loud its occurrence is rare in comparison to rain. The spectra of the noise produced by hail has a broad peak in the region of 2 - 5 kHz [72]. In the Baltic Sea during winter months snowfall can be more frequent than rain. The noise produced by snow is reported to be quieter and at different frequencies than by rain. The noise from snowfall was reported to be important at ultrasonic frequencies above 20 kHz [72] or 40 kHz [79].

As introduced in the subsection 3.3 of the thesis and shown in Fig. 4, during winter months ice forms over parts of the Baltic Sea. The appearance of ice is expected to significantly alter and contribute to the soundscapes in its vicinity [80]. During some periods the under ice sound level can be significantly below the levels measured in sea state zero conditions in a similar ice free region [81]. Rapid decreases in temperature are known to cause thermal stress in the ice sheets leading to formation of cracks and resulting in impulsive slip-stick sounds [82]. The peak energy of the cracking sounds by ice are generally below 100 Hz [83]. The edges of formed ice are also known to be zones louder than their surrounding and the noise is generated by interaction between the ice-edge and surface waves [84].

In water with instantaneous increases in the horizontal turbulent velocity an excess of shear stresses drive the sediment transport near the sea bottom which also generates sound [85]. The sediment transport (gravel, clay or fine sand) creates sound as result of the interparticle collisions [86]. The sound levels are dependent on the sediment type and the friction velocity near the sea bottom. According to Basset the sound from the sediment transport can be detectable between frequencies 1 kHz to 30 kHz and rises significantly in frequency range 4 kHz - 30 kHz [87].

Lightning strikes are very rare but powerful events that can also create briefly lasting loud underwater sounds [88]. An example of the loudness is the detection of a lightning strike sound 46 km from the lightning in shallow 20 m water [89]. Upon occurrence the lightning over the sea surface can generate impulsive sound in the range 10 Hz - 250 Hz with the duration of a thunder signal related to one lightning strike can vary from 20 s to 60 s [90]. A good overview of relatively recent 9 year lightning data analysis in the Baltic Sea area can be found in the following article [91].

Another important naturally existing part of the underwater soundscape is often contributed by marine animals. A long known and loud example in warm coastal waters is the biological noise produced by the snapping shrimp [92]. Another notable group of marine animals who can intermittently dominate a soundscape in large sea areas are the whales [93]. The contribution by biological sound sources to the Baltic Sea long-term sound levels is expected to be mostly negligible. Which doesn't mean that the Baltic Sea lacks soniferous animals. Among the Baltic Sea soniferous animals are marine mammals: the harbour porpoise, harbour -, ringed -, and grey seal. The harbour porpoise creates echolocation

signals that are ultrasonic clicks within frequencies 110 - 150 kHz [94]. Distribution of the harbour porpoises was studied in a project Static Acoustic Monitoring of the Baltic Sea Harbour Porpoise (SAMBAH). The monthly probabilities of detecting porpoise clicks as a function of spatially-referenced covariates and time are published in the following article [95]. The harbour seals produce various vocalisations that lie between frequencies 25 Hz - 4.0 kHz [96]. Ringed seals produce vocalisation broadly in frequency range of 50 Hz - 2.5 kHz [97] and grey seals 100 Hz - 3.0 kHz [98]. Overview about the population distribution of the three Baltic Sea seal species can be found in the following report [99]. Beside the marine mammals some fish species are known to produce sound. Among them are Baltic Sea species like the atlantic cod and atlantic herring. The cod makes grunts in frequencies 95 Hz - 1 kHz [100]. The herring creates sound by releasing gas from the anal opening that is observed when the fish is scared or during ascent and descent [101]. A herring in a school can make brief sounds with a spectrum that has a peak around 2 kHz [102]. The peak rolls off gently toward higher frequencies and declines sharply toward lower frequencies [102].

4.2 Anthropogenic sound sources

The most widespread preponderant anthropogenic underwater sound in the seas and oceans is created as an unintended by-product of maritime shipping [14]. The sound from vessels can be generated by different mechanisms that Urick has divided into machinery noise, propeller noise and hydrodynamic noise [54]. The machinery noise originates from inside the vessel by the mechanical vibration of its various parts. For example vibration can be caused by some unbalanced rotation or the reciprocating engines. This vibration can be coupled to the sea via the hull of the vessel. In contrast, the propeller noise originates mostly from the outside of the vessel - from the rotation of propellers. Principally the propeller noise is due to the cavitation induced by the propeller but it is also the noise caused by the vibration of the propeller's shaft. The hydrodynamic or flow noise comes from the irregular and fluctuating flow of fluid past the moving vessel. These mentioned mechanisms all have the ability to vary differently with the ship's speed [103].

The removal of material from the sea bottom *i.e.* dredging creates unintended underwater noise. There are different techniques used for dredging and the dredgers fall in two broad categories - hydraulic or mechanical dredgers. The hydraulic dredgers work by sucking a mixture of dredged material along with water from the bottom. In case of mechanical dredges the material is scooped from the bottom [104]. Beside the sound created by the dredgers, additional sound is created by tugs and workboats assisting the operations. Altogether the sounds from a dredging operation depend on the type of dredger used, the substrate type being removed, geomorphology of the site, hydrodynamic conditions, equipment maintenance status, and skill of the dredger operator [105]. The sound emissions by dredgers have been measured to be loudest in lower frequencies < 1 kHz [106]. Dredging operation by a backhoe dredger was monitored in Estonian waters 2018 for the construction of the Balticconnector gas pipeline in the bay of Lahepera.

The first offshore wind farm was built in the Baltic Sea already in the beginning of 1990s [107]. As setting up wind farms offshore offers some significant advantages and with declining cost of building their construction has been ever expanding with several developments planned in Estonian coastal waters. An overview of Baltic Sea offshore wind farms and the planned developments can be found in [108]. Offshore wind farms create sounds during construction, operation and decommissioning stages of their life cycle. While the construction phase is usually the loudest especially when pile driving, the operation can also create continuous low-intensity underwater noise [109]. A measurement of three types of offshore wind turbines have shown that sound was above the natural ambient at

frequencies below 500 Hz and this only in the close proximity (14 and 20 m) from the turbines [110]. The noise from wind farms can be recognised by the tonal components caused by the rotating machinery [111]. Besides offshore wind farms there are some offshore oil developments near the coast of Poland [108] and Kaliningrad Region of the Russian Federation (Kravtsovskoye oil field). Offshore drilling can also produce nearly continuous noise at moderate source levels [112].

Impulsive noise events in the Baltic Sea are collected into a central impulsive noise events registry [113]. From there one can find the reported use of impact pile driving, active sonars, acoustic deterrent devices, airgun arrays and explosions. According to the registry the most numerous impulsive sound source is the explosions. Often the Baltic Sea explosions are related to clearance of unexploded ordnances. During the world wars ∼175 000 mines were laid in the Baltic Sea of which 10 - 30 % are estimated to remain in the sea [114]. The clearance of these mines is ongoing and each year a number of controlled explosions are carried out. Besides the ordnance clearance the explosions can be related to military ship hull integrity trials, blasting rock beds during construction, decommissioning offshore wind turbines, and deterrence of wildlife (seal bombs). The spectral and amplitude characteristics of explosions vary with the weight of the charge and the depth of the detonation [14]. The dominant parts of the sound energy by ordnance clearance explosion shock wave are expected to be contained in low frequencies < 1 kHz [115].

In areas of their use the acoustic deterrent devices can create intentional anthropogenic underwater noise in order to deter animals from approaching a specific area that can be for example a location of an aquaculture site or a pile driving operation. Near aquaculture sites they are used with the aim of mitigating pinniped depredation through the emission of loud and pervasive noise. With the expanding aquaculture the use of these devices has multiplied [116] and they have been used also widely in the Baltic Sea [117]. The majority of the deterrent devices produce sounds in the range 2-40 kHz [116].

Active sonars transmit underwater sound signals as an integral part of their operation fur using the signals' reflections times. Active sonars are widely used and can include bathymetric echo sounders for water depth measurement (30 - 400 kHz), fish finders for locating schools of fish (12 - 200 kHz), sub-bottom profilers for mapping layers of sediment or rock under the seafloor (2 - 13 kHz), sidescan sonars for seabed imaging (≈100 kHz), and multibeam echosounders for seafloor mapping [63]. The naval active sonars can be conventionally divided into low- (< 1 kHz), mid- (1-10 kHz), and high-frequency (> 10 kHz) systems [118]. According to Lurton the naval sonars are among the most powerful anthropogenic sound sources at sea. Different military search sonars and their characteristics are listed in [63, 14]. According to Ainslie [63] for at least one mine hunting sonar (TSM 2022) transmits in search mode signals in frequency 165 kHz.

In seismic exploration of the seabed for offshore oil and gas the reflections of artificially induced shock waves that penetrate the deeper seabed layers have been widely used. The shock wave is generated by airguns that rapidly release compressed air from an airgun cylinder. Although the airguns are designed to produce most energy below 100 Hz (or 250 Hz [119]), the resulting oscillating air bubble pulses act as a source of loud, broadband, and impulsive sound that can contain substantial energy up to 10 kHz [120].

In marine construction piles are driven into seabed, in order to provide foundation support for docks, bridges, wind turbines, and offshore oil and gas platforms. There are two main types of techniques used for pile driving: impact- and vibratory pile driving. In impact pile driving a heavy weight is lifted and dropped on top of a pile for driving it into the seabed generating loud impulsive sounds at low frequencies. The predominant energy from pile driving is at frequencies ranging from 100-500 Hz [121] (50 Hz to 1 kHz [122]). In

vibratory pile driving there are a series of oscillating weights that continuously transfer vertical vibrations into the pile at a specific frequency. The dominant spectral features of radiated underwater sound in vibratory pile driving is related to the frequency of the driving hammer that is typically 15 - 35 Hz, producing spectral lines at intervals of this frequency [123]. Altogether, the sound from pile driving is dependent on various factors that include the method of pile driving, pile material, diameter of the pile, and the seabed substrate.

Anthropogenic underwater sound is also created by underwater wireless acoustic communications devices for remote vehicle command and control, diver communications, underwater monitoring and data logging, trawl net monitoring and other applications [14]. Human recreational activities can be important factors in some coastal areas like the recreational small boats and jet skis [124]. Also loud sources far above the water can radiate sound underwater. One of the loud sources can be an airplane [125]. When an airport is close to water planes have been measured significantly contributing to the underwater soundscapes in vicinity [126]. The largest airport in the Baltic Sea region close to water is the Copenhagen airport.

4.3 Ship traffic density

The distance to the shipping lanes, the intensity of traffic on the lane, and the ship type along with the environmental conditions affect the low frequency anthropogenic sound levels in a given location. The ship traffic data is available from the automatic identification system (AIS). The AIS data for the BIAS project was provided by Baltic Marine Environment Protection Commission - Helsinki Commission (HELCOM).
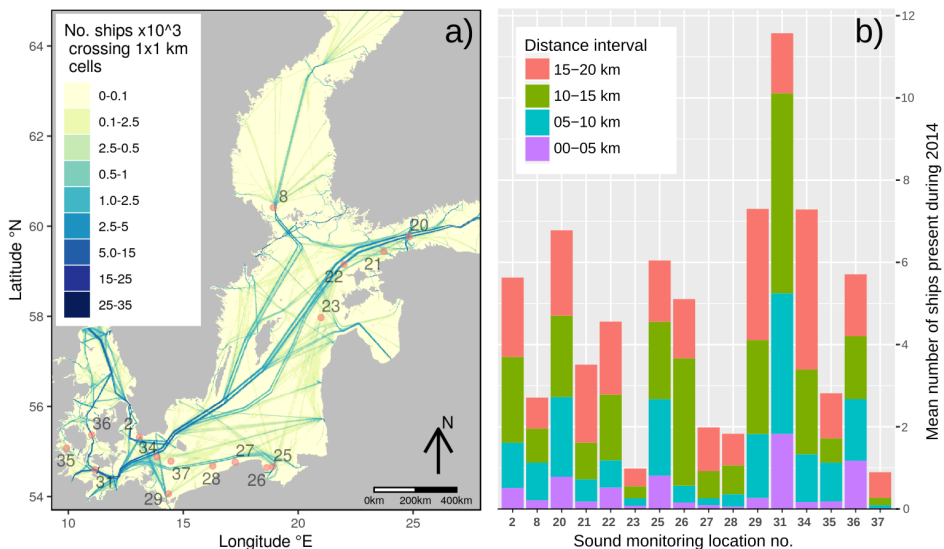

Figure 6: *a)* Ship density (number of ships crossing a 1x1 km grid cell) during 2014 in the Baltic Sea. The data originated from HELCOM. *b)* Average ship traffic intensity at different distance intervals within 20 km maximum range from the monitoring locations in 2014. The intensity calculation is based on 20 second time-regularised ship location data from the automatic identification system (AIS). The mean number of ships corresponds to the most likely number of ships within a distance interval at a randomly selected time during 2014. The figure *b)* is modified from [Publication IV].

Figure 6-a shows the mapped selected BIAS sound monitoring locations on top of the density of ships map in the Baltic Sea. The density colors represent the number of ships times 1000 crossing a 1x1 km grid cell during the whole year of 2014. The maximum number crossings amount to 35 000 in the busiest locations. The ship density map in Fig 6-a draws out clearly the areas with the busiest shipping lanes in the Baltic Sea and the selected BIAS monitoring locations in relation to the shipping lanes.

For a better comparison of the ship traffic intensities around the sound monitoring locations the AIS data was normalised for distances from the monitoring location and time regularised. The time regularisation of the AIS data was necessary as the intervals for the systems location reporting are irregular in time. AIS data reporting frequency is dependent on the rate of turn and speed of the ships as well as the class of AIS transceivers. The time regularised AIS ship distances were normalised to give the mean number of ships most likely to be present at any time during 2014. Figure 6-b shows the differences in the mean number of ships near monitoring locations and originally printed in [Publication IV]. Locations 37 (Rønne Banke) and 23 (Saaremaa) stand out as having the lowest shipping intensities in the radius of 20 km where on average only one vessel was present. Figure 6-b also shows that in location 37 most of the ships occured in the distance interval 15-20 km. In contrast, location 31 (Fehmarn Belt), was exposed to the most intensive shipping. In this location, on average two vessels were on average present at any given time within 5 km and more than eleven vessels within 20 km.

It has to be noted that using only AIS for determining the abundance of shipping in a sea area can have some problems. For example in areas with considerable amounts of recreational vessels not using the AIS transmitters the ship traffic intensity can be severely underreported [127]. An attempt of mapping the intensity of leisure boat activities in the Baltic Sea with the aim of approximating their emissions has been realised in the following preprint [128]. Besides, the AIS data can be erroneous as some users are known to intentionally broadcast errors or falsify the information sent by their AIS tranceivers [129].

5 The BIAS monitoring results

The year-long sound level monitoring of the BIAS project has been the most complete attempt to measure the Baltic Sea soundscapes. Therefore, an effort was made to analyse the annual SPL values along with the gathered shipping intensities and the wind speeds. This analysis and information presented in this section of the thesis was put out in [Publication IV]. The temporal and spatial variability in the sound pressure level is expected to be larger in the shallow Baltic Sea than in the deep water [54]. Also the contribution by the higher frequencies should be proportionally more important than in the deep water. The latter is explained by the cut-off phenomena reducing sound propagation in the lower frequencies [54, 130]. The statistical analysis from [Publication IV] presented in this thesis section was performed using bespoke software written in the programming language R [131].

5.1 Spatial variability of measured sound

The spatial variability analysis of ambient noise is based on the 2014 year long sound monitoring in the selected BIAS sound monitoring locations highlighted in Fig. 1 with coordinates listed in Table 1. As discussed in the section 4 of the thesis the underwater ambient sound in the Baltic Sea is expected to be a mixture of the natural sounds, mostly caused by wind driven sea surface agitation, and the anthropogenic sounds, mostly produced by commercial ship traffic. Therefore, one of the drivers of the spatial variability arises from the spatial variability of these dominant sound sources. The spatial variability of the ship traffic intensity is shown in Fig. 6-a while the wave heights and wind speeds in the selected monitoring locations are shown in Figures 4-a and 4-b. Another major factor affecting the spatial variability is the regional differences in sound propagation conditions. The sound propagation can vary due to geographical differences in water column properties (Fig. 3), bathymetry (Fig. 2-b) and seabed substrates (Fig. 2-a).

The annual underwater SPL values in different locations are concisely presentable by the estimated probability density function (PDF). A good way to compare different PDFs of the one-third octave band SPL values is to compile them in the form of violin plots. As common for PDFs, the area of each violin plot equals unity. The abscissa of the plots shows the probability for the occurrence of the SPL value displayed on the vertical axis. Various statistical measures are added to the violin plots for making them visually comparable and readable. The added statistical measures are the geometric mean (GM) and exceedance levels L5, L10, L25, L50, L75, L90, and L95. In the case of sound monitoring, exceedance level L95 is a low SPL value that is exceeded 95% of the time and therefore can be related to the infrequent quieter natural sound levels. The exceedance level L5 is the SPL value that is exceeded only 5% of the time. In most cases it is related to occasional louder events when vessels pass close by the monitoring location. Similarities of the annual sound pressure level PDFs by regions have been presented previously in a study about the level in UK waters [53]. This study presented the 125 Hz one-third octave band PDFs of shorter deployments from ten monitoring locations in the North Sea.

Resulting violin plots presenting the annual SPLs in 16 BIAS sound monitoring locations are shown in Figs. 7 to 9 which were taken from [Publication IV]. The long and thin upper tails of the PDFs in Figs. 7 to 9 represent the rarely occurring louder events that in most cases are close passages of vessels. The differences in the upper ends of the tails indicate that the recorded sound was indeed not subject to significant clipping. The lower tails of the violin plots are bounded by the limit imposed by the self-noise level of the SM2M recorder standard hydrophone with no gain. The self-noise levels are listed in Table 5
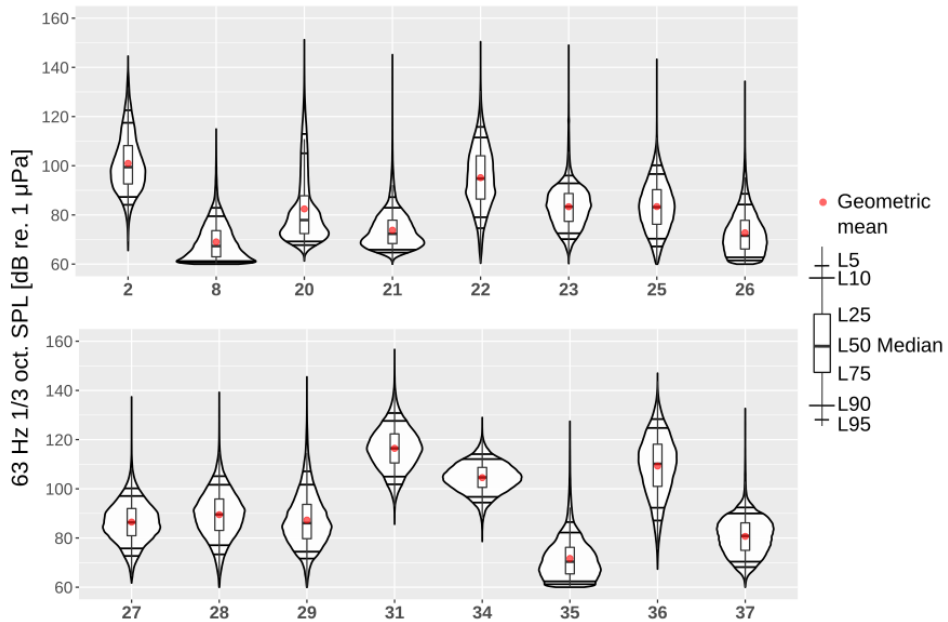
Figure 7: The estimated probability density functions in the form of violin plots of the measured annual SPLs in sixteen different locations in the 63 Hz one-third octave band for the year 2014. The horizontal black lines represent L95, L90, L10, L5; the red dot marks the geometric mean (GM); the upper and the lower lines of the boxplot mark L25, L75; the thicker black line in the middle of the boxplot marks the median of the data. This figure is taken from [Publication IV].

found in appendix B.1. In monitoring locations 8, 26 and 35, there might have occurred relatively low SPL values, often well below the self-noise level. Examples of time series of the SPLs where the noise floor is reached are shown in Figure 11. In order to avoid hitting the noise floor equipment with lower self-noise should be used. It is important to note that while the geometric mean values are affected by occurrence of self-noise, the median or exceedance levels L5, L10, L25 remain unaffected. When the effect of the self-noise level on the violin plots is acknowledged, they are still very useful for interpreting the soundscape at a specific location.

Figures 7 to 9 show the annual estimated PDFs as the violin plots for the selected monitoring locations and frequency bands taken from [Publication IV]. Figures 7, 8 exhibit the 63 Hz and 125 Hz one-third octave band SPL being highly dependent on the sound monitoring location. As noted in [Publication IV] the difference between the median SPL values of the quietest location, no. 8 (Sea of Åland) and the loudest location, no. 31 (Fehmarn Belt), is around 50 dB for the 63 Hz one-third octave band and 40 dB for the 125 Hz one-third octave band. This observation confirms the prediction made by Urick [54] about the expected large spatial variability of the low frequency sound levels in the shallow seas. Figure 9 from [Publication IV] shows that within the higher 2 kHz one-third octave band the spatial variability in SPL is much lower. As stated in [Publication IV] median SPL is 15 dB lower in 26 (Puck Bay) from the highest annual median SPL in location 31 (Fehmarn Belt). At this higher frequency band, the sea surface agitation should be more dominant than the shipping noise. In spite of the apparent variability, some similarities in the PDFs can be found, mostly by regions and by similar conditions:
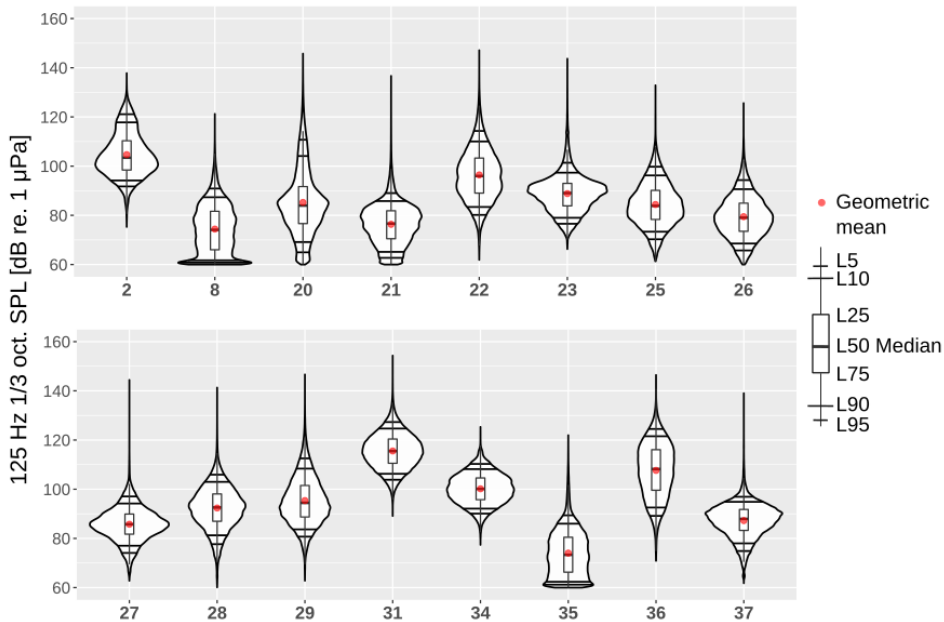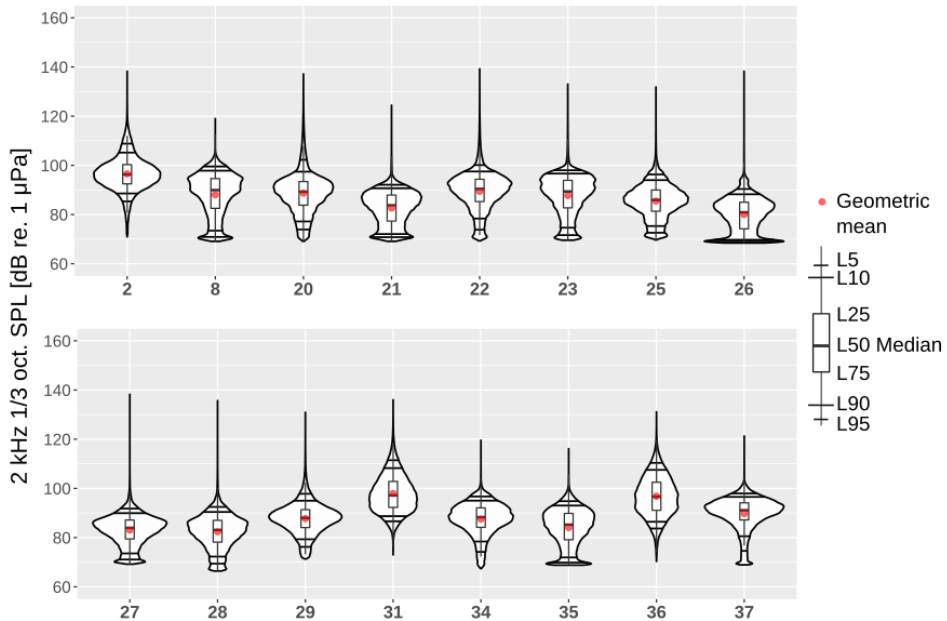
Figure 8: The annual estimated probability density functions of the SPL measured in sixteen different locations in the 125 Hz one-third octave band during the year 2014. This figure was originally printed in [Publication IV].

1. As said in [Publication IV] the highest annual SPL values in all the one-third octave bands were recorded in the Great Belt and Fehmarn Belt (locations 31, 36). Figure 6-b shows that these locations had also the highest shipping intensities within the dist. interval < 5 km among the monitoring locations. Both locations have frequent close-by ferry traffic and numerous cargo ships, tankers, including the largest ships, on route into the Baltic Proper. Seasonally, there are also a high number of sailing and leisure boats.

2. Among the quieter locations are 26, 35 as noted in [Publication IV]. Figure 4-a shows that locations 26 and 35 have the lowest significant wave height among the monitoring locations. Location 26 is in Bay of Puck that is separated from the open sea by the Hel Peninsula and 35 is in a winding Danish strait the Little Belt. The locations have similar water depths and distances to land as listed in Table 2. Although the annual 63 Hz and 2 kHz one-third octave band SPL values from these locations have relatively similar PDFs, they differ considerably in the 125 Hz one-third octave band.

3. Within the two lower frequency bands the quietest location was 8 (Sea of Åland) [Publication IV]. This location is not in sheltered waters or with the lowest intensity of shipping. Its lowest levels can partly be explained by the different data coverage as the recordings are not available during the first four months of the year. As seen from an annual time series in Fig. 19 these months can be the loudest. Although location 8 was the quietest even when comparing the median SPL of the locations on a monthly basis.

4. As revealed in [Publication IV] the annual sound levels in the Gulf of Finland loca-

Figure 9: The annual estimated probability density functions of the SPL measured in sixteen different locations in the 2 kHz one-third octave band during the year 2014. This figure was originally printed in [Publication IV].

tions 20 and 21 are similar according to the PDFs. Figure 4-a shows that due to being protected from the South-Westward winds the significant wave heights are lower in these locations when compared to the Baltic Proper locations 22 and 23. Therefore, it is anticipated that the natural ambient SPL values are lower in locations 20 and 21 than in the Baltic Proper. Figure 4-b shows that the annual mean wind speed is lower in location 21 from location 20. The ship traffic intensity is higher in location 20, which is situated near busy shipping lanes (Fig. 6). All this leads to the annual SPL values at location 20 being expectedly higher at all frequency bands when compared to location 21.

5. The levels and their PDFs recorded in locations 37 and 23 are very similar [Publication IV]. As shown in Fig. 6-b the overall ship traffic was lowest in these locations. Therefore, the recorded sound may be considered mostly natural. The modeled wind speed in these locations was almost the same (Fig. 4-b). Although, the sea depth (88 m in loc. 23 and 15 m in loc 37) and significant wave heights are considerably different (Fig. 4-a).

6. The recorded levels in locations 25, 27, 28 and 29 at the coast of Poland are quite similar as seen from their PDFs from [Publication IV]. Differences in the levels follow loosely the shipping intensities, wind speeds and sea depths. Locations 27 and 28 have both very low shipping intensities. In location 28 the higher annual mean wind speed and deeper water probably leads to the higher SPL values. While the location 27 is closest to land (Tab. 2) being most exposed to surf noise its levels are still lower. When comparing location 29 with the other Polish locations, the shipping intensity is considerably higher, which leads to higher SPL levels in the 125 Hz and 2 kHz one-

third octave bands. The very shallow depth of this location (12 meters) has probably constrained the higher SPL values due to the cut-off effect.
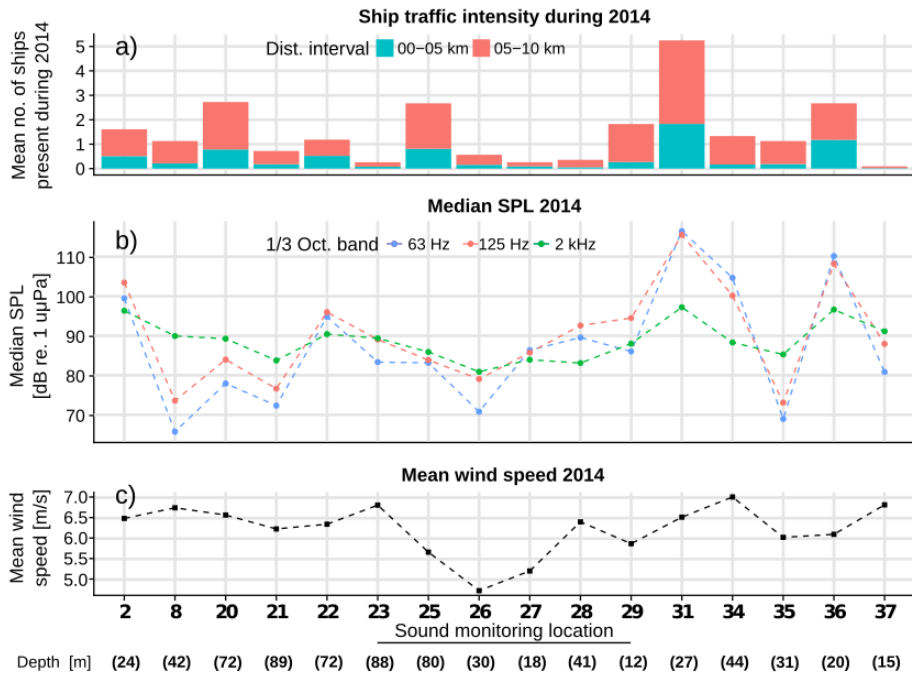

Figure 10: **a)** The annual mean values of the ship traffic intensity around the monitoring locations. **b)** Annual median one-third octave band SPL values at all monitoring locations. **c)** Mean wind speeds and the water depths. The dashed lines in both **a)** and **b)** joining the points are to be considered as aids for visualising the data and not as indicating the intermediate values between the locations. The wind speed data originates from the SMHI open-access data from the MESAN weather analysis model. This figure with mean wind speeds in knots printed in [Publication IV].

For a better overview of all the relevant collected data Fig. 10 presents the annual median SPLs for all one-third octave bands together with the sea depths, annually averaged shipping intensities and mean wind speeds. Figure 10 was published in [Publication IV] with wind speeds in knots instead of meters per second. Comparison of the graphs in Fig. 10 shows the following results published in [Publication IV]:

- The annual median SPL values of 63 Hz and 125 Hz one-third octave bands have strong correlation. The 125 Hz one-third octave band annual median SPL values in monitoring locations are on average 3 dB higher.

- The 2 kHz one-third octave band annual median SPL values correlate weakly with the lower frequency octave bands.

- As expected, the two lower frequency band median SPL values seem to be more affected by the ship traffic intensity than is the 2 kHz one-third octave band.

- The median 2 kHz one-third octave band values in locations with very intense traffic are higher. Otherwise, some dependence on mean wind speeds can be noted.

5.2 The effects of ice cover

In the Baltic Sea the occurrence of ice causes spatial and temporal variability of its soundscapes. As discussed in subsection 3.3 ice forms only in certain areas of the sea and has its maximum extent between March and February. The extent of ice during a moderate winter of 2014 is exemplified with the ice-chart in Figure 4-c. The noise created by ice is discussed in the subsection 4.1 of the thesis. The change in the sound levels due to ice cover was recorded in the middle of the Bay of Bothnia BIAS sound monitoring location 11 during the winter of 2016. This location is mapped in Fig. 1 showing all the BIAS sound monitoring locations and in the ice chart in Figure 4-c. The ice cover data originated from the Finnish meteorological Institute and was provided for the [Publication IV] along with the sound monitoring data by Jukka Pajala.
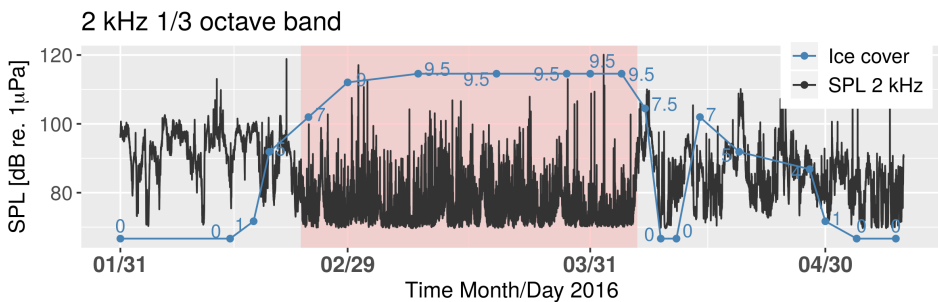
Figure 11: The effect of ice on the measured 2 kHz one-third octave band SPL in the Bothnian Bay BIAS sound monitoring location 11. The ice concentration is a fraction that expresses the sea surface ice cover in one-tenths (1/10). The complete coverage by ice corresponds to 10/10. This figure was taken from [Publication IV].

Figure 11 from [Publication IV] shows that prior to the formation of ice the SPL varied in a way expected from natural wind driven sounds. During this time only a few possible passes of individual ships can be seen. The formation of ice cover highlighted with a pink background in Fig. 11 seems to lower the 2 kHz one-third octave band SPL. This decrease was estimated in [Publication IV] to be around 10 dB. Although the true decrease might be even larger as the recorders self-noise level restrict measuring the SPL lower than 70 dB within 2 kHz one-third octave band (Tab. 5 in Appendix B.1). During ice cover a wide selection of ice dynamics driven impulsive sounds are apparent in Figure 11. As can be seen in Fig. 6 the ship traffic intensity in the Bay of Bothnia is relatively low. It was claimed that the recordings made during the ice cover contained the sounds of some ships breaking through ice. The lower bound of the values show some short period increases that might be connected to higher wind speeds.

5.3 Temporal variability in ambient noise

The ambient noise levels in the Baltic Sea are known to be periodic at different time scales. Firstly the diel changes were investigated and the preliminary analysis of the data for [Publication IV] showed significant variations in SPL values within this time scale. In locations with more intense ship traffic these variations coincided with the diel changes in the number of ships present around a monitoring location. This is understandable as the ferry boats have daily schedules and fishing/leisure/sailing boats have their daily routines. Therefore, the anthropogenic component of the soundscape should also have a diel pattern. Otherwise the vertical migration of marine organisms has been found to be related

to the diel variation in SPL in the southern Baltic Sea [132].

The seasonal variability of the recorded sound can mostly be related to the periodic variations in the sound speed profile of the water column. The upper layers of the water column get warmer during summer months. As a result, the sound waves refract down towards the bottom, causing faster loss of the propagating acoustic energy [133]. Besides, the sea surface agitation in the Baltic Sea is also known to have seasonal changes. The wind speeds and wave heights are both higher during the winter according to [58] and the SMHI data. The analysis of the AIS data for [Publication IV] showed that some ship types can also have seasonal occurrence patterns.

In the southern Baltic Sea the seasonal variability in the SPL values has been measured to be in the range of 12 dB [134], or 10-15 dB [132] with greater levels during the winter. The BIAS sound monitoring analysis for [Publication IV] also showed the highest monthly median SPL values during the winter and the lowest in the summer months. In most locations the minimum in the monthly medians for all the one-third octave bands was recorded in July. The month with the highest median varied according to the frequency band. In the 63 Hz and 2 kHz one-third octave bands, the loudest month in most locations was December. As for the 125 Hz one-third octave band, in most locations, the loudest months were either January or February. The difference between the medians of the loudest and the quietest month was on average 10 dB [Publication IV]. In the monitoring locations with intense shipping, the monthly medians changed less throughout the year when compared to other locations. For example, location 31 with most intense shipping had only 2 dB seasonal difference in the 63 Hz, 3 dB in the 125 Hz and 6 dB in the 2 kHz one-third octave bands [Publication IV]. Examples of the seasonal SPL variations in the four Estonian BIAS sound monitoring locations during 2014 can be seen in the time series in Figure 18.

According to monitoring in the North Sea the interannual variability of sound level should be low [53]. The interannual variability was investigated for [Publication IV] in location 20 and 26 where sound monitoring has continued after the end of the BIAS project. The post-BIAS sound monitoring data for the location 26 was provided by Radomił Koza for [Publication IV]. Figure 12 from [Publication IV] presents the comparison of two years of monitored SPLs in these locations. Figure 12 shows clearly that the PDFs of two consecutive annual periods are similar for all three frequency bands. This hints at the yearly averaged soundscape in a given location remaining relatively unchanged despite high seasonal variability. Therefore, when conducting sound monitoring one should cover most of the year to give a representative estimate to the prevailing SPL values in a location. Also, only the yearly SPL values serve as a baseline for locations, against which to compare any measurements in the following years. Comparison of the two years with the Mann-Whitney U test (significant if p-value < 0.05) in [Publication IV] noted the following results:

- In location 20, the 63 Hz one-third octave band had no statistically significant change in the annual SPL values, while in the 125 Hz and 2 kHz one-third octave bands there was a statistically significant increase in the SPL values. The annual median value in the 125 Hz one-third and 2 kHz octave bands was about 1.7 dB higher in the second monitoring period [Publication IV].

- In location 26 for all the one-third octave bands, there was no significant change in the annual SPL values. The difference in the medians between the two monitoring periods was less than 0.25 dB [Publication IV].
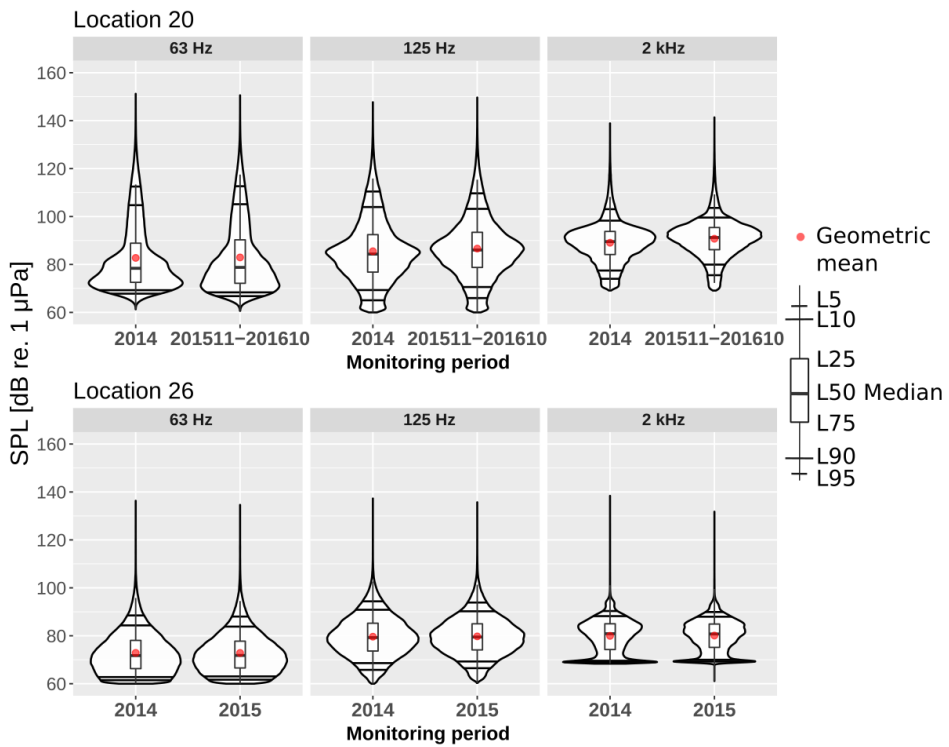
Figure 12: Estimated probability density functions of the measured SPL at three different one-third octave bands for the measurement location 20 (Tallinn, EST) and location 26 (Puck Bay, POL) for two annual monitoring periods. This figure is taken from [Publication IV].

6 Wind-driven sound level estimation

The extensive BIAS sound monitoring analysis presented in section 5 adapted from [Publication IV] showed that the soundscape in a location has both natural and anthropogenic components that often exist simultaneously. As marine life has evolved to live in an acoustic environment without the interference of loud man-made sounds, it is reasonable to assume that the natural sounds are not harmful for marine life. Therefore, the assessment of the anthropogenic component's excess over the underlying natural level is a key task when considering the environmental pressure of man-made underwater sound.

One approach is to construct detectors for finding time periods where anthropogenic sound is present in the monitored data. This approach was presented in [Publication III]. Therefore, the results within subsections 6.1, 6.2 originates from [Publication III]. The other approach investigated was based on the estimation of natural sound level from wind speed. This approach was presented in [Publication V] and the results in subsections 6.3, 6.4 are from [Publication V]. The estimation method is based on fitting the dependence of the lower measured sound levels and the wind speed. The dependence enables the estimation of natural sound levels in case the anthropogenic component exceeds the natural.

6.1 Anthropogenic sound detection

The most widespread anthropogenic sound comes from maritime shipping. Therefore, using AIS data is a straightforward method for detecting the anthropogenic sound. The AIS ship locations can be time regularised and when integrated with the monitored sound data it is possible to estimate the 'audible distance' of passing ships. In this case 'audible distance' means the distance of ships from the monitoring locations at which they are audible in the recordings. This distance allows us to separate the time periods when ships sound should be present in a monitoring location. Although, using AIS has some obvious drawbacks. As discussed in subsection 4.3 some ships do not have AIS transponders and the AIS data can be erroneous. Problems are also posed by the differences in the source levels of ships and the seasonal changes in the underwater sound propagation conditions. If the data analysed is from a single month, the seasonal changes do not affect the results significantly.
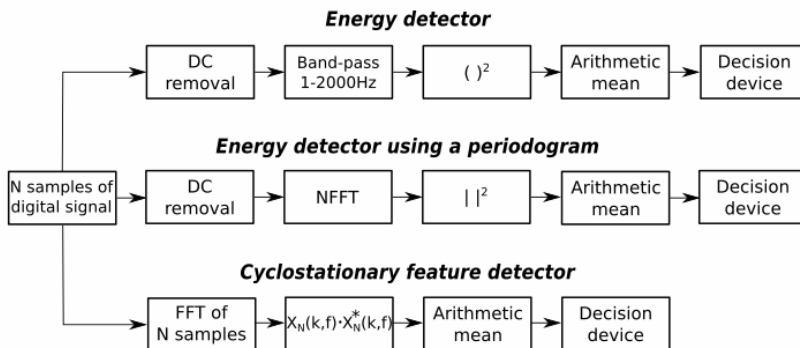

Figure 13: Block diagrams of the three anthropogenic sound detectors. This figure taken from [Publication III].

Besides the AIS data the recorded audio files with anthropogenic noise detectors can

be used. For his master thesis Mihkel Tomingas investigated the energy detector, energy detector using a periodogram, and cyclostationary feature detector for anthropogenic sound detection. The threshold selection process was revised and reimplemented in [Publication III] by the author of this thesis.

The energy detector described in [Publication III] calculates the "energy" value associated with the ADC output values from the audio files over a specified number of samples and frequency range. Figure 13 from [Publication III] shows the block diagram with the main parts of the energy detector algorithm. As first steps the DC bias of a one second length ADC output signal was removed and a band-pass filter for the frequency range 1-2000 Hz was applied. The energy detector using a periodogram differs from the previous by being implemented in the frequency domain. As shown in Fig. 13 following the DC removal, the numerical fast Fourier transform (NFFT) was applied to the 1 second length recorded sound data. The modulus of the N complex numbers produced by NFFT was squared and an "energy" value using a periodogram was received.

The cyclostationary feature detector differs intrinsically from the other implemented detectors in [Publication III]. This detector is based on finding the periodicities in the sound intensity instead of considering just the intensity itself. Ship propeller creates a periodic cavitation that has an acoustic signature characterised by a periodically modulated amplitude [135] and with broadband spectrum [136]. Therefore, the natural wind-driven sounds are expected to be stationary, while the ships produce predominantly cyclostationary sound. Figure 13 shows the implementation of the cyclostationary feature detector consisting of a fast Fourier transform of N samples of the recorded ADC output signal. The N complex values produced by the Fourier transform were multiplied with their complex conjugates as these two steps are equivalent to the calculation of the Fourier transform of the signal's autocorrelation. The arithmetic mean of this result gives the cyclostationarity value for a given time period of the recorded signal.
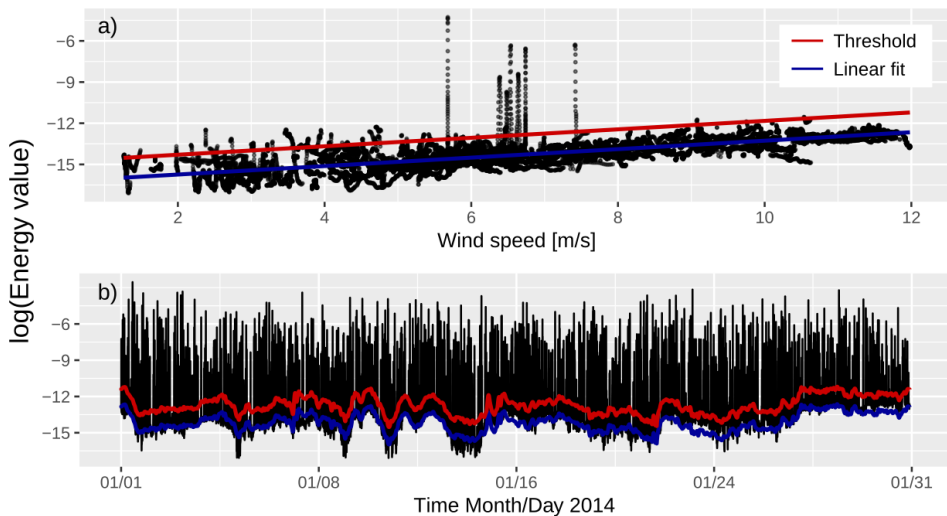
Figure 14: **a)** Wind speed against the logarithm of the calculated energy values, their linear fit and the threshold. Figure is redrawn version of a figure published in [Publication III]. **b)** Time series of the energy values along with the linear fit and threshold. The energy values were found from data where according to AIS there were no ships closer than 7.5 km in location BIAS 20 during January of 2014.

An important part in the implementation of the three detectors in [Publication III] was setting of the threshold values. This was done with the help of the AIS and the SMHI modeled wind speeds. Time periods where according to AIS no ships were in the vicinity of the monitoring locations was used to calculate characteristic values attributable to the natural sound. The least squares method was used to fit a linear relationship between the wind speed and the logarithm of each calculated characteristic. The threshold values for a given wind speed were set as an exceedance of the linearly fitted value by two standard deviations. If the calculated characteristic value exceeds the threshold value, the recorded sound will be marked as anthropogenic. Figure 14-a illustrates the wind dependence of the energy value and the setting of the threshold according to the linear least squares fit of the dependence. The peaks in the middle of Fig. 14-a can be attributed to close passages of ships that did not use AIS. The exceedances of the threshold in lower wind speeds indicate that linear approximation might be not the suitable model for lower sea states. Another interpretation of this exceedance can be related to the increase of the audible distance at the lower sea states. All the energy values shown in Fig. 14-b that exceed the red line are classified as anthropogenic.

6.2 Detector sound categorisation

As discussed in subsection 6.1 and 4.3, the AIS detection has its faults. The detection using only the sound monitoring data can also yield false results due to the errors produced by setting the threshold. Therefore, it seems reasonable to use the ensemble of AIS detection along with the sound detectors. In [Publication III] all of the four detection methods were averaged to produce a binary detection value for every 20 seconds where zero corresponds to not detecting the anthropogenic sound and one to the detection of anthropogenic sound. The four different detection values were combined to give the overall detection score. According to the detection score, the recorded sound was categorised into three different groups in [Publication III]. If the score was none or only one the sound was considered as natural. When the score was at least three the sound was categorised as anthropogenic. The mixed category was assigned when only half of the detectors sense the sound as anthropogenic.

This categorisation is set up to find the certain occurrences of anthropogenic sound. Therefore, it has to be stressed that the natural and mixed categories probably contain the quieter anthropogenic sounds. This is due to the threshold for the anthropogenic noise detection being relatively high compared to the linear fit of the dependence between wind speeds and sound values. Figure 15 adapted from [Publication III] shows the decomposition of the sound pressure level PDFs in the four Estonian sound monitoring locations during January of 2014. The decompositions in Fig. 15 reveals the anthropogenic sound raising the overall sound levels in the four locations in different amounts. The relative sizes of the anthropogenic components correspond to the ship traffic densities in Figures 10-a and 6-b. In location 23 the ship traffic is sparsest and is the densest in location 20. The overall sound levels are categorised the most as natural in location 23 and least in location 20.

Besides providing a visual overview an increase in the SPL values due to the presence of ships can be estimated from the categorisation. For this the difference in the median SPL with and without the anthropogenic component was calculated in [Publication III]. The median SPL values were 1 dB higher with the anthropogenic component in monitoring locations 21 and 23 for both of the analysed one-third octave bands. As noted in [Publication III] the increase in the location 20 was 5 dB for both frequency bands. In location 22, the estimated increase was 5 dB in the 63 Hz and 3 dB in the 125 Hz one-third octave band
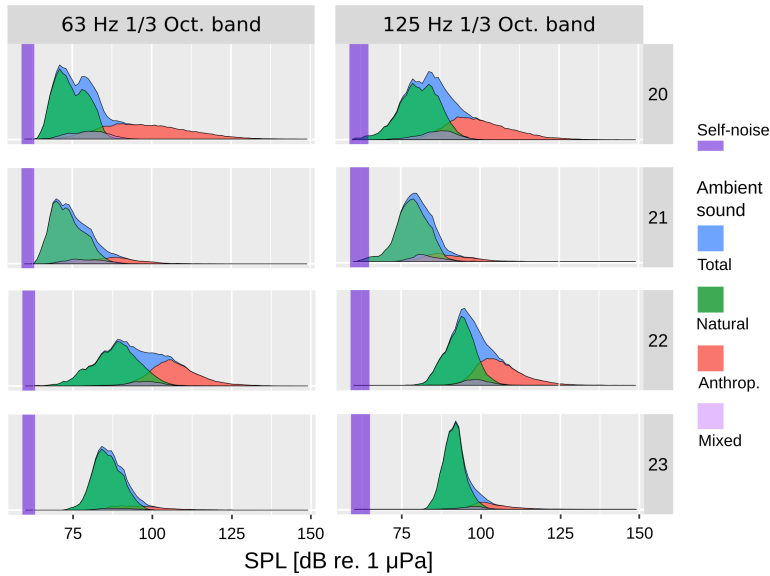
Figure 15: Estimated decompositions of the probability density functions (PDFs) of 2014 January recorded SPL values in four different monitoring locations (20, 21, 22 and 23) for two one-third octave bands (63 Hz and 125 Hz). The overall or total PDFs in the background are depicted with blue color. The overall PDF is decomposed into the anthropogenic, natural and mixed categories. The anthropogenic is colored red, the natural - green and the mixed - light purple. The self noise levels of the SM2M recorders are indicated by the purple color bands. The apparent difference in the decomposed areas indicates the proportions of the different categories. Figure adapted from [Publication III].

[Publication III]. The sound levels of the sound levels categorised as natural in locations 20 and 21 are expectedly similar as they are situated in the same region (Gulf of Finland). The sound levels of the estimated natural component in the Baltic Proper locations 22 and 23 were higher than the Gulf of Finland. This follows the wind speeds and wave heights being higher in the Baltic Proper (Figure 4-a and 4-b).

6.3 Wind-driven sound models

Whereas in the two previous subsections the anthropogenic sound detectors were investigated, this subsection shows the [Publication V] method for estimating the natural sound level from wind speed. As discussed in subsection 4.1 the sea-surface agitation accounts for the most omnipresent and continuous natural underwater sound. Also as stated in subsection 3.3 the wind speed is usually considered a good first order descriptor for the characterisation of the sea-surface agitation. The dependence of the natural sound level on the wind speed is variable across different frequency ranges [11]. Piggott [137] has suggested that in the lower frequency bands, the noise level tends to be a result of a wind independent background and a wind dependent component. According to Piggott, within certain wind speed ranges, the noise level increases linearly with the logarithm of the wind speed:

$$L(f, u) = S_1(f) + 20 n(f) \log_{10}(u),$$
(3)

where L is the ambient sound spectrum level at frequency f, $S_1(f)$ is the sound level at a unit wind speed, $n(f)$ is a fitted coefficient, and u the wind speed at 10 meters above the sea surface [132]. Equation (3) models the wind dependent regime, under the consideration that the wind independent component is exceeded. For modeling low wind speed conditions, Poikonen [8] used a logarithmic model based on three parameters that describe the two regimes of the wind-driven ambient sound:

$$L(f,u) = S_0(f) + 10 \log_{10}\left[1 + \left(\frac{u}{u_c(f)}\right)^{k(f)}\right],$$ (4)

where S_0 is the spectrum level of the wind independent background, u_c is the critical wind speed below which background dominates over the wind dependent component, and k is the wind speed dependence factor. Above some critical wind speed, higher sound attenuation takes place due to the presence of dense bubble clouds and persistent bubble layers [8]. Therefore, there exists a maximum wind speed above which Eq. (4) does not hold. However, such high wind speeds were rare in the Baltic Sea.
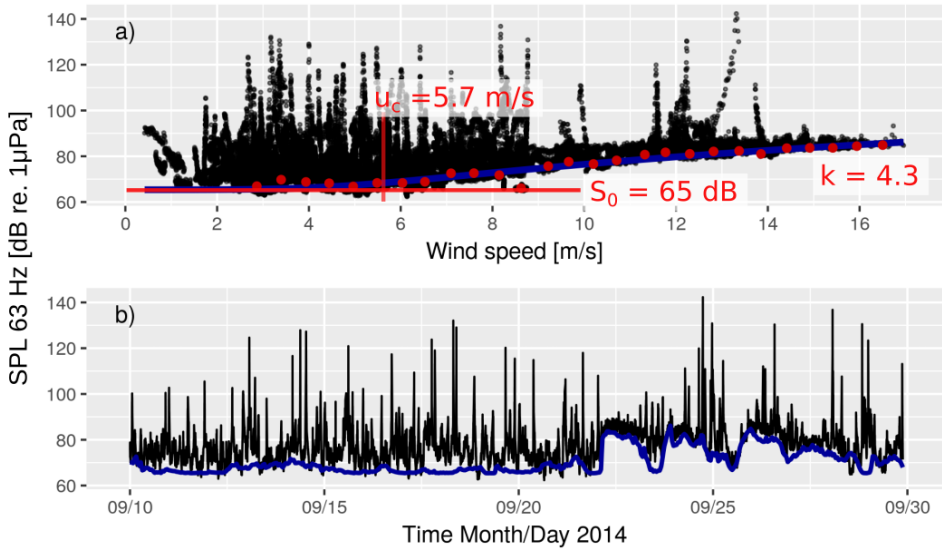
Figure 16: **a)** Black dots mark the recorded SPL values plotted against MESAN wind speeds recorded in sound monitoring location 23 between 10th and 30th of September 2014. The red dots represent 10th percentile values of 0.5 m/s wide wind speed ranges. The blue line shows the model fit with the parameters $S_0 = 65$ dB, $u_c = 5.7m/s$, and $k = 4.3$. **b)** The time series of the 63 Hz one-third octave band SPL in sound monitoring location 23 between 10th and 30th of September 2014. The blue line shows the model predicted wind-driven ambient sound levels. This figure was originally printed in [Publication V].

Finding the wind dependence in a location dominated by sounds from maritime traffic needs some additional considerations. The main assumption proposed in [Publication V] is that between passing ships the ambient sound returns to the natural level. If a relatively stable wind speed dependence exists it can be approximated from the occurrences of these natural sound levels and known wind speeds. For demonstrating the validity of this assumption, Figs. 16-a and 16-b from [Publication V] show 20-day long one-third octave band 63 Hz SPL values recorded in monitoring location 23 between 10th and 30th

of September 2014. The highest narrow peaks visible in these figures correspond to the closest passes of ships. Figure 16-a shows recorded SPL values in 63 Hz one-third octave band plotted against the wind speed. In this plot, a distinct wind-dependence of the lower bound can be observed for wind speeds higher than 6 m/s. The lower bound was first extracted by finding lower percentile values of the recorded SPL within fixed width ranges of wind speed. The uniformly distributed extracted data points are shown in Fig. 16-a by red dots. These data points were found to follow the model given by Eq. (4). Fitting the lower percentile SPL values with the model gave estimates for the parameters S_0, u_c, and k. The resulting fit is shown in Fig. 16-a with a blue line.
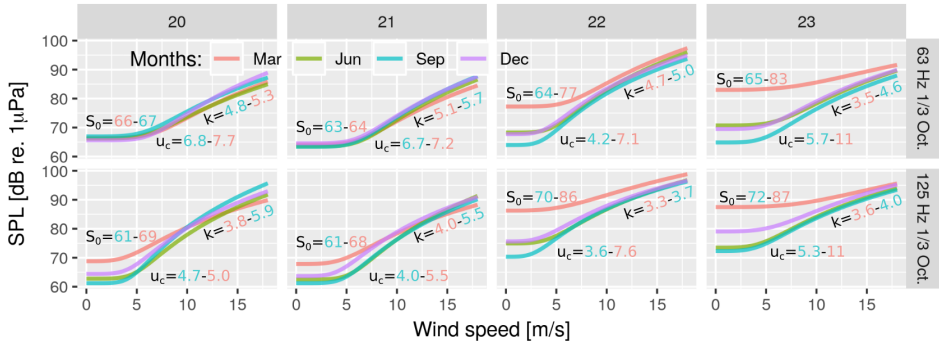
Figure 17: The fitted averaged wind dependencies of the natural ambient sound for four months of the year (March, June, September and December) in the four monitoring locations and two one-third octave bands. The fitted parameter S_0, u_c and k values for the noisiest (March) and the quietest (September) months are listed with red and blue coloured numbers accordingly. Figure is adapted from [Publication V].

The fitted wind dependencies for different seasons, locations and frequency bands are shown in Figure 17 from [Publication V]. It can be seen that seasonal variability in the dependencies is larger in the Baltic Proper locations and in 125 Hz one-third octave band. The fitted parameters vary with seasons the most in location 23. There the parameter S_0, marking the level of the wind independent background, was found to vary in [Publication V] between March and September up to 18 dB. As shown in the [Publication IV] the seasonal variation of the sound pressure levels can exceed 10 dB in the analysed low frequency bands. This variation can be attributed to the seasonal changes in the sound speed profile (see Fig. 3). During the summer months, the rising temperature of the mixed layers causes downward refraction and larger propagation losses. Therefore, the choice of a time window is crucial for the proposed method: time period for fitting has to be long enough to cover a variety of different wind speeds while not too long to minimise the effect of the seasonal changes. For this reason, in [Publication V] three different length rolling time windows (10, 15, 30 days) were used to find statistically significant fits for the parameters throughout the year. The shorter time window of 10 days sufficed for periods with highly variable wind speeds. It has to be noted that in the case of dense ship traffic, the time intervals when the sound level returns to the natural level are scarce. In most cases, if the rolling time window exceeded 30 days, the seasonal changes made fitting more difficult. Besides seasonality, the noise floor of the sound recorder has to be considered. In some locations, from June to November, the ambient sound level was below the self-noise level of the measurement instruments. The self-noise of the SM2M recorder is listed in Table 5 found in appendix B.1.

6.4 Exceedance estimation

The method described in [Publication V] and the previous subsection allows estimating the wind-dependent component of the recorded one-third octave band sound pressure levels. However, as with the anthropogenic sound detectors discussed in [Publication III] and subsection 6.1 it is quite complicated to determine the exact bound between the natural and the anthropogenic sound. After inspection of the recorded data, it was assumed in [Publication V] that when the SPL exceeded the estimated wind dependent levels by 4 dB, they mostly correspond to the anthropogenic sound. This assumption enabled the division of the measured SPL values into the natural and anthropogenic components accordingly. The outcome of the division is demonstrated in Fig. 18 from [Publication V] with an overview of the annual 2014 SPL time series and Fig. 19 adapted from [Publication V] with their PDFs. The time series in Fig. 18 show the different extent of the seasonal changes. Thus, the very low seasonal variations seen from the fitted dependencies in Fig.17 for 63 Hz one-third octave band SPL values are apparent in the Fig. 18 time series for the monitoring locations 20 and 21. Some seasonality is apparent in these locations for the 125 Hz one-third octave band for these locations. This seasonality can hardly be quantified due to the self-noise limit being reached from May until November. The noise floor for each one-third octave band is indicated by transparent horizontal violet bands. In locations 22 and 23, the effect of the seasonal change is clearly visible in both one-third octave bands.
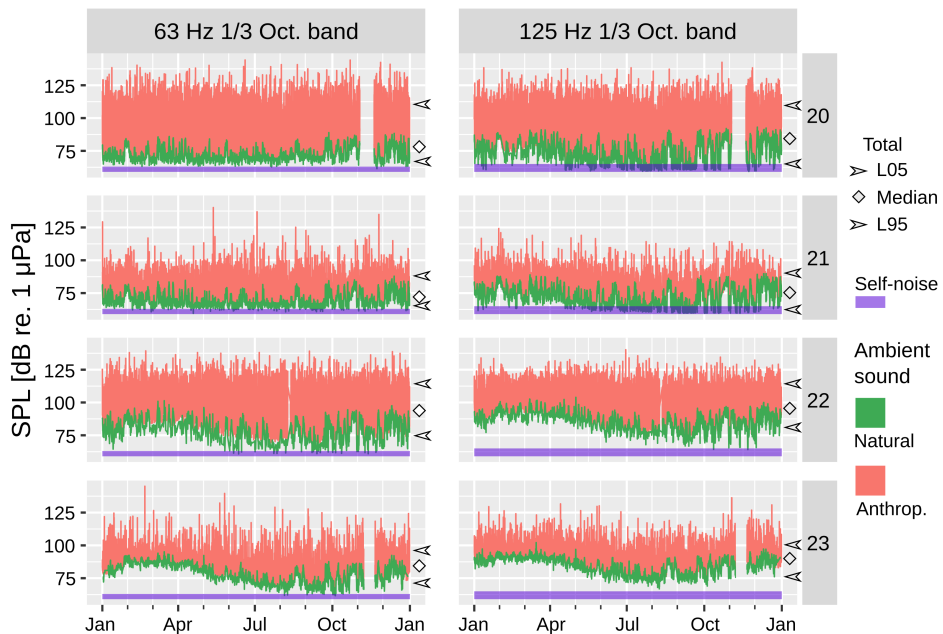
Figure 18: Time series of 2014 recorded 63 Hz and 125 Hz one-third octave bands SPL values in four sound monitoring locations (20, 21, 22 and 23) with estimated decompositions into natural and anthropogenic components. This figure was originally printed in [Publication V].

The PDFs in Fig. 19 demonstrate the prevalence of the measured sound levels by the frequency bands and locations. The total PDFs (blue) are presented with the superimposed wind-driven natural (green) and anthropogenic (red) components. Exceedance lev-
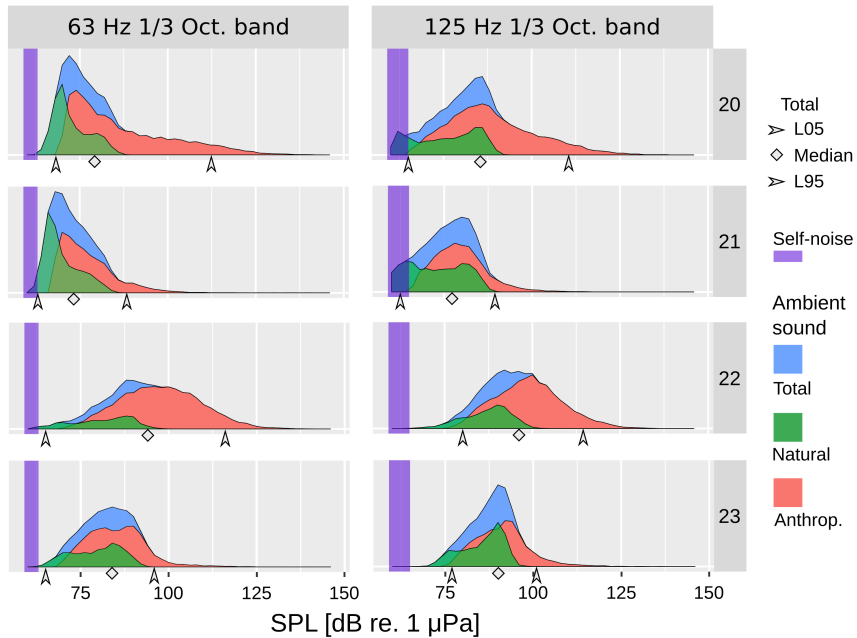
Figure 19: Estimated decompositions the probability density functions (PDFs) of 2014 recorded SPL values in four different monitoring locations (20, 21, 22 and 23) for two one-third octave bands (63 Hz and 125 Hz). Figure redrawn from [Publication V].

els L05, L95, and median (L50) of the total PDFs are shown by arrows and diamond marks accordingly (exceedance levels discussed in subsection 5.1). The depicted categorisation enabled to draw several conclusions published in [Publication V]:

- Gulf of Finland locations 20 and 21.

  – The estimated natural sound levels were relatively similar, being slightly quieter in the more harbored location 21 where annual median wind speeds are also slightly higher (see Fig. 4-b for reference). The estimated anthropogenic component was significantly higher in monitoring location 20 than in location 21. This difference is caused by the proximity of busy shipping lanes in location 20. The differences in shipping intensity are shown in Fig. 6-b, where within the distance of 10 km at any given time, on average two more vessels are present in location 20 than in location 21.

- Baltic Proper locations 22 and 23.

  – In modeling the wind-driven sound is often represented by sources in a layer that is assumed to exist just below the sea surface [138]. Apparently, with the formation of thermocline during the summer period (see Fig. 3), the distant natural ambient sound sources contribute less in low frequency bands, as their generated sound is downward refracted, causing comparatively higher propagation loss. As a result, the seasonal variation of the lower bound values in Figure 18 Baltic Proper locations are clearly visible.

– Compared to the Gulf of Finland locations, the median natural ambient sound levels were found to be around 10 dB higher in the Baltic Proper locations in [Publication V]. The median natural levels in location 23 are only slightly higher. Figure 4-b shows that the yearly median wind speed was lower in location 22 where it was 6.0 m/s and higher in location 23 where it was 6.8 m/s.

– In subsection 5.1 it was noted that soundscapes in geographically close locations have similar annual SPL values. The categorisation of the PDFs also showed that in locations 22 and 23 the proximity can lead to considerable similarities in the PDFs of the natural sound.

– The anthropogenic component was contrastingly different for the Baltic Proper locations. This was expected as location 22 is exposed to widely different shipping intensity compared to location 23, as shown in Fig. 6-b.

Numerical values of the total exceedance levels from Fig. 19 along with estimated natural exceedance levels are listed in Table 4.

Table 4: Estimated natural sound level (Nat) and recorded total (Tot) values with the added excess levels (Ex) in four different monitoring locations for two one-third octave bands. The BSN marks that the value was below the self-noise limit of the SM2M data logger and therefore no reliable comparison can be made. The table taken from [Publication V].

	SPL 63 Hz 1/3 Oct. [dB re. 1μPa]								
Exceedance	L95			L50			L05		
Mon locs\Val	Nat	Tot	Ex	Nat	Tot	Ex	Nat	Tot	Ex
20, Tallinn	66	68	2	68	79	11	79	112	33
21, Paldiski	63	65	2	66	73	7	77	88	11
22, Hiiumaa	65	75	10	75	94	19	88	116	28
23, Saaremaa	65	70	5	76	84	8	87	96	9
	SPL 125 Hz 1/3 Oct. [dB re. 1μPa]								
Exceedance	L95			L50			L05		
Mon locs\Val	Nat	Tot	Ex	Nat	Tot	Ex	Nat	Tot	Ex
20, Tallinn	BSN	65	4	72	85	13	85	110	25
21, Paldiski	BSN			70	77	7	82	89	7
22, Hiiumaa	73	80	7	83	96	13	93	114	21
23, Saaremaa	73	77	4	84	90	6	91	101	10

7 Ship source level, directivity

Better description of ships as sources of underwater noise is a topic that needs to be specified in more detail. More accurate descriptions of sound radiated by individual vessels is important for soundscape modeling and thereafter the pressure estimation posed by noise from marine traffic. Typically in modeling a ship is considered to be a point monopole source. Although a good first approximation, measurements have shown that actual sound radiation patterns of ships are are more complex and their source levels are dependent on the direction of measurement [139].

For the measurement of ship source characteristics in deep water there already exist standardised procedures [140]. The methodology for estimating the ship's source level in shallow water conditions and other information presented in this section is published in [Publication I] and [Publication II]. Estimating the source level from different directions to a ship yields a more precise description of the ships as sources of underwater noise.

7.1 Source level estimation

A hydrophone senses the sound pressure at a sound monitoring location $p(\vec{x})$ from which the sound pressure level in that location $L_p(\vec{x})$ can be calculated (see subsecsion 2.2 and appendix B.2). This measured SPL is also called the received level (RL) and denoted L_p. The underwater sound sources can be characterised by their source levels (SL) and denoted L_S. In case of a hypothetical point source the SL of a sound source in a specified direction is equal to the mean-square sound pressure at a 1 m distance [31]. The L_p is related to source level L_S by the equation:

$$L_p = L_S - N_{PL}, \tag{5}$$

where N_{PL} denotes propagation loss (PL). To be able to assess source level L_S from received level L_p one must know the propagation loss in the larger area around the monitoring location. In the deep water conditions spherical spread of acoustic waves can be considered for the back-calculation and N_{PL} can be expressed as:

$$N_{PL} = 20 \log \frac{r}{r_1}, \tag{6}$$

where r is the distance between the acoustic acoustic centre of the sound source and the hydrophone while $r_1 = 1$ m. In shallow water conditions the influence of the sea bottom characteristics on the sound propagations can not be neglected. Considering the relatively low frequency ranges of the MSFD one-third octave bands, the inhomogeneous medium and preferred one-way propagation direction from the ship to the hydrophone, the parabolic equation method was used for the PL estimation in [Publication I, II]. In particular the implementation of the parabolic equation method named the range-dependent acoustic model (RAM) [141, 142] was used to solve the problem. As input the RAM requires information between the positions of the source (ship) and the receiver (hydrophone) about the bathymetry, sea bottom characteristics and sound speed profile of the water column. The bathymetry around monitoring locations is available from the Baltic Sea Bathymetry Database and is shown in Figure 2-b. An indication about the Baltic Sea bottom characteristics can be found from the EMODnet seabed substrates database shown in Figure 2-a. The sound speed profiles of the water column were available from measurements from which the summer and winter profiles are shown in Figure 3. The relative locations of the ships can be extracted from the AIS data. As a first order approach it was assumed in [Publication I, II] that the acoustic center of the ship is located in their stern at the effective depth derived from the AIS reported draught.
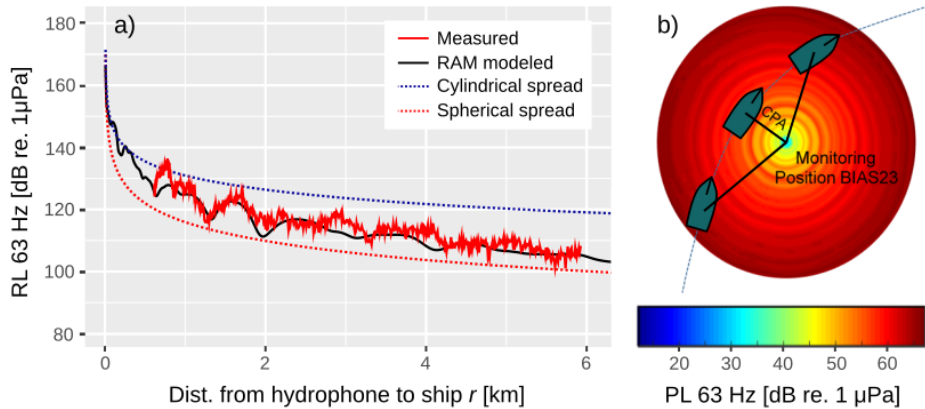
Figure 20: **a)** *The 63 Hz one-third octave band received level (RL) against distance r between the hydrophone (receiver) and the ship (source) in monitoring location 23. The 14 January measured RL for a 152 m long container ship (speed 18.3 kn) is shown with a continuous red line. The red dotted line shows the RL in case of spherical spreading (Eq. (6)) and blue line in case of cylindrical spreading. The RAM modeled RL (when SL is 176 dB) and r dependence for a bottom type sandy mud is shown with a black line. Figure adapted from [Publication I]. **b)** The 63 Hz one-third octave band propagation loss within 20 km radius from the sound monitoring location 23 corresponding to sandy mud bottom and sound speed profile from January showing a halocline in the bottom. Figure adapted from [Publication II].*

The RAM based PL estimation was validated for [Publication I] in the monitoring location 23 where the bathymetry is very flat. As listed in Table 2 the standard deviation in depth within 5 km from this monitoring location is only 2 m. Also, by using the data from the month of January, the sound speed profile is more uniform and does not have a thermocline that forms during summer months (see Fig. 3 for reference). Figure 20-a from [Publication I] shows the validation of the sound propagation modeling in the location 23. The red line in Fig. 20-a represents the RLs from a 152 m long container ship and its dependence on the distance r between the ship and the hydrophone. As seen in Fig. 20-a, during the voyage past the hydrophone the minimal distance or the closest point of approach (CPA) was around 0.7 km. Figure 20-a also shows the recorded RL dependence being roughly in the middle between what would be expected in the cases of the spherical and cylindrical spread models. The measured RL dependence was fitted with the dependence found from the RAM model for seabed with a sandy mud bottom. This also coincides with the EMODnet seabed substrate listed in Table 2. For the 63 Hz one-third octave band the RAM model RL fitted best the monitored RL when the SL of the ship in the modeling was equal to 176 dB. This RAM modeled RL dependence on the r is shown in Fig. 20-a with a continuous black line. The validated PL within a 20 km radius around the monitoring location 23 is shown in Figure 20-b adapted from [Publication II].

7.2 Ship source level directivity

The validated PL around a monitoring location enables to find the source level if ships during their voyages pass by the hydrophone. Knowing the propagation loss N_{PL} around a monitoring location, the received level L_p and the location of sources relative to the receiver the source level L_S can be calculated with equation (5). When a ship passes the hydrophone its SL is being recorded from the various different directions enabling the

possibility of measuring the directivity of the ship's SL. The azimuthal directivity angle γ is measured between the ship's course over ground (COG) and the cartographical azimuth between the hydrophone location and the ship location. Due to low water depth and relatively large distances between the ship and hydrophone, all directivity diagrams from [Publication I, II] neglect the depression angle under the ship. The azimuthal directivity angle γ is demonstrated in Figure 21-a from [Publication I]. During a normal voyage of the ship past the hydrophone when the ship does not change its course significantly, the azimuthal directivity angle γ changes between 0°-180° during a starboard side pass by or 180°-360° during a port side pass by. For minimising the interference by other ships the AIS data was checked for the absence of other ships during the measurements.
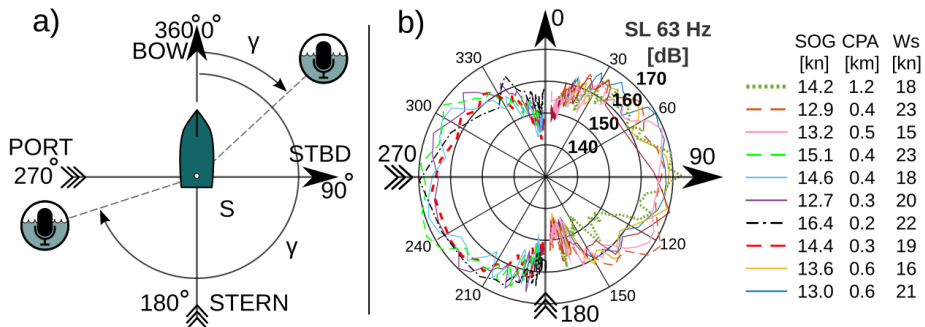
Figure 21: **a)** The azimuthal directivity angle γ measured relative to the ship (S) course and the position of the hydrophone. Figure taken from [Publication I]. **b)** Polar plot of the location 23 measured 63 Hz one-third octave band source level dependence on the azimuthal angle γ for different passes of a 190 m Ro-Ro cargo ship. Each line represents a single voyage of the ship past the hydrophone having different speed over ground (SOG), closest point of approach (CPA) and wind speed (Ws) during the voyage. Figure adapted from [Publication I].

The measured Ro-Ro cargo ship SLs with respect to its azimuthal directivity angles for 10 different voyages past the sound monitoring location 23 are presented in Fig. 21-b from [Publication I] for the 63 Hz one-third octave band. Each line in the Fig. 21-b polar plot represents a single voyage of the ship past the hydrophone. The speed over ground (SOG) of the 190 m length cargo ship varied between 12.7 to 16.4 knots. The measured 63 Hz one-third octave band SL directivity diagrams in Fig. 21-b show no significant dependence on the ship's speed within this range. The minimal distance between the ship and the hydrophone during a voyage is also called the closest point of approach (CPA) and is illustrated in Figure 20-b. During each voyage the wind-driven ambient sound level is indicated by the wind speed (Ws). The measured SL shown in Fig. 21-b from [Publication I] ranged from around 140 to 170 dB.

Figure 22-a from [Publication II] shows the measured 125 Hz one-third octave band SLs of a cargo ship with respect to its azimuthal directivity angles for 11 different voyages past the sound monitoring location 23. Figure 22-b from [Publication II] shows the dependence when averaging over the different passages of the vessel as well as over every 15 degrees of the azimuthal directivity angle. The standard deviation shown Fig. 22-b of the SL's dependence on the azimuthal directivity angle was found in [Publication II] to remain between 3 and 5 dB. Considering the robustness of the estimation method the result is encouraging. The lack of symmetry in the SLs directivity angle dependence can be explained by the bigger average draught for the starboard passes of the ship past the hydrophone. The estimated average effective depth of the ships acoustic center in [Publication II] for
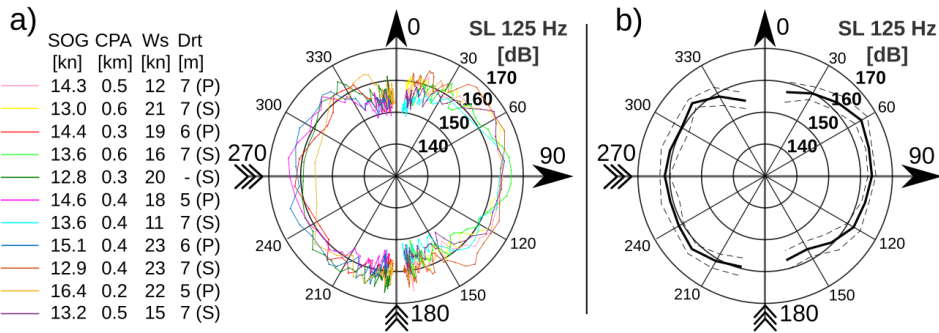
Figure 22: *a)* Polar plot of source level (SL) dependence on the azimuthal angle *γ* measured in location 23 in 63 Hz one-third octave band for different passes of a cargo ship. Each line represents a single voyage of the ship past the hydrophone having different speed over ground (SOG), closest point of approach (CPA), wind speed (Ws) during the voyage and draught (Drt). The S and P within the brackets show whether the ship passed the hydrophone from its port side (P) or starboard side (S). Figure adapted from [Publication II]. *b)* Polar plot showing the averaged 125 Hz one-third octave band source level (SL) dependence on the azimuthal angle *γ* where the averaging is done over the different voyages of the vessel as well as over every 15 degrees. Figure adapted from [Publication II].

the port aspect passes of the ship was 2.4 meters and for the starboard side passes 3.4 meters. RAM modeling in [Publication II] showed that the difference in the PL for two effective depths is around 3 dB explaining the higher SL values for the starboard aspect. Figure 22-b also shows the stern direction SL is about 5 dB higher than for the bow direction. This difference between the stern's and the bow's SL noted in [Publication II] was in agreement with the results reported by other authors [143]. It has to be noted that the estimation of the SL becomes increasingly inaccurate at larger distances between the ship and the hydrophone location corresponding to the bow and stern directions.

Conclusions

The BIAS project sound monitoring has been pioneering in terms of its coordinated cross-bordering effort, longevity and spatial coverage. The Baltic Sea underwater ambient sound was monitored in frames of the BIAS project annually in the year 2014. The collected data offered an opportunity to analyse the measured soundscapes of this shallow brackish sea. Also the gathered data enabled quantify the spatial and temporal variability of the ambient sound. The analysis was restricted to 16 selected BIAS-project monitoring locations. The choice was driven by the annual data coverage and the aim to be representative of the different natural conditions and ship traffic intensities.

1. The annual SPL values from the different monitoring locations show high variability with some clear regional similarities. The difference between the loudest and quietest location was almost 50 dB in 63 Hz one-third octave band [Publication IV]. The locations with the lowest recorded annual median SPL were in calm sheltered waters, while the highest annual median SPL values were in the Danish straits where a lot of vessels are present at any given time. For most of the locations, the recorded SPL had clear relation with prevailing wave/wind weather and shipping intensity.

2. The temporal variability was shown to be highly dependent on the time scale. When monitoring noise at the same locations for two yearly periods, the overall sound levels of the two periods were found to be very similar. This low variability of the annual PDFs indicates that it is a good measure of the baseline SPL values at a given location. The seasonal variations of sound pressure levels were found to be in the range of 10 dB [Publication IV] with lower variation in locations with heavier traffic.

3. The anthropogenic sound detection was demonstrated for differentiating time periods in the sound monitoring with the prevailing natural or anthropogenic sounds. The detector based sound categorisation showed an increase in the median of the MSFD one-third octave bands due to the presence of ships was estimated to be in the order of 5 dB in location with high intensity of maritime traffic and 1 dB in the locations with distant or sparse ship traffic [Publication III]. Although it must be noted these values can be considered as the lower bound due to the miscategorisation of quieter anthropogenic sounds as natural or mixed by the method. Simultaneously, the method can be computationally expensive and the detection threshold values vary with natural ambient sound levels.

4. Another method for the separation of the anthropogenic component of measured ambient sound was based on the fitting of the empirical natural sound level dependence with the measured SPLs. The method can be applied to the assessment period of any duration provided that the wind speed data is available.

5. It must be noted that there will always be uncertainty in distinguishing low anthropogenic sound levels from the natural background, but the method based on finding the wind dependence of the natural ambient sound can be considered more useful for the assessment of the environmental pressure posed by continuous underwater noise. This can be stated as the method only requires the monitored SPLs and wind speed data from the same region. Therefore, the proposed method of the ambient sound characterisation can be used for the assessment of the proportion of anthropogenic sound in the recorded data by determination of the excess levels over the natural sound level. The excess levels can be used as a basis for the assessment of anthropogenic pressure on marine wildlife.

6. A method for measuring the source level of a ship in shallow water conditions was demonstrated. The method was tested in the case of flat bathymetry and range-independent propagation conditions. The modeled propagation loss around a sound monitoring location enabled finding the source levels dependence on its direction of measurement. The averaged source level value dependence on the direction had standard deviation in the range of 3-5 dB [Publication II].

List of Figures

List of Tables

References

[1] John William Strutt Baron Rayleigh. *The theory of sound*. Dover, 1945.

[2] Marvin Lasky. Review of undersea acoustics to 1950. *The Journal of the Acoustical Society of America*, 61(2):283–297, February 1977. Publisher: Acoustical Society of America.

[3] YA S. Karlik, VA Semendyaev, and YU F. Tarasyuk. A Brief History of Russian Hydroacoustics. In *History of Russian Underwater Acoustics*, pages 19–68. World Scientific Publishing Co., 2008.

[4] J. N. Westwood. Submarine Construction. In *Russian Naval Construction, 1905–45*, pages 106–125. Springer, 1994.

[5] Herbert Lichte. On the influence of horizontal temperature layers in sea water on the range of underwater sound signals. *Physikalische Zeitschrift*, 17:385–389, September 1919.

[6] Arto Oll. *Kalev ja Lembit. Eesti allveelaevade lugu*. ARGO, 2017.

[7] Vern O. Knudsen, R. S. Alford, and J. W. Emling. Underwater ambient noise. *Journal of Marine Research*, 7:410–429, 1948. Publisher: Yale University.

[8] Ari Poikonen. *Measurements, analysis and modeling of wind-driven ambient noise in shallow brackish water*. Doctoral Dissertation, Aalto University, 2012.

[9] Peter C. Wille and Detlef Geyer. Measurements on the origin of the wind-dependent ambient noise variability in shallow water. *The Journal of the Acoustical Society of America*, 75(1):173–185, 1984. Publisher: Acoustical Society of America.

[10] NN Fedorov and RI Eikhenfeld. The History of Development of Hydroacoustic Measurements at the CRI Morfizpribor. In *History Of Russian Underwater Acoustics*, pages 987–1007. World Scientific Publishing Co., 2008.

[11] Gordon M. Wenz. Acoustic ambient noise in the ocean: spectra and sources. *The Journal of the Acoustical Society of America*, 34(12):1936–1956, 1962. Publisher: Acoustical Society of America.

[12] W. John Richardson, Charles R. Greene Jr, Charles I. Malme, and Denis H. Thomson. *Marine mammals and noise*. Academic press, 2013.

[13] Regina Asariotis, Hassiba Benamara, Jan Hoffmann, Anila Premti, Vincent Valentine, and Frida Youssef. Review of Maritime Transport, 2016. Technical Report UNCTAD/RMT/2016, 2016.

[14] John A. Hildebrand. Anthropogenic and natural sources of ambient noise in the ocean. *Marine Ecology Progress Series*, 395:5–20, 2009. Publisher: Inter-Research Science Center.

[15] Donald Ross. *Mechanics of Underwater Noise*. Elsevier, October 2013. Google-Books-ID: sdwgBQAAQBAJ.

[16] Jennifer L. Miksis-Olds and Stephen M. Nichols. Is low frequency ocean sound increasing globally? *The Journal of the Acoustical Society of America*, 139(1):501–511, 2016. Publisher: Acoustical Society of America.

[17] Mark A. McDonald, John A. Hildebrand, and Sean M. Wiggins. Increases in deep ocean ambient noise in the Northeast Pacific west of San Nicolas Island, California. *The Journal of the Acoustical Society of America*, 120(2):711–718, 2006. Publisher: Acoustical Society of America.

[18] Roger Payne and Douglas Webb. Orientation by means of long range acoustic signaling in baleen whales. *Annals of the New York Academy of Sciences*, 188(1):110–141, 1971. Publisher: Blackwell Publishing Ltd.

[19] Frants Havmand Jensen, Lars Bejder, Magnus Wahlberg, N. Aguilar Soto, M. Johnson, and Peter Teglberg Madsen. Vessel noise effects on delphinid communication. *Marine Ecology Progress Series*, 395:161–175, 2009. Publisher: Inter-Research Science Center.

[20] Christopher W. Clark, William T. Ellison, Brandon L. Southall, Leila Hatch, Sofie M. Van Parijs, Adam Frankel, and Dimitri Ponirakis. Acoustic masking in marine ecosystems: intuitions, analysis, and implication. *Marine Ecology Progress Series*, 395:201–222, 2009. Publisher: Inter-Research Science Center.

[21] Rogelio Sierra-Flores, Tim Atack, Hervé Migaud, and Andrew Davie. Stress response to anthropogenic noise in Atlantic cod Gadus morhua L. *Aquacultural Engineering*, 67:67–76, 2015. Publisher: Elsevier.

[22] Robert Williams, Andrew J. Wright, Erin Ashe, L. K. Blight, R. Bruintjes, R. Canessa, C. W. Clark, S. Cullis-Suzuki, D. T. Dakin, and Christine Erbe. Impacts of anthropogenic noise on marine life: publication patterns, new discoveries, and future directions in research and management. *Ocean & Coastal Management*, 115:17–24, 2015. Publisher: Elsevier.

[23] Christine Erbe, Rebecca Dunlop, and Sarah Dolman. Effects of noise on marine mammals. In *Effects of Anthropogenic Noise on Animals*, pages 277–309. Springer, 2018. Publisher: Springer.

[24] Danuta Maria Wisniewska, Mark Johnson, Jonas Teilmann, Ursula Siebert, Anders Galatius, Rune Dietz, and Peter Teglberg Madsen. High rates of vessel noise disrupt foraging in wild harbour porpoises (Phocoena phocoena). *Proceedings of the Royal Society B: Biological Sciences*, 285(1872):20172314, 2018. Publisher: The Royal Society.

[25] European Parliament and of the Council. Directive 2008/56/EC of the European Parliament and of the Council of 17 June 2008 establishing a framework for community action in the field of marine environmental policy. *Official Journal of the European Union L*, 164:19–40, 2008.

[26] M. L. Tasker, M. Amundin, M. Andre, A. Hawkins, W. Lang, T. Merck, A. Scholik-Schlomer, J. Teilmann, F. Thomsen, and S. Werner. Marine Strategy Framework Directive – Task Group 11 Report. Underwater Noise and Other Forms of Energy. *JRC Sci. Policy Rep. EUR 24341 EN, Publ. Off. Eur. Union, Luxemb*, 2010.

[27] R. P. A. Dekeling, M. L. Tasker, A. J. Van der Graaf, M. A. Ainslie, M. H. Andersson, M. André, J. F. Borsani, K. Brensing, M. Castellote, and D. Cronin. Monitoring guidance for underwater noise in European seas. *JRC Sci. Policy Rep. EUR 26557 EN, Publ. Off. Eur. Union, Luxemb*, 2014.

[28] European Commission. Decision 2017/848/EC of the European Commission of 17 May 2017 laying down criteria and methodological standards on good environmental status of marine waters and specifications and standardised methods for monitoring and assessment, and repealing. *Official Journal of the European Union L*, 125:43–74, 2017.

[29] Peter Sigray, Mathias Andersson, Jukka Pajala, Janek Laanearu, Aleksander Klauson, Jaroslaw Tegowski, Maria Boethling, Jens Fischer, Jakob Tougaard, Magnus Wahlberg, and others. BIAS: A Regional Management of Underwater Sound in the Baltic Sea. In *The Effects of Noise on Aquatic Life II*, Advances in Experimental Medicine and Biology, pages 1015–1023. Springer, 2016. Publisher: Springer.

[30] Anna Nikolopoulos, Peter Sigray, Mathias Andersson, Julia Carlström, and Emilia Lalander. *BIAS Implementation Plan: Monitoring and assessment guidance for continuous low frequency sound in the Baltic Sea*. BIAS LIFE11 ENV/SE/841, 2016.

[31] ISO. *ISO 18405:2017 - Underwater acoustics – Terminology*. International Organization for Standardization Geneva, 2017.

[32] L. Wang and S. P. Robinson. *Standard for terminology*. Report of the EU INTERREG Joint Monitoring Programme for Ambient Noise North . . . , 2018.

[33] Loggerhead Instruments. *Manual and specification sheet*. 2020.

[34] WildlifeAcoustics. *User Manual Supplement SM2M+*. WildlifeAcoustics, 2013.

[35] K Betke, Thomas Folegot, Rainer Matuschek, Jukka Pajala, Leif Persson, Jaroslaw Tegowski, and Magnus Wahlberg. BIAS Standards for Signal Processing. Aims, Processes and Recommendations. Amended version. Technical report, 2015.

[36] S. P. Robinson, P. A. Lepper, and R. A. Hazelwood. Good Practice Guide for Underwater Noise Measurement. NPL Good Practice Guide No. 133/National Measurement Office, Marine Scotland. *The Crown Estate*, (NPL Good Practice Guide No. 133), 2014.

[37] Nathan Merchant, Adrian Farcas, and Claire Powell. JOMOPANS WP6 - Acoustic metric specification. Report of the EU INTERREG Joint Monitoring Programme for Ambient Noise North Sea (JOMOPANS), September 2019.

[38] Aarno Voipio. *The Baltic Sea*. Elsevier, 1981.

[39] BORIS Winterhalter. Late-Quaternary stratigraphy of Baltic Sea basins—a review. *Bulletin of the Geological Society of Finland*, 64(Part 2):189–194, 1992. Publisher: Geological Society of Finland.

[40] Boris Katsnelson, Valery Petnikov, and James Lynch. *Fundamentals of shallow water acoustics*. Springer Science & Business Media, 2012.

[41] Anu Kaskela, Aarno Kotilainen, Ulla Alanen, Rhys Cooper, Sophie Green, Janine Guinan, Sytze van Heteren, Susanna Kihlman, Vera Van Lancker, Alan Stevenson, and the EMODnet Geology Partners. Picking Up the Pieces—Harmonising and Collating Seabed Substrate Data for European Maritime Areas. *Geosciences*, 9(2):84, February 2019. Publisher: MDPI.

[42] O. B. Wilson Jr, Stephen N. Wolf, and Frank Ingenito. Measurements of acoustic ambient noise in shallow water due to breaking surf. *The Journal of the Acoustical Society of America*, 78(1):190–195, 1985. Publisher: Acoustical Society of America.

[43] V. I. Bardyshev. Underwater surf noise near sea coasts of different types. *Acoustical Physics*, 54(6):814–822, 2008. Publisher: Springer.

[44] Matti Leppäranta and Kai Myrberg. *Physical oceanography of the Baltic Sea*. Springer Science & Business Media, 2009.

[45] Peter Winsor, Johan Rodhe, and Anders Omstedt. Baltic Sea ocean climate: an analysis of 100 yr of hydrographic data with focus on the freshwater budget. *Climate Research*, 18(1-2):5–15, 2001. Publisher: Inter-Research Science Publisher.

[46] Germo Väli, HE Markus Meier, and Jüri Elken. Simulated halocline variability in the Baltic Sea and its impact on hypoxia during 1961–2007. *Journal of Geophysical Research: Oceans*, 118(12):6982–7000, 2013. Publisher: Wiley Online Library.

[47] Colin Pounder. Sodium chloride and water temperature effects on bubbles. In *Oceanic Whitecaps*, pages 278–278. Springer, 1986.

[48] M. R. Loewen and W. K. Melville. A model of the sound generated by breaking waves. *The Journal of the Acoustical Society of America*, 90(4):2075–2080, October 1991. Publisher: Acoustical Society of America.

[49] Rainer Feistel, Günther Nausch, and Norbert Wasmund. *State and evolution of the Baltic Sea, 1952-2005: a detailed 50-year survey of meteorology and climate, physics, chemistry, biology, and marine environment*. John Wiley & Sons, 2008.

[50] Jüri Elken, Pentti Malkki, Pekka Alenius, and Tapani Stipa. Large halocline variations in the Northern Baltic Proper and associated meso-and basin-scale processes. *Oceanologia*, 48(S), 2006. Publisher: Institute of Oceanology PAS.

[51] Juss Pavelson. *Mesoscale physical processes and the related impact on the summer nutrient fields and phytoplankton blooms in the western Gulf of Finland*. Tallinn University of Technology Press, 2005.

[52] Christopher Bassett, Jim Thomson, Peter H. Dahl, and Brian Polagye. Flow-noise and turbulence in two tidal channels. *The Journal of the Acoustical Society of America*, 135(4):1764–1774, April 2014. Publisher: Acoustical Society of America.

[53] Nathan D. Merchant, Kate L. Brookes, Rebecca C. Faulkner, Anthony WJ Bicknell, Brendan J. Godley, and Matthew J. Witt. Underwater noise levels in UK waters. *Scientific Reports*, 6, 2016. Publisher: Nature Publishing Group.

[54] Robert J. Urick. *Principles of underwater sound*. Peninsula Pub, Los Altos, Calif, originated 1983 edition edition, August 1996.

[55] NRRC Booij, Roeland C. Ris, and Leo H. Holthuijsen. A third-generation wave model for coastal regions: 1. Model description and validation. *Journal of Geophysical Research: Oceans*, 104(C4):7649–7666, 1999. Publisher: Wiley Online Library.

[56] Lars Häggmark, Karl-Ivar Ivarsson, Stefan Gollvik, and Per-Olof Olofsson. Mesan, an operational mesoscale analysis system. *Tellus A: Dynamic Meteorology and Oceanography*, 52(1):2–20, 2000. Publisher: Taylor & Francis Group.

[57] William M. Carey and Richard B. Evans. *Ocean ambient noise: measurement and theory*. Springer Science & Business Media, 2011.

[58] Andrus Räämet and Tarmo Soomere. The wave climate and its seasonal variability in the northeastern Baltic Sea. *Estonian Journal of Earth Sciences*, 59(1):100–113, March 2010. Publisher: Estonian Academy Publishers.

[59] Mats Granskog, Hermanni Kaartokallio, Harri Kuosa, David N. Thomas, and Jouni Vainio. Sea ice in the Baltic Sea–a review. *Estuarine, Coastal and Shelf Science*, 70(1-2):145–160, 2006. Publisher: Elsevier.

[60] Ethan H. Roth, John A. Hildebrand, Sean M. Wiggins, and Donald Ross. Underwater ambient noise on the Chukchi Sea continental slope from 2006-2009. *The Journal of the Acoustical Society of America*, 131(1):104–110, 2012. Publisher: Acoustical Society of America.

[61] BIM Baltic Icebreaking Management. Baltic Sea Icebreaking Report 2013-2014. Technical report, BIM - Baltic Icebreaking Management, 2014.

[62] BIM Baltic Icebreaking Management. Baltic Sea Icebreaking Report 2014-2015. Technical report, BIM - Baltic Icebreaking Management, 2015.

[63] M. A. Ainslie, C. A. F. De Jong, H. S. Dol, G. Blacquière, and C. Marasini. Assessment of natural and anthropogenic sound sources and acoustic propagation in the North Sea. Technical Report TNO-DV 2009 C085, TNO, Den Haag, February 2009.

[64] National Marine Fisheries Service (NMFS). *2018 revision to: Technical guidance for assessing the effects of anthropogenic sound on marine mammal hearing (version 2.0): Underwater thresholds for onset of permanent and temporary threshold shifts*. US Dept. of Commer., NOAA, 2018.

[65] Fred K. Duennebier, Roger Lukas, Eva-Marie Nosal, Jérome Aucan, and Robert A. Weller. Wind, waves, and acoustic background levels at Station ALOHA. *Journal of Geophysical Research: Oceans*, 117(C3), 2012. Publisher: Wiley Online Library.

[66] Michael Selwyn Longuet-Higgins. A theory of the origin of microseisms. *Philosophical Transactions of the Royal Society of London. Series A, Mathematical and Physical Sciences*, 243(857):1–35, 1950. Publisher: The Royal Society London.

[67] L. M. Brekhovskikh. Generation of sound waves in a liquid by surface waves. *Soviet Physics: Acoustics*, 12:323–325, 1967. Publisher: American Institute of Physics.

[68] Douglas H. Cato. Theoretical and measured underwater noise from surface wave orbital motion. *The Journal of the Acoustical Society of America*, 89(3):1096–1112, March 1991. Publisher: Acoustical Society of America.

[69] M. A. Isakovich and B. F. Kuryanov. To the Theory of Low Frequency Ocean Noises. *Soviet Physics: Acoustics*, 16(1):62, 1970. Publisher: American Institute of Physics.

[70] JE Ffowcs Williams and Y. P. Guo. Mechanisms of sound generation at the ocean surface. In *Sea Surface Sound*, pages 309–324. Springer, 1988.

[71] Barry B. Ma, Jeffrey A. Nystuen, and Ren-Chieh Lien. Prediction of underwater sound levels from rain and wind. *The Journal of the Acoustical Society of America*, 117(6):3555–3565, June 2005. Publisher: Acoustical Society of America.

[72] Joseph A. Scrimger, Donald J. Evans, Gordon A. McBean, David M. Farmer, and Bryan R. Kerman. Underwater noise due to rain, hail, and snow. *The Journal of the Acoustical Society of America*, 81(1):79–86, 1987. Publisher: Acoustical Society of America.

[73] Marcel Minnaert. On musical air-bubbles and the sounds of running water. *The London, Edinburgh, and Dublin Philosophical Magazine and Journal of Science*, 16(104):235–248, 1933. Publisher: Taylor & Francis.

[74] William M Carey, James W Fitzgerald, Edward C Monahan, and Qin Wang. Measurement of the sound produced by a tipping trough with fresh and salt water. *The Journal of the Acoustical Society of America*, 93(6):15, 1993. Publisher: Acoustical Society of America.

[75] Jim Rohr, Ray Glass, and Brett Castile. Effect of monomolecular films on the underlying ocean ambient-noise field. *The Journal of the Acoustical Society of America*, 85(3):1148–1157, March 1989. Publisher: Acoustical Society of America.

[76] T. E. Heindsmann, R. H. Smith, and A. D. Arneson. Effect of Rain upon Underwater Noise Levels. *The Journal of the Acoustical Society of America*, 27(2):378–379, March 1955. Publisher: Acoustical Society of America.

[77] Y. P. Guo and JE Ffowcs Williams. A theoretical study on drop impact sound and rain noise. *Journal of Fluid Mechanics*, 227:345–355, 1991. Publisher: Cambridge University Press.

[78] Hugh C. Pumphrey and Paul A. Elmore. The entrainment of bubbles by drop impacts. *Journal of Fluid Mechanics*, 220:539–567, 1990. Publisher: Cambridge University Press.

[79] Steven O. McConnell, Michael P. Schilt, and J. George Dworski. Ambient noise measurements from 100 Hz to 80 kHz in an Alaskan fjord. *The Journal of the Acoustical Society of America*, 91(4):1990–2003, April 1992. Publisher: Acoustical Society of America.

[80] Sebastian Menze, Daniel P. Zitterbart, Ilse van Opzeeland, and Olaf Boebel. The influence of sea ice, wind speed and marine mammals on Southern Ocean ambient sound. *Royal Society Open Science*, 4(1):160370, 2017. Publisher: The Royal Society publishing.

[81] R. H. Mellen and H. W. Marsh. Underwater sound in the Arctic Ocean. Technical report, AVCO Marine Electronics Office, New London, CT, 1965.

[82] A. R. Milne and J. H. Ganton. Ambient Noise under Arctic-Sea Ice. *The Journal of the Acoustical Society of America*, 36(5):855–863, 1964. Publisher: Acoustical Society of America.

[83] G. Bazile Kinda, Yvan Simard, Cedric Gervaise, Jérôme I. Mars, and Louis Fortier. Arctic underwater noise transients from sea ice deformation: Characteristics, annual time series, and forcing in Beaufort Sea. *The Journal of the Acoustical Society of America*, 138(4):2034–2045, 2015. Publisher: Acoustical Society of America.

[84] Nicholas C. Makris and Ira Dyer. Environmental correlates of Arctic ice-edge noise. *The Journal of the Acoustical Society of America*, 90(6):3288–3298, 1991. Publisher: Acoustical Society of America.

[85] Peter D. Thorne, Jon J. Williams, and Anthony D. Heathershaw. In situ acoustic measurements of marine gravel threshold and transport. *Sedimentology*, 36(1):61–74, 1989. Publisher: Wiley Online Library.

[86] P. D. Thorne. An overview of underwater sound generated by interparticle collisions and its application to the measurements of coarse sediment bedload transport. *Earth Surface Dynamics*, 2(2):531–543, December 2014. Publisher: Copernicus Publications.

[87] Christopher Bassett, Jim Thomson, and Brian Polagye. Sediment-generated noise and bed stress in a tidal channel. *Journal of Geophysical Research: Oceans*, 118(4):2249–2265, April 2013. Publisher: Wiley Online Library.

[88] R. D. Hill. Investigation of lightning strikes to water surfaces. *The Journal of the Acoustical Society of America*, 78(6):2096–2099, December 1985. Publisher: Acoustical Society of America.

[89] Roy T. Arnold, Henry E. Bass, and Anthony A. Atchley. Underwater sound from lightning strikes to water in the Gulf of Mexico. *The Journal of the Acoustical Society of America*, 76(1):320–322, July 1984. Publisher: Acoustical Society of America.

[90] N. A. Dubrovskiy and S. V. Kosterin. Noise in the ocean caused by lightning strokes. In *Natural Physical Sources of Underwater Sound*, pages 697–709. Springer, 1993.

[91] Antti Mäkelä, Sven-Erik Enno, and Jussi Haapalainen. Nordic lightning information system: thunderstorm climate of Northern Europe for the period 2002–2011. *Atmospheric Research*, 139:46–61, 2014. Publisher: Elsevier.

[92] Martin W. Johnson, F. Alton Everest, and Robert W. Young. The role of snapping shrimp (Crangon and Synalpheus) in the production of underwater noise in the sea. *The Biological Bulletin*, 93(2):122–138, 1947. Publisher: The Marine Biological Laboratory.

[93] Joseph H. Haxel, Robert P. Dziak, and Haru Matsumoto. Observations of shallow water marine ambient sound: The low frequency underwater soundscape of the central Oregon coast. *The Journal of the Acoustical Society of America*, 133(5):2586–2596, May 2013. Publisher: Acoustical Society of America.

[94] Karin Tubbert Clausen, Magnus Wahlberg, Kristian Beedholm, Stacy Deruiter, and Peter Teglberg Madsen. Click communication in harbour porpoises Phocoena phocoena. *Bioacoustics, The International Journal of Animal Sound and its Recording*, 20(1):1–28, 2011. Publisher: Taylor & Francis.

[95] Ida Carlén, Len Thomas, Julia Carlström, Mats Amundin, Jonas Teilmann, Nick Tregenza, Jakob Tougaard, Jens C. Koblitz, Signe Sveegaard, Daniel Wennerberg, Olli Loisa, Michael Dähne, Katharina Brundiers, Monika Kosecka, Line Anker Kyhn, Cinthia Tiberi Ljungqvist, Iwona Pawliczka, Radomil Koza, Bartlomiej Arciszewski, Anders Galatius, Martin Jabbusch, Jussi Laaksonlaita, Jussi Niemi, Sami Lyytinen, Anja Gallus, Harald Benke, Penina Blankett, Krzysztof E. Skóra, and Alejandro Acevedo-Gutiérrez. Basin-scale distribution of harbour porpoises in the Baltic Sea provides basis for effective conservation actions. *Biological Conservation*, 226:42–53, October 2018. Publisher: Elsevier.

[96] Evelyn B. Hanggi and Ronald J. Schusterman. Underwater acoustic displays and individual variation in male harbour seals, Phoca vitulina. *Animal Behaviour*, 48(6):1275–1283, 1994. Publisher: Elsevier.

[97] Daisuke Mizuguchi, Masatoshi Tsunokawa, Mamoru Kawamoto, and Shiro Kohshima. Underwater vocalizations and associated behavior in captive ringed seals (Pusa hispida). *Polar Biology*, 39(4):659–669, 2016. Publisher: Springer.

[98] Sylvie Asselin, Mike O. Hammill, and Cyrille Barrette. Underwater vocalizations of ice breeding grey seals. *Canadian Journal of Zoology*, 71(11):2211–2219, 1993. Publisher: NRC Research Press.

[99] Jonas Teilmann, Anders Galatius, and Signe Sveegaard. Marine mammals in the Baltic Sea in relation to the Nord Stream 2 project: Baseline report. 2017. Publisher: Aarhus Universitet.

[100] A. D. Hawkins and Knud Just Rasmussen. The calls of gadoid fish. *Journal of the Marine Biological Association of the United Kingdom*, 58(4):891–911, November 1978. Publisher: Cambridge University Press.

[101] M Wahlberg. Sounds produced by herring (Clupea harengus) bubble release. *Aquatic Living Resources*, 16(3):271–275, July 2003. Publisher: Elsevier.

[102] Thomas R. Hahn and Gary Thomas. Passive acoustic detection of schools of herring. *The Journal of the Acoustical Society of America*, 125(5):2896, 2009. Publisher: Acoustical Society of America.

[103] John Carlton. *Marine propellers and propulsion*. Butterworth-Heinemann, fourth edition edition, December 2018.

[104] Burton Suedel, Andrew McQueen, Justin Wilkens, and Morris Fields. Evaluating effects of dredging-induced underwater sound on aquatic species : a literature review. Technical report, Engineer Research and Development Center (U.S.), September 2019.

[105] Douglas Clarke, Charles Dickerson, and Kevin Reine. Characterization of underwater sounds produced by dredges. In *Dredging'02: Key Technologies for Global Prosperity*, pages 1–14. 2003.

[106] D. Jones, K. Marten, and K. Harris. Underwater sound from dredging activities: Establishing source levels and modelling the propagation of underwater sound. *Proceedings from Central Dredging Association's Dredging Days*, 2015.

[107] M. B. Zaaijer. Review of knowledge development for the design of offshore wind energy technology. *Wind Energy: An International Journal for Progress and Applications in Wind Power Conversion Technology*, 12(5):411–430, 2009. Publisher: Wiley Online Library.

[108] Johannes Hüffmeier and Mats Goldberg. Offshore Wind and Grid in the Baltic Sea – Status and Outlook until 2050. Technical report, Swedish Agency for Marine and Water Management, March 2019.

[109] Jakob Tougaard, PETER T. MADSEN, and Magnus Wahlberg. Underwater noise from construction and operation of offshore wind farms. *Bioacoustics, The International Journal of Animal Sound and its Recording*, 17(1-3):143–146, 2008. Publisher: Taylor & Francis.

[110] Jakob Tougaard, Oluf Damsgaard Henriksen, and Lee A. Miller. Underwater noise from three types of offshore wind turbines: Estimation of impact zones for harbor porpoises and harbor seals. *The Journal of the Acoustical Society of America*, 125(6):3766–3773, 2009. Publisher: Acoustical Society of America.

[111] JR Nedwell, SJ Parvin, B Edwards, R Workman, AG Brooker, and JE Kynoch. Measurement and interpretation of underwater noise during construction and operation of offshore windfarms in UK waters. Subacoustech Report 544R0738, December 2007.

[112] Jesse Spence, Ray Fischer, Mike Bahtiarian, Leo Boroditsky, Nathan Jones, and Ron Dempsey. Review of existing and future potential treatments for reducing underwater sound from oil and gas industry activities. NCE 07-001, Joint Industry Programme on E&P Sound and Marine Life, 2007.

[113] Antonio Novellino and Marco Alba. EMODnet physics: towards an European impulsive noise register. *Instrumentation viewpoint*, (20):12–13, 2018. Publisher: SARTI.

[114] Gunnar Möller. From a DC-3 to BOSB: The Road to a Breakthrough in Military Safety Measures Against the Risks of Historic, Explosive Ordnance. *Marine Technology Society Journal*, 45(6):26–34, November 2011. Publisher: Marine Technology Society.

[115] Alexander M. von Benda-Beckmann, Geert Aarts, H. Özkan Sertlek, Klaus Lucke, Wim C. Verboom, Ronald A. Kastelein, Darlene R. Ketten, Rob van Bemmelen, Frans-Peter A. Lam, and Roger J. Kirkwood. Assessing the Impact of Underwater Clearance of Unexploded Ordnance on Harbour Porpoises (Phocoena phocoena) in the Southern North Sea. *Aquatic Mammals*, 41(4), 2015.

[116] C. R. Findlay, H. D. Ripple, F. Coomber, K. Froud, O. Harries, N. C. F. van Geel, S. V. Calderan, S. Benjamins, D. Risch, and B. Wilson. Mapping widespread and increasing underwater noise pollution from acoustic deterrent devices. *Marine Pollution Bulletin*, 135:1042–1050, 2018. Publisher: Elsevier.

[117] Arne Fjälling, Magnus Wahlberg, and Haakan Westerberg. Acoustic harassment devices reduce seal interaction in the Baltic salmon-trap, net fishery. *ICES Journal of Marine Science*, 63(9):1751–1758, 2006. Publisher: Oxford University Press.

[118] Xavier Lurton. *An introduction to underwater acoustics: principles and applications*. Springer Science & Business Media, 2002.

[119] Stacy L. DeRuiter, Peter L. Tyack, Ying-Tsong Lin, Arthur E. Newhall, James F. Lynch, and Patrick JO Miller. Modeling acoustic propagation of airgun array pulses recorded on tagged sperm whales (Physeter macrocephalus). *The Journal of the Acoustical Society of America*, 120(6):4100–4114, 2006. Publisher: Acoustical Society of America.

[120] Line Hermannsen, Jakob Tougaard, Kristian Beedholm, Jacob Nabe-Nielsen, and Peter Teglberg Madsen. Characteristics and propagation of airgun pulses in shallow water with implications for effects on small marine mammals. *PloS one*, 10(7), 2015. Publisher: Public Library of Science.

[121] Michael A. Ainslie, Christ AF de Jong, Stephen P. Robinson, and Paul A. Lepper. What is the source level of pile-driving noise in water? In *The Effects of Noise on Aquatic Life*, number 730 in Advances in Experimental Medicine and Biology, pages 445–448. Springer, New York, NY, 2012. Publisher: Springer.

[122] Christ A. f De Jong and Michael A. Ainslie. Underwater radiated noise due to the piling for the Q7 Offshore Wind Park. *The Journal of the Acoustical Society of America*, 123(5):2987, 2008. Publisher: Acoustical Society of America.

[123] Peter H. Dahl, David R. Dall'Osto, and Dara M. Farrell. The underwater sound field from vibratory pile driving. *The Journal of the Acoustical Society of America*, 137(6):3544–3554, June 2015. Publisher: Acoustical Society of America.

[124] Christine Erbe. Underwater noise of small personal watercraft (jet skis). *The Journal of the Acoustical Society of America*, 133(4):EL326–EL330, 2013. Publisher: Acoustical Society of America.

[125] Robert J. Urick. Noise signature of an aircraft in level flight over a hydrophone in the sea. *The Journal of the Acoustical Society of America*, 52(3B):993–999, 1972. Publisher: Acoustical Society of America.

[126] Christine Erbe, Rob Williams, Miles Parsons, Sylvia K. Parsons, I. Gede Hendrawan, and I. Made Iwan Dewantama. Underwater noise from airplanes: An overlooked source of ocean noise. *Marine Pollution Bulletin*, 137:656–661, 2018. Publisher: Elsevier.

[127] Line Hermannsen, Lonnie Mikkelsen, Jakob Tougaard, Kristian Beedholm, Mark Johnson, and Peter T. Madsen. Recreational vessels without Automatic Identification System (AIS) dominate anthropogenic noise contributions to a shallow water soundscape. *Scientific Reports*, 9(1):1–10, 2019. Publisher: Nature Publishing Group.

[128] Lasse Johansson, Erik Ytreberg, Jukka-Pekka Jalkanen, Erik Fridell, K. Martin Eriksson, Maria Lagerström, Ilja Maljutenko, Urmas Raudsepp, Vivian Fischer, and Eva Roth. Model for leisure boat activities and emissions – implementation for the Baltic Sea. preprint, Numerical Models/Chemical Tracers/Surface/Baltic Sea, January 2020.

[129] Clement Iphar, Cyril Ray, and Aldo Napoli. Uses and Misuses of the Automatic Identification System. In *OCEANS 2019 - Marseille*, pages 1–10, Marseille, France, June 2019. IEEE.

[130] J. K. Garrett, Ph Blondel, Brendan J. Godley, S. K. Pikesley, M. J. Witt, and L. Johanning. Long-term underwater sound measurements in the shipping noise indicator bands 63 Hz and 125 Hz from the port of Falmouth Bay, UK. *Marine Pollution Bulletin*, 110(1):438–448, 2016. Publisher: Elsevier.

[131] R. Core Team. R: A language and environment for statistical computing. 2013. Publisher: Vienna, Austria.

[132] Zygmunt Klusek and Aliaksandr Lisimenka. Seasonal and diel variability of the underwater noise in the Baltic Sea. *The Journal of the Acoustical Society of America*, 139(4):1537–1547, 2016. Publisher: Acoustical Society of America.

[133] L. M. Brekhovskikh and Yu P. Lysanov. *Fundamentals of Ocean Acoustics*. Modern Acoustics and Signal Processing. Springer-Verlag, New York, 3 edition, 2003.

[134] R. A. Wagstaff and J. Newcomb. Omnidirectional ambient noise measurements in the southern Baltic Sea during summer and winter. In *Progress in Underwater Acoustics*, pages 445–452. Springer, 1987.

[135] Evandro Luiz Da Costa. Detection and Identification of Cyclostationary Signals. Master's thesis, Naval Postgraduate School, Monterey, CA, March 1996.

[136] David Hanson, Jerome Antoni, Graham Brown, and Ross Emslie. Cyclostationarity for ship detection using passive sonar: progress towards a detection and identification framework. In *Proceedings of ACOUSTICS 2009*, pages 1–8, Adelaide, Australia, 2009. Australian Acoustical Society.

[137] C. L. Piggott. Ambient sea noise at low frequencies in shallow water of the Scotian Shelf. *The Journal of the Acoustical Society of America*, 36(11):2152–2163, 1964. Publisher: Acoustical Society of America.

[138] William A. Kuperman and Frank Ingenito. Spatial correlation of surface generated noise in a stratified ocean. *The Journal of the Acoustical Society of America*, 67(6):1988–1996, 1980. Publisher: Acoustical Society of America.

[139] Paul T. Arveson and David J. Vendittis. Radiated noise characteristics of a modern cargo ship. *The Journal of the Acoustical Society of America*, 107(1):118–129, January 2000. Publisher: Acoustical Society of America.

[140] American National Standards Institute (ANSI) and Acoustical Society of America (ASA). *Quantities and Procedures for Description and Measurement of Underwater Sound from Ships–Part 1: General Requirements*. International Organization for Standardization, Geneva, 2009.

[141] Michael D. Collins. A split-step Padé solution for the parabolic equation method. *The Journal of the Acoustical Society of America*, 93(4):1736–1742, 1993. Publisher: Acoustical Society of America.

[142] Michael D. Collins, Robert A. Coury, and William L. Siegmann. Beach acoustics. *The Journal of the Acoustical Society of America*, 97(5):2767–2770, 1995. Publisher: Acoustical Society of America.

[143] Martin Gassmann, Sean M. Wiggins, and John A. Hildebrand. Deep-water measurements of container ship radiated noise signatures and directionality. *The Journal of the Acoustical Society of America*, 142(3):1563–1574, 2017. Publisher: Acoustical Society of America.

[144] U. K. Verfuß, M. Andersson, T. Folegot, J. Laanearu, R. Matuschek, J. Pajala, P. Sigray, J. Tegowski, and J. Tougaard. BIAS Standards for noise measurements, 2014.

[145] N. Crawford, S. Robinson, and L. Wang. Standard procedure for equipment performance, calibration and deployment. Report of the EU INTERREG Joint Monitoring Programme for Ambient Noise North Sea (Jomopans), 2018.

Acknowledgements

Abstract

Natural and Anthropogenic Underwater Ambient Sound in the Baltic Sea

The favourable propagation conditions for acoustic waves inside the seas and oceans has made the marine organisms adapted to using sounds for communication, prey locating, and predator avoidance. There has long been a growing concern that underwater sound-scapes are becoming increasingly dominated by man-made sounds which can have negative effects on the marine biota. In tackling this problem one needs to map and quantify the sound levels in marine areas. [Publication IV] presents the analysis of the annual sound pressure levels from a year-long sound monitoring in Baltic Sea covering 37 different measuring locations, along with the ship traffic information and the wind speed data. Additionally, the temporal and spatial variability of the sound levels were quantified. The monitored and presented sound levels can be used as the baseline against which any future monitoring results can be compared.

In monitoring both the natural and anthropogenic components of the soundscape exist simultaneously. A key question for environmental pressure assessment is to estimate the anthropogenic component's exceedance over the underlying natural level. An approach based on detecting the anthropogenic sound is presented in [Publication III]. Another approach based on estimating the natural sound level from wind speed is presented in [Publication V]. This method was based on fitting the dependence of the lower measured sound levels and the wind speed. The fitted dependence enables the estimation of natural sound levels in case the anthropogenic component exceeds the natural.

The most widespread anthropogenic sound source is the marine traffic. Therefore, a better description of ships as sound sources is beneficial for soundscape modelling and mitigation efforts. The source levels of different types of ships and the source level directivity are two of the characteristics describing ships as sound sources to be measured. Although measurement standards exist for deep water, their methodologies are not well suited for use in shallow water and are not cost effective. A measurement methodology addressing these shortcomings is presented in [Publication I] and [Publication II] along with the measurement results of the ships' source level's directivity.

Kokkuvõte
Läänemere looduslik ja inimtekkeline veealune ümbrusheli

Mered ja ookeanid on helilainete levimiseks soodne keskkond ning seetõttu on sealne elustik kohanenud kasutama helisid kommunikatsiooniks, saaklooma leidmiseks ja röövlooma saagiks langemise vältimiseks. Üha enam on kasvanud mure veealuste helimaastike inimtekkelistest helidest küllastumisest ja selle võimalikest kahjulikest mõjudest mere elustikule. Antud probleemiga tegelemiseks on vajalik helitasemete mõõtmete ja kaardistamine merealadel. In tackling this problem one needs to map and quantify the sound levels in a given marine area. Publikatsioonis IV esitatakse 37 erinevas Läänemerd katvas mõõtmispunktis aastaste helirõhutasemete mõõtmistulemuste, laevaliikluse andmete ja tuulekiiruste analüüsi. Täiendavalt määrati helirõhutasemete ajaline ja ruumiline muutlikkus. Mõõdetud ja esitatud helirõhutasemeid võib kasutada lähtetasemetena, mis on võrdlusaluseks tulevikus sooritatud mõõtmistele.

Mõõdetud helirõhutasemetes esinevad looduslikud ja inimtekkelised komponendid samaaegselt. Seetõttu on keskkonnamõjude hindamises võtmeküsimuseks hinnata looduslikku komponendi ületamise määra inimtekkelise komponendi poolt. Üheks lahenduseks on inimtekkeliste helide tuvastamine, mida esitatakse Publikatsioonis III. Teine lahendus, mis on esitatud Publikatsioonis V põhineb looduslike helitasemete hindamisel tuule kiirustest. Antud meetod tugineb mõõdetud madalamate helitasemete ja tuule kiiruste vahelise seose lähendamisel. Antud lähendatud seos võimaldab hinnata looduslikke helitasemeid juhul, kui inimtekkeline komponent ületab looduslikku.

Enim levinud inimtekkeliseks heliallikaks on laevaliiklus. Seetõttu on laevade, kui heliallikate täpsem kirjeldamine vajalik veealuste helimaastike modeleerimiseks ja leevendusmeetmete planeerimiseks. Erinevate laevatüüpide allikatasemed ja nende tasemete suunasõltuvused on kaks laevu kui heliallikaid kirjeldavatest omadustest mida mõõdetakse. Kuigi leiduvad standardid antud mõõtmisteks sügavas vees ei ole neis kirjeldatavad metodoloogiad kuluefektiivsed ega sobivaimad mõõtmisteks madalas vees. Antud puudujääkidest lähtuv mõõtmismetodoloogia on esitatud Publikatsioonides I ja II koos laevade allikataseme suunasõltuvuse mõõtmistulemustega.

Appendix A

PUBLICATIONS

Publication I

Mirko Mustonen, Aleksander Klauson, Janek Laanearu, Madis Ratassepp, Thomas Folegot, and Dominique Clorennec. Passenger ship source level determination in shallow water environment. *Proceedings of Meetings on Acoustics 4ENAL*, 27:070015, 2016

Fourth International Conference on the Effects of Noise on Aquatic Life

Dublin, Ireland
10-16 July 2016

Dublin 2016
10-16 July

The Effects of Noise on Aquatic Life

Passenger ship source level determination in shallow water environment

Mirko Mustonen, Aleksander Klauson, Janek Laanearu and Madis Ratassepp
Department of Mechanics, Tallinn University of Technology, Ehitajate tee 5, 19086, Tallinn, Estonia;
mirkomustonen@gmail.com, aleksander.klauson@ttu.ee, janek.laanearu@ttu.ee, madis.ratassepp@ttu.ee

Thomas Folegot and Dominique Clorennec
Quiet Oceans, 65 Place Nicolas Copernic, 29280 Plouzané, France; thomas.folegot@quiet-oceans.com,
dominique.clorennec@quiet-oceans.com

To study sound radiation from an individual ship, it is required to analyze its spectral and spatial distribution. For an analysis in deep water, standard measurement procedures can be used. Such approach may not be valid in shallow water conditions, where the loss must be determined by sound propagation modelling. In the ambient noise measurements in the Baltic Sea, the shipping noise sources were identified by temporal tracking of their distances from the measuring hydrophone using the Automatic Identification System (AIS). The large dataset obtained from the recorded, identified and tracked ship noise events enabled us to assess transmission loss between the measurement point and each tracked ship location. Accurate modelling needs a sound speed profile in the water column, which can be found by measurements. For calculations at the sea bottom, some typical data sets can be used that fit best the attenuation rate of the measured ship noise data. Once the dependence of the loss upon azimuth and the range is estimated, it can be used for the back-calculation of the source level (SL), allowing us to find the radiated underwater noise directivity patterns of the ship in shallow water conditions.

1. INTRODUCTION

The Marine Strategy Framework Directive (MSFD) requires that European Member States develop strategies for achieving or maintaining Good Environmental Status (GES) in the European seas. For the indicator concerning the ambient underwater noise, a combined use of measurements and modelling is considered a very effective way to ascertain the levels and trends of underwater noise in the relevant frequency bands for larger sea areas. Close studies of the spatial distribution of sound radiation from individual ships would further improve the modelling in the combined method.

Controlled measurements of commercial ship source level and its directionality have been performed in previous investigations (Arveson and Vendittis, 2000). An effort has been made to obtain uniform distribution of measurements at all angles on a hemisphere centred at the ship propeller. For lower frequencies (up to 24 Hz), nearly circular directivity pattern in azimuthal direction was found. For higher frequencies (340-350 Hz) that are dominated by propeller cavitation, the directivity was slightly decreased in the front and rear directions as the bow aspect radiation is partially blocked by the hull, and the stern aspect radiation is partially absorbed in the bubble wake of the ship. A difficulty of shipping noise prediction by modelling due to discrepancies in the environmental and ship data was reported by Heitmeyer *et al.*, (2003). Extensive research on the spectral characteristics of commercial ships has been described by McKenna *et al.*, (2012). These studies address underwater measurements in deep water conditions. However, the procedures there may be inapplicable in the shallow water conditions of the Baltic Sea. Focus in the present study was on underwater recordings made in shallow water conditions. The aim was to assess the directivity patterns of commercial ships.

Figure 1. Passenger ship in the Gulf of Finland.

2. UNDERWATER NOISE MONITORING

In the frames of BIAS Life+ project (Sigray *et al.,* 2016), the ambient noise was measured in four different positions in the Estonian EEZ during the year 2014. The monitoring equipment and procedures are described in the BIAS standards for noise measurements (Verfuß *et al.*, 2015). Fig. 2a presents the BIAS rig design used for the measurements in Estonia.

Ship traffic is quite intense across the Baltic Sea as well as in the Estonian EEZ. Density of ships per square kilometre during January 2014 and the location of Estonian measurement positions are shown in Fig. 2b. The highest density of passenger ships in the Baltic Sea is between Tallinn and Helsinki where the BIAS20 recording station is located. At this position, it was possible to record individual noise signatures from several regularly operated passenger ships.
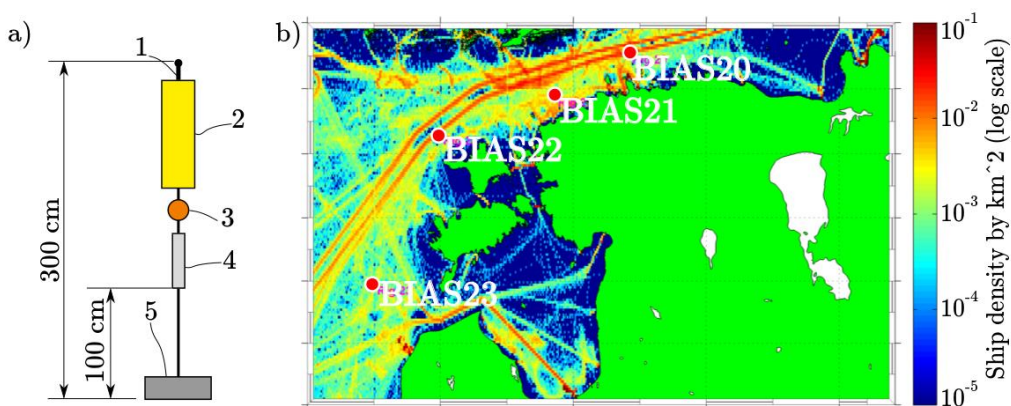

Figure 2. a - Sketch of a BIAS standard rig: (1) hydrophone, (2) SM2M logger, (3) buoy, (4) acoustic releaser, (5) anchor (min 20 kg wet weight); b - Recording positions on the map of the overall density of ships around Estonia (January 2014).

Table 1 presents the geographical coordinates of the deployment positions, water depths, position types and recording times in days. According to the recommendations made by Dekeling *et al.,* (2014), category A stations were located further from the shipping lanes. The aim of these stations was to record ambient noise from distant shipping. Category B stations were located close to the shipping lanes. Their aim was to record the noise generated by individual ships. As seen from Table 1, type B station BIAS20 recorded almost continuously during the year 2014.

Table 1. Underwater noise recording positions in Estonian waters

Name	Latitude	Longitude	Depth, m	Category	Rec. time, days
BIAS20, Tallinn	59°46.5'N	24°50.5'E	73	B	324,5
BIAS21, Paldiski	59°27.2'N	23°43.4'E	81	A	201.5
BIAS22, Hiiumaa	59°09.0'N	21°59.4'E	80	B-A	203.5
BIAS23, Saaremaa	57°58.3'N	21°00.0'E	82	A	179.5

3. SHIP POSITIONING WITH AIS

Automatic Identification System (AIS) is intended to enhance safety of life at sea, the safety and efficiency of navigation and protection of the marine environment (Revised Guidelines, 2016). AIS equipment aboard vessels transmits continuously and autonomously information about the vessel including its identity, position, course and speed (Tetreault, 2005). These data were used to position the ships relative to recording positions. Due to irregular sampling, interpolation was used. Speed over ground (SOG) and course over ground (COG) were interpolated uniformly between the AIS data points. The directivity angle γ can be approximated from the COG and the cartographical azimuth between the recording station and the ship (Fig. 3). On a normal pass of the ship from the recording station, the azimuthal directivity angle γ changes between 0-180° or 180-360° depending on the ship's and the recording station's relative positions.

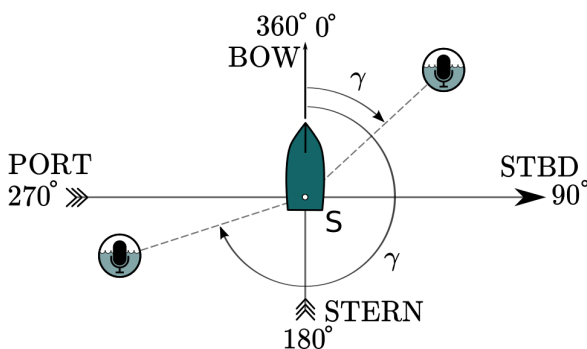*Figure 3. Ship and recorder position geometry. The azimuthal angle γ is measured between the ship's COG and the location of the hydrophone.*

4. TRANSMISSION LOSS MODELLING

Received level (RL) indicates the sound pressure level received by the measurement station. To calculate the RL 1/3 octave band values from the measured data, the data were processed according to the BIAS Standards for Signal Processing (Betke *et al*., 2015). The RL is related to the source level (SL) by the equation

$$RL = SL - TL,$$

where TL denotes transmission loss. SL is defined as the sound pressure level at 1 meter of the source in the direction of reception. All terms of the equation are expressed in decibels relative to 1 μPa. To be able to assess SL, the TL must be known. In deep water conditions, spherical spread of acoustic waves can be considered for the back-calculation and TL can be expressed as

$$TL = 20\log(r/r_{=1m})$$

In shallow water conditions, the influence of the sea bottom cannot be neglected. In this case, sound propagation modelling must be used to take into account the influence of bathymetry, acoustical properties of the sea bottom (sediments) and the sound speed profile. Considering the

needed relatively low frequency ranges, inhomogeneous medium and preferred one-way propagation direction from the ship to the hydrophone, the parabolic equation (PE) method can be used. In particular, the PE method implementation RAM, i.e. the range-dependent acoustic model (Collins, 1993, 1995), was used to solve the problem. The inputs of the RAM include bathymetry, sound speed profiles and acoustical properties of the waveguide, as well as the position of the source and the receiver. The output of the code is the TL in the plane of the source and the receiver.
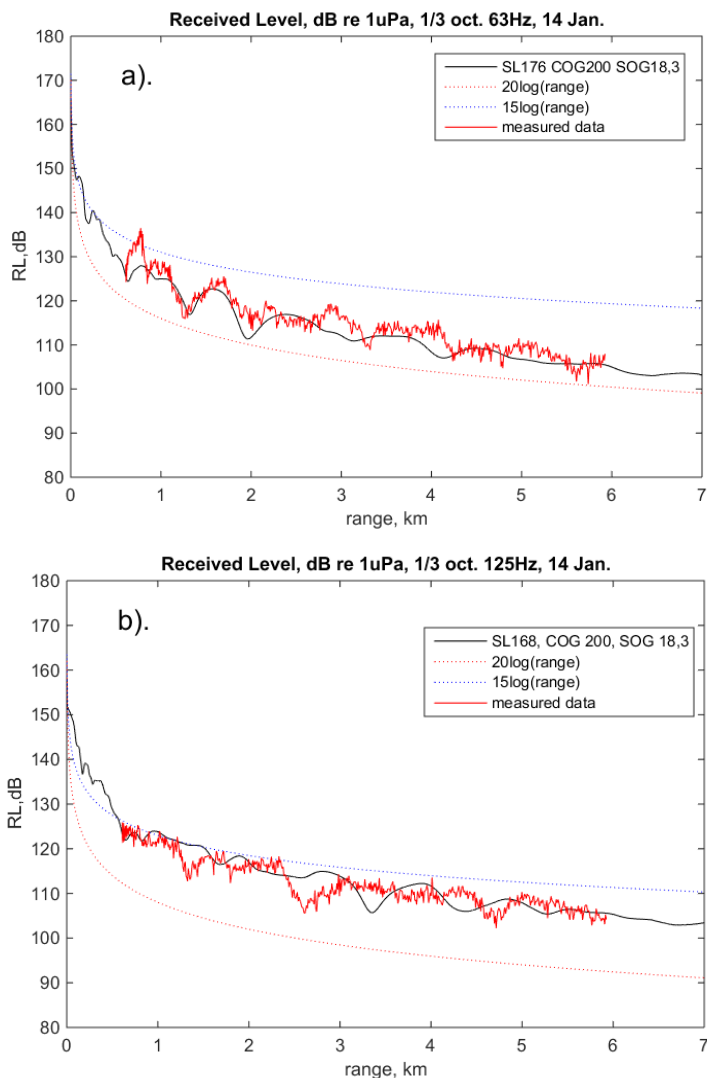
Figure 4. Red line - data measured from a container ship (L=152m), limiting dotted lines - RL for 20log(r) and 15log(r) spreading, black line - modelling with the bottom type sandy mud. a – 63 Hz ⅓ octave band and b – 125 Hz ⅓ octave band results.

To validate the method, position BIAS23 near the Island of Saaremaa was chosen because of its rather flat bathymetry and less intensive ship traffic, resulting in less interference from distant shipping. It must be pointed out that in January the sound speed profile is quite constant with the water depth in this region, which will also simplify validation. The ship positions can be found using the AIS data. For the ships passing close to the hydrophone position, the 2D sound propagation can be derived by the hydrophone location and the estimates of the ship position. Although the sediment probes were locally taken during deployments, uncertainty about the sediment type remains. However, the attenuation rate of measured data helps to determine a suitable sediment type for the model. It can be seen that sandy mud bottom gives quite realistic results to the distances up to 6 kilometres [Fig. 4]. Finally, the SL must be fitted to the modelling and measured data. For example, in Fig. 4a and b, the measured data from a cargo ship 1 were best fitted in the case of sandy mud bottom and SL=176 dB re 1 μPa for 63 Hz and SL=168 dB re 1 μPa for 125 Hz ⅓ octave bands. The measured data (RL) were averaged for every second. The proximity of other ships was systematically checked to minimize distant shipping noise interference.

Once the sea bottom parameters are chosen, it is possible to determine the TL around the hydrophone position as a function of range r and azimuthal angle γ to be used further for back-calculation of the SL of the ships with arbitrary trajectories inside the 7-km ring centred around the hydrophone. An example of the TL at the position BIAS20 in January 2014 is shown in Fig.5.

Transmission Loss, dB re 1uPa, 1/3 oct. 63Hz, B20
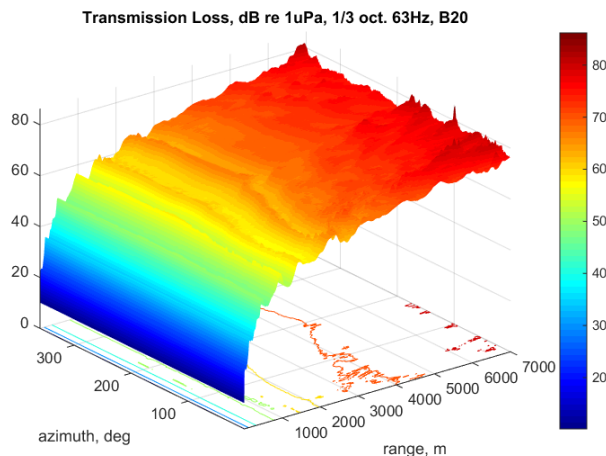
Fig.5. TL centred at the position BIAS20 (depth 70m) in January 2014 as a function of range and azimuth of the source. Reception at the depth of 73 m, depth of the source at 3 m. Bottom sediment - coarse silt.

5. DIRECTIVITY PATTERN CALCULATION

For different azimuthal angles γ, the SL was back-calculated from the known positions of the ship. Due to low water depth and considerably great distances between the ships and hydrophone, all directivity diagrams neglect the depression angle under the ship. The following

directivity diagrams present the SL for the 63 Hz and 125 Hz ⅓ octave bands. All measured data used in Figs. 6-7 correspond to the period of January 2014. At the angular diagrams, data points were averaged for the time intervals of 10 seconds. Each curve of the plot corresponds to a different recording of the same ship. In the legend, SOG is speed over ground in knots, CPA - the closest point of approach in km and Ws - wind speed in knots. The latter reveals the sea state during the recording.

Directivity diagrams in Figs. 6-7 are quite symmetrical with respect to the ship axis, in particular at similar ship speeds and distances. Fig. 6 shows side lobes in the directivity diagrams at 45° and 135°. For the angles close to bow and stern directions, the results of the directivity diagram are not reliable enough, as the distance used for back-calculation grows considerably and ambient noise starts to interfere with distant recordings. The directivity is slightly decreased in the front and rear directions where the propeller radiation is masked by the hull or partially absorbed in the bubble wake of the ship, as reported by Arveson and Vendittis (2000). In Fig. 7, the directivity diagram is quite omnidirectional for the ⅓ octave band centred around 125 Hz. The differences in the angular diagrams of the same ship can be explained by inaccurate modelling resulting from averaging of sediment and water column properties in the region of interest. Also, time drift of the logger, if not properly considered, can mislead in terms of timing of the acoustical event and its real distance from the logger. Thus, time drift will produce an angular shift of lobes in the directivity diagram. The results obtained show spread exceeding the requirements in deep water (ISO/PAS 17208-1:2012), but they can be considered as a cost-effective alternative for the assessment of ship source level and directivity in shallow water.
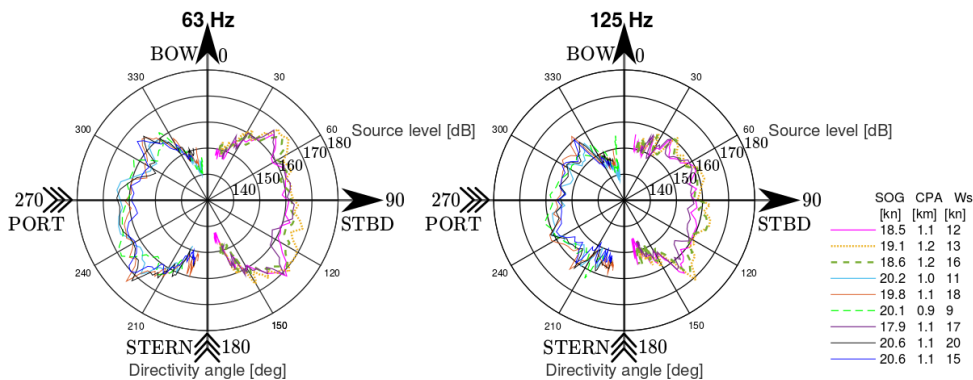

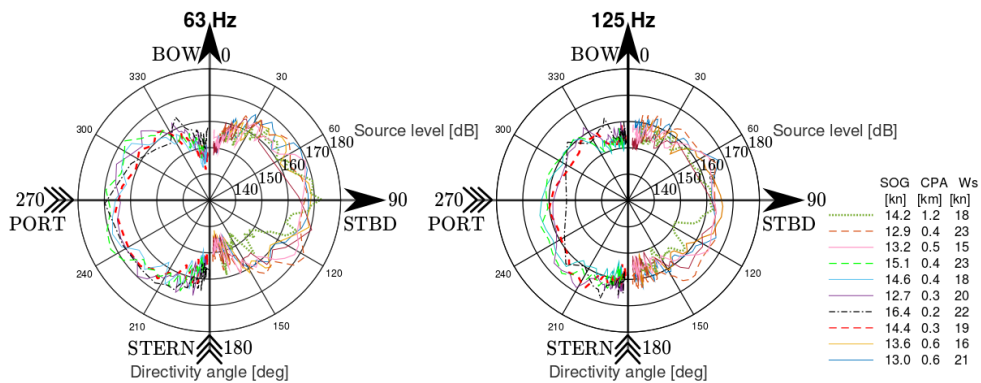*Figure 6. Passenger ship (Length = 185 m) BIAS20 directivity diagrams.*

Figure 7. Ro-Ro Cargo Ship (Length = 190 m) BIAS23 directivity diagrams.

6. CONCLUSION

Our analysis shows that it is possible to calculate the source level based on ship noise recordings in shallow water, if modelling is accurate and AIS data are available and a transmission loss map for the region around the recording station can be composed. In this case, the ship SL can be back-calculated. Further refinement of the model will improve the results and reduce their variation. Our approach has its natural limits for directivity angles approaching 0° and 180° where the reduction of the signal to the ambient noise ratio lowers the reliability of the results. Particular care should be taken for accurate synchronization of the AIS data with the acoustical recordings, as time drift of the datalogger clock can give inaccurate estimates of the ship's range and angle. There is significant angular variability of the SL in the frequency band ⅓ octave centred around 63 Hz, showing that in several cases, the omnidirectional ship source model broadly implemented can be disputed. Typically, the maxima of the diagrams are in the ship beam aspect (90° and 270°) but quite high side lobes in the angular diagrams can occur, as shown for a passenger ship (Fig. 6). To provide more information about the directivity of a ship's acoustical radiation, other frequency bands should be further investigated.

ACKNOWLEDGMENTS

REFERENCES

Arveson, P. T., and Vendittis, D. J. (**2000**). "Radiated noise characteristics of a modern cargo ship," J. Acoust. Soc. Am. **107**, pp. 118–129.

Betke K., Folegot T., Matuschek R., Pajala J., Persson L., Tegowski J., Tougaard, J., Wahlberg M. (**2015**). "BIAS Standards for Signal Processing. Aims, Processes and Recommendations. Amended version," editors: Verfuß U.K., Sigray P.

Collins, M. D. (**1993**). "A split-step Padé solution for the parabolic equation method," in The Journal of the Acoustical Society of America, **93**(4), pp. 1736-1742.

Collins, M. D., R. A. Coury and W.L. Siegmann. **(1995)** "Beach acoustics", in The Journal of the Acoustical Society of America, **97**(5), Pt.1, pp. 2767-2770.

Dekeling, R.P.A., Tasker, M.L., Van der Graaf, A.J., Ainslie, M.A, Andersson, M.H., André, M., Borsani, J.F., Brensing, K., Castellote, M., Cronin, D., Dalen, J., Folegot, T., Leaper, R.,Pajala, J., Redman, P., Robinson, S.P., Sigray, P., Sutton, G., Thomsen, F., Werner, S., Wittekind, D., Young, J.V. **(2013)** Monitoring Guidance for Underwater Noise in European Seas . Part II: Monitoring Guidance Specifications. JSR Scientific and Policy Report of the MSFD Technical Subgroup on Underwater Noise (TSG Noise).

Heitmeyer, R. M., Wales, S. C., and Pflug, L. A. **(2003)**. "Shipping noise predictions: Capabilities and limitations," Mar. Technol. Soc. J. 37, pp. 54-65.

ISO/PAS 17208-1:2012 Acoustics: "Quantities and procedures for description and measurement of underwater sound from ships", Part 1: General requirements for measurements in deep water.

McKenna, M. F., Ross, D.,Wiggins, S. M. & Hildebrand, J. A. **(2012)**. "Underwater radiated noise from modern commercial ships," J. Acoust. Soc. Am. **131**, pp. 92−103.

Revised Guidelines for onboard operational use of ship Automatic Identification Systems (AIS), **(2016)** St. Vincent and the Grenadines, Maritime Administration, Circular nr. SOL 064.

Sigray, P., Andersson, M., Pajala, J., Laanearu, J., Klauson, A., Tegowski, J., Boethling, M., Fischer, J., Tougaard, J., Wahlberg, M. and Nikolopoulos, A. **(2016)**. "BIAS: A Regional Management of Underwater Sound in the Baltic Sea," in The Effects of Noise on Aquatic Life II (Springer New York), pp. 1015-1023.

Tetreault, C. B. J. **(2005)**. "Use of the Automatic Identification System (AIS) for maritime domain awareness (MDA)," in OCEANS, 2005. Proceedings of MTS/IEEE (pp. 1590-1594). IEEE.

Verfuß, U.K., Andersson, M., Folegot, T., Laanearu, J., Matuschek, R., Pajala, J., Sigray, P., Tegowski, J., Tougaard, J. **(2015)**. "BIAS Standards for noise measurements. Background information, Guidelines and Quality Assurance. Amended version."

Publication II

174th Meeting of the Acoustical Society of America

New Orleans, Louisiana

04-08 December 2017

Underwater Acoustics: Paper 4aUW6

Ship source strength estimation in shallow water

Aleksander Klauson and Mirko Mustonen
Department of Civil Engineering and Architecture, Tallinn University of Technology, Tallinn, Harjumaa, 19086, ESTONIA; aleksander.klauson@ttu.ee; mirkomustonen@gmail.com

Continuous underwater noise from commercial ship traffic is an important pressure on the marine environment that has to be taken into account as stated in the Marine Strategy Framework Directive adopted in the EU. Monitoring of the underwater ambient noise level has been performed in the frame of the Life+ BIAS project together with underwater noise propagation modelling resulting in noise maps. In order to improve the modelling of anthropogenic noise based on AIS traffic data, it is essential to provide better source level (SL) input for individual ships. The SL can be obtained using the data from the underwater noise monitoring. Long-term recordings provide information about ships' multiple passages. In shallow water, sound prop-agation modelling should be applied for accurate loss estimation. If the modelling is performed for some particular frequency bands, estimation of the loss needs even more calculation effort. This paper proposes a simplified approach for more efficient calculation of the losses. The calculated results are compared with the measurements in different geographical positions and sea conditions. The topic of ship source directionality is addressed. The repeatability of the results is checked for the different passages of the same ship during the year.

1. INTRODUCTION

Continuous underwater noise from commercial ship traffic is an important pressure on the marine environment that has to be assessed, as stated in the Marine Strategy Framework Directive adopted in the EU. Long-term monitoring of the underwater ambient noise in the Baltic Sea was started as part of the Life+ BIAS project.[1] The recorded data helped to calibrate underwater noise propagation modeling that was used for making the noise maps of the Baltic Sea. In order to improve the modeling of anthropogenic noise propagation that is based on Automatic Identification System (AIS) traffic data, it is essential to provide as input better source level (SL) estimates for individual ships. The SL can be found using some simplified models.[2] In deep water conditions, the back-calculation of the SL can be estimated by the spherical spread model. In shallow water, this type of approach is inapplicable because of the multiple interactions of the sound with the sea surface and the bottom. Hence sound propagation modeling should be applied for accurate loss estimation. Also, long-term monitoring data provides valuable information about ships performing regular passages near to a recorder. This paper proposes a simplified approach for a more efficient calculation of the transmission losses and the SL. The calculated results are compared with measurements made for the different ship speeds and sea conditions. The approach is also used to study the topic of SL directionality. The repeatability of the results is checked for ships making regular passages during the winter season.

2. STATEMENT OF THE PROBLEM

Over the low frequency band, shipping is recognized as the principal source of ambient underwater anthropogenic noise.[3] Continuous anthropogenic noise has come into focus because of its potential negative impact on marine life. The known effects of continuous noise on marine species are the reduction of communication space,[4] increased stress levels, reduction in the foraging and energetic budget.[5]

Anthropogenic underwater noise is recognized as a form of pollution in European legislation through the Marine Strategy Framework Directive (MSFD descriptor 11: 2010/477/EU, 2017/848) and should be at levels that do not adversely affect the marine environment. These levels should be expressed as the annual average of the squared sound pressure in each of two 1/3-octave bands, one centered at 63 Hz and the other at 125 Hz, or another suitable metric agreed at regional or sub-regional level.

In 2012 an extensive anthropogenic sound monitoring program has been launched as part of the Life+ project "Baltic Sea Information on the Acoustic Soundscape" (BIAS). Scientists from six Baltic Sea countries - Sweden, Denmark, Germany, Poland, Estonia and Finland - measured the ambient noise at 36 monitoring locations during the year 2014. Passive acoustic monitoring (PAM) was performed by deploying autonomous omnidirectional marine recorders.[6] It is presumed that the natural noise in the Baltic Sea is mainly generated by wind-driven surface waves, while the main anthropogenic noise source is commercial maritime traffic.

In the BIAS project the underwater anthropogenic sound pressure levels in the sea have been derived using sound propagation modeling.[6] The length and speed of ships provided by the AIS and VMS data were used to determine the source level of the individual ships using the RANDI3 model.[7] As a result of long-term underwater ambient sound monitoring of the BIAS project, a large amount of recorded sound and AIS data has been collected. The sound monitoring was done with a sampling frequency of 32 kHz and with duty-cycling varying from 20 to 59 minutes per hour. This high resolution data contains a lot of valuable information that can be used to improve the sound propagation modeling. The propagation model requires many input parameters, such as seafloor sediment properties, the sound speed profile and the acoustical characteristics of the source, to be set beforehand.

A single ship is a complex multi-parametric acoustic source. Among the important parameters influencing a ship's sound radiation are its speed over ground and engine power, which in turn is related to the ship's deadweight.[8] The ship's SL can be measured in deep water by following procedures specified in the corresponding standards.[9] Significant technical effort is required for the measurement of a ship's SL and its directivity.[10] The methods developed for deep water conditions are not applicable in shallow seas, where multiple reflections from the bottom have to be taken into account. However, the ship SL and its directivity can be assessed by an indirect approach that uses the available underwater sound monitoring and AIS data. In our previous study, the back-calculation of the ship SL was tested for passenger ships making regular passages in the Gulf of Finland.[6] However, the uneven bathymetry of the site in the previous study increased the uncertainty of the modelling results. In the present paper, the methodology is tested in a location with flat bathymetry. Parametric research was used to find the best fit for the acoustical properties of the bottom. Ensemble averaging of the different passages of the same ship made it possible to calculate the SL directivity of the ship.

A. MAIN ASSUMPTIONS

- Automatic Identification System (AIS) broadcasts the vessel's coordinates, speed, course and various other parameters useful for estimation of its SL. Generally the ship's position reports in AIS are broadcast at irregular intervals. The intervals get shorter with the increasing speed and rate of turn of the vessel.
- As a simplification, it is assumed that the acoustic center of the ship is located in the stern. In the modeling, a ship is considered as a monopole source located at the effective depth derived from the AIS reported and design draught.
- It is assumed that the sound speed profile (SSP) and sediment properties remain unchanged around the monitoring position.
- Bathymetry around the monitoring position is sufficiently flat to enable the use of a 2D sound propagation model.
- The exact physical properties of the sediments (sound speed and density) for the area are *a priori* unknown but can be derived from the curve fitting of the 2D modeling of a ship's passage close to the monitoring location with the measured data.
- For the initial guess the acoustic center of the ship is assessed from its draught and remains unchanged for every trip.

B. MONITORING LOCATIONS AND ENVIRONMENTAL DATA

The Baltic Sea is quite shallow and the depths at the monitoring locations range from 70 to 90 meters (Fig. 1). The typical sediment type at these depths is mud, which has been confirmed by bottom probes.

In the Estonian EEZ, the BIAS project underwater noise monitoring locations were:

BIAS20 – Tallinn, very close to the shipping lane, quite flat bathymetry, depth 73 meters;

BIAS21 – Paldiski, 14 km from a shipping lane, flat bathymetry, depth 81 meter;

BIAS22 – Hiiumaa, 2 km from a shipping lane, uneven bathymetry, depth 80 meters;

BIAS23 – Saaremaa, 30 km from a shipping lane, flat bathymetry, depth 82 meters.
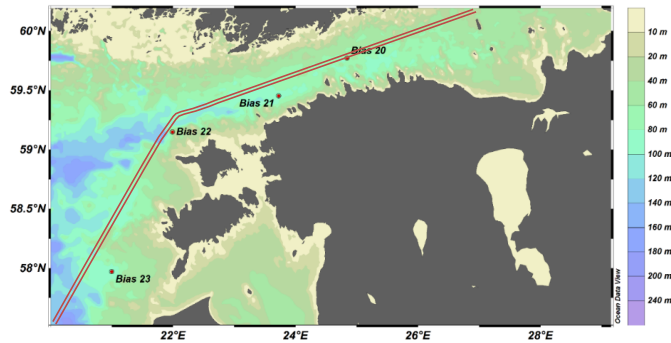
Figure 1. Bathymetry of the BIAS monitoring sites in Estonia and approximate position of the shipping lanes.

During the winters the temperature and therefore the sound speed profile (SSP) of the water column in the Baltic Sea are close to being constant. However, saline water from the ocean which infiltrates from the Danish straits forms a layer near the sea bottom. As a result, a visible halocline can be seen in the SSPs shown in Figure 2.
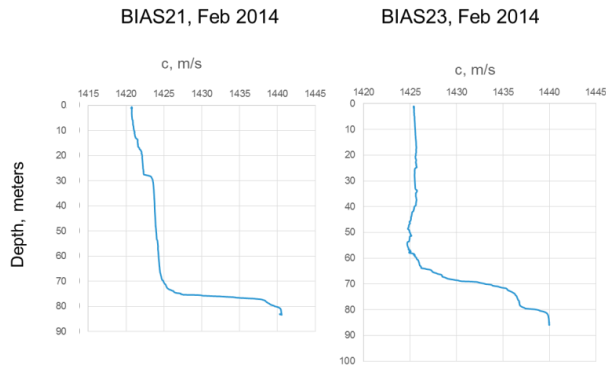
Figure 2. Measured sound speed profiles from two sound monitoring locations.

3. SHIP SOURCE STRENGTH ESTIMATION

SPL in one-third octave band centered at 63 Hz is known to be a good indicator of the presence of shipping. Higher levels within this frequency band can be identified as passages of individual vessels. Although the omnidirectional hydrophones cannot capture the position of the source, the AIS data can fill this gap. Synchronization of the time domain SPL with the AIS vessel locations makes it possible to get a good overview of the positions of the sources with respect to the hydrophone as well as their identification. The underwater sound propagation model[11] needs correct input parameters to give reliable results. Better known among them are the sound speed profile, bathymetry and the locations of the source and receiver. Less well known are the acoustic properties of the sea bottom and the SLs of the ships. In the first stage, the acoustic properties are determined by a sensitivity analysis. The sea bottom parameters considered

essential for sound propagation modelling are the relative density $\rho = \rho_b / \rho_w$, sound attenuation in the bottom β expressed in dB/λ, and the sound speed in the bottom c_b. Figure 3 a-d presents the sensitivity analysis of the dependence of transmission loss upon the selected parameters. All curves represent the received level as a function of the range. Figure 3a shows that the density of the bottom influences sound propagation much less than the other parameters. As the sound speed influences reflection from the sea bottom, for small attenuations the decay curve approaches that of the spherical spread law. Except for higher attenuation rates, the decay curve lies between the curves indicating the spherical spread and that described by 15log($range$) low.
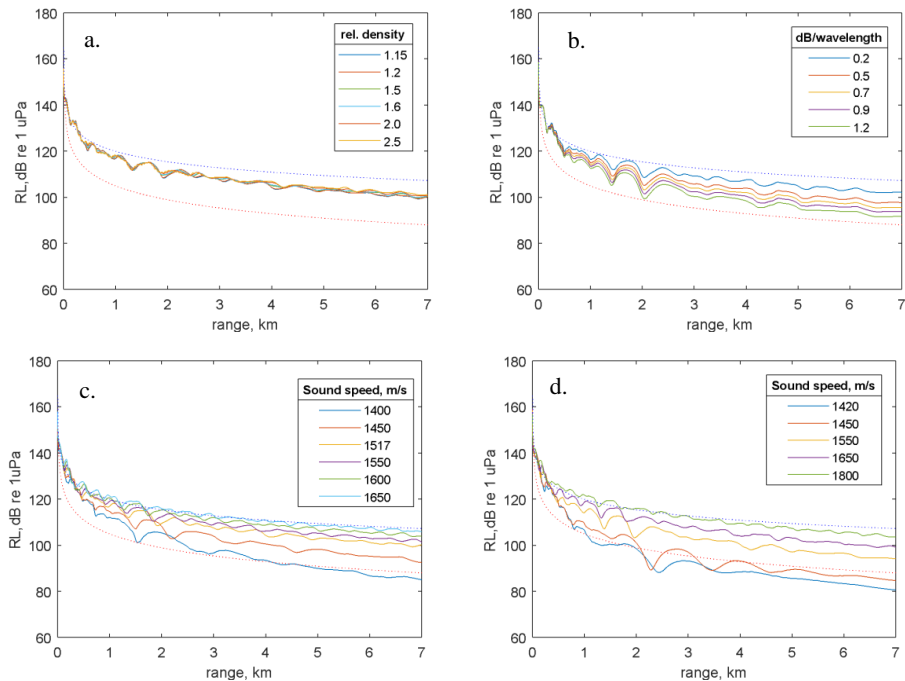
Figure 3. Dependence of the received level (RL) on the range (SL=165dB, 1/3-octave band 63Hz) for the selected parameters: a – relative densities ρ (c_b=1550m/s, α=0.2), b - attenuations β (c_b =1550m/s, ρ=1.2), c - sound speeds c_b (ρ=1.2, β=0.2), d - sound speeds c_b (ρ=1.2, β=1.2). Dotted blue and red lines show spherical and 15log(range) decay curves.

The effective depth of the source can be estimated according to Gray $et\ al.$[12] to be equal to the ship draft minus 85% of the propeller diameter. Diameter can be estimated as 65% of the ship design draught.[13] Based on this considerations and AIS reporting, the depth of the source could vary in the interval z_s=2.4 …3.4m. The modeled result was compared with the measured data, as shown in Fig. 4. Based on the analysis, the acoustic properties of coarse silt (ρ =1.2, c=1555 m/s, and β=1.2 dB/λ) were chosen as the sea bottom substrate for the modeling.
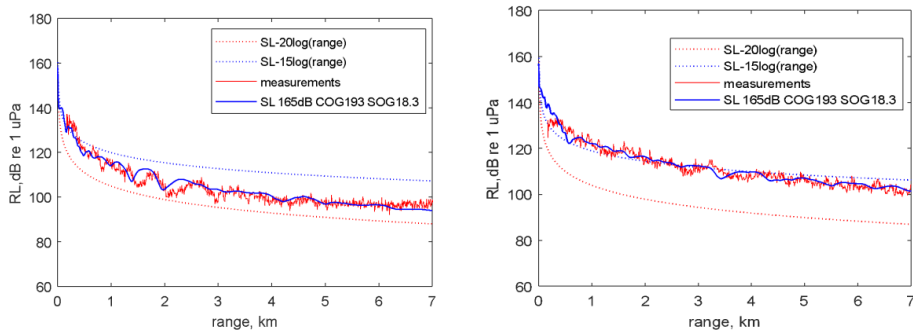
Figure 4. Measured (red line) and modeled (blue line) received level dependence on the range for 1/3-octave bands 63 Hz (left) and 125 Hz (right). Dotted blue and red lines show spherical and 15log(range) low decay curves.

Once the acoustic properties of the sea bottom are chosen, the transmission loss (TL) map can be calculated around the monitoring location. This map enables the SL to be calculated by adding the TL value to the received level. Moreover, calculating the source levels at the different aspects of a ship with respect to the monitoring position amounts to finding its directivity. Figure 5 shows the TL map around monitoring location 23. This map can be further used for the back-calculation of the SL for every ship crossing the area.
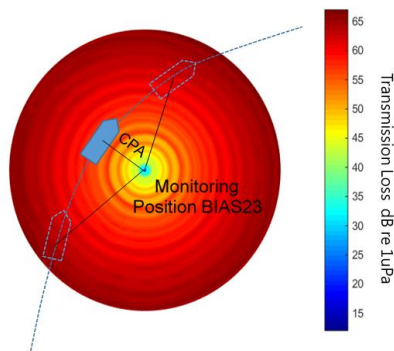
Figure 5. TL map around monitoring position 23 (Saaremaa island).

4. SHIP SOURCE LEVEL DIRECTIVITY ASSESSMENT

Cargo ships on the regular lines offer an opportunity to capture from various passes their underwater acoustic emission at different speeds (SOG – speed over ground in knots), aspects and distances (CPA – closest point of approach in kilometers). To minimize interference, it is important to check from the AIS data that no other ships are present at a distance less than 12 km from the monitoring location. This ultimate audible distance was determined based on the analysis of the underwater sound recordings. Resulting directivity plots are presented in Fig.6 for 1/3 octave band 125Hz. The wind speed (Ws in knots) and draught (Drt in meters) is shown for every directivity curve of the ship's passes. This demonstrates an

expected outcome that the ship's SLs are mostly independent from the changing natural sound levels. The calculated directivity curves can be further analyzed and averaged. Averaging over the different passages of the vessel as well as over every 15 degrees gives an estimate of the true source level directivity for small inclination angles (8…20º for CPA interval 0.6 …0.2 km) projected to the horizontal plane. The standard deviation of the SL's directivity remained between 3 and 5 dB. This is a quite encouraging result considering the robustness of the method. Lack of symmetry of the angular diagram is due to the bigger average draught of the starboard aspect ship tracks. Estimated average effective depth of the acoustic center for the port aspect is 2.4 meters and for the starboard 3.4 meters. Calculations show that the difference in the TL for two effective depths is about 3dB, which can explain higher SL values for the starboard aspect. In the stern aspect SL is about 5dB higher than for the bow aspect. This is in agreement with the results reported by other authors.[14] It should be noted that the SL estimation becomes increasingly inaccurate at larger distances between the ship and the monitoring location, which corresponds to the bow and stern aspect in the directivity plots. Better accounting for the effective depth of acoustic center of the ship through more advanced measurement technique could probably enhance the results.
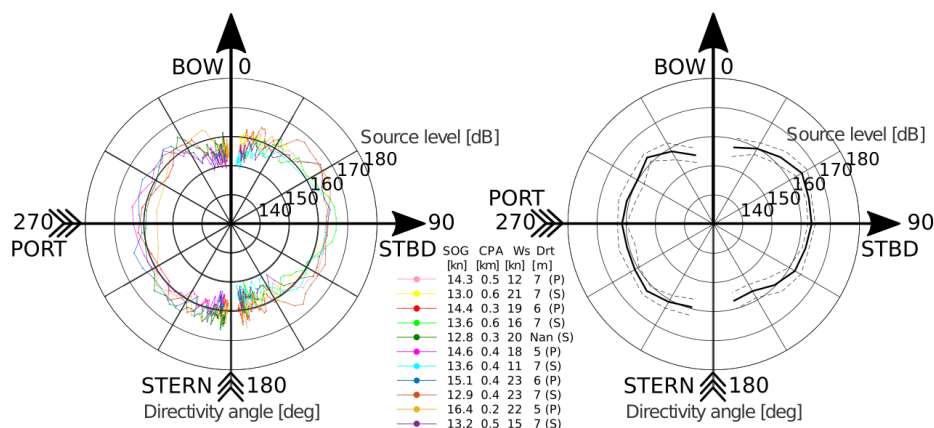
Figure 6. SL directivity plots of a cargo ship for 1/3 octave band 125Hz during its different passages (left) and the averaged result (right). In the legend SOG – speed over ground, CPA – closest point of approach, Ws – wind speed, Drt –draught of the ship.

5. CONCLUSIONS

- It was demonstrated that the source level of a ship in shallow water can be estimated from the PAM data. The method has been tested for the case of flat bathymetry and range-independent propagation conditions.
- The transmission loss can be found by the application of sound propagation modeling. More detailed information about the sediment structure and its acoustical properties is beneficial to improve the reliability of the results.
- The averaged SL directivity values gave the estimate for a ship's SL at different aspects with a standard deviation of 3–5 dB.

ACKNOWLEDGEMENTS

REFERENCES

[1] Sigray, P., Andersson, M., Pajala, J., Laanearu, J., Klauson, A., Tegowski, J., Boethling, M., Fischer, J., Tougaard, J., Wahlberg, M., Nikolopoulos, A. (2016). "BIAS: A Regional Management of Underwater Sound in the Baltic Sea," in The Effects of Noise on Aquatic Life II. Springer New York, 1015-1023.

[2] Frisk, G., Bradley, D., Caldwell, J., D'Spain, G., Gordon, J. (2003). Ocean noise and marine mammals. NRC Ocean Studies Board, Washington DC: National Academies Press.

[3] Urick, R.J. (1983). Principles of Underwater Sound, 3rd ed. McGraw-Hill, New York.

[4] Clark, C.W., Ellison, W.T., Southall, B.L., Hatch, L., Van Parijs, S.M., Frankel, A., Ponirakis, D. (2009). Acoustic masking in marine ecosystems: intuitions, analysis, and implication. Marine Ecology Progress Series 395, 201–222.

[5] Williams, R., Wright, A.J., Ashe, E., Blight, L.K., Bruintjes, R., Canessa, R., Clark, C.W., Cullis-Suzuki, S., Dakin, D.T., Erbe, C., Hammond, P.S., Merchant, N.D., O'Hara, P.D., Purser, J., Radford, A.N., Simpson, S.D., Thomas, L., Wale, M.A. (2015). Impacts of anthropogenic noise on marine life: publication patterns, new discoveries, and future directions in research and management. Ocean Coast. Manag. 115, 17–24.

[6] Mustonen, M., Klauson, A., Laanearu, J., Ratassepp, M., Folegot, T., Clorennec, D. (2017). "Passenger ship source level determination in shallow water environment," 4th Int. Conf. on the Effects of Noise on Aquatic Life, Dublin, Ireland, 10-16 July 2016, Proc. of Meetings on Acoustics, Vol. 27, 070015.

[7] Folegot, T., Clorennec, D., Chavanne, R., Gallou, R. (2016). Mapping of ambient noise for BIAS. Quiet-Oceans technical report QO.20130203.01.RAP.001.01B, Brest, France, December 2016.

[8] McKenna, M.F., Ross, D., Wiggins, S.M. & Hildebrand, J.A. (2012). Underwater radiated noise from modern commercial ships. J. Acoust. Soc. Am. 131, 92–103.

[9] ANSI/ASA S12.64-2009 part1: Quantities and Procedures for Description and Measurement of Underwater Sound from Ships –Part 1 General Requirements.

[10] Arveson, P.T., Vendittis, D.J. (2000). Radiated noise characteristics of a modern cargo ship. J. Acoust. Soc. Am. 107, 118–129.

[11] Collins, M.D., Cederberg, R.J., King, D.B. (1996). Comparison of algorithms for solving parabolic wave equations. J. Acoust. Soc. Am., 100, 178-182.

[12] Gray, L.M. and Greeley, D.S. (1980) Source level model for propeller blade rate radiation for the world's merchant fleet. J. Acoust. Soc. Am., 67(2):516– 522.

[13] MAN diesel & turbo. Basic principles of ship propulsion. Dec 2011.

[14] Gassmann M, Wiggins SM, Hildebrand JA. (2017) Deep-water measurements of container ship radiated noise signatures and directionality. J Acoust Soc Am. Sep; 142(3):1563-1574.

Publication III

174th Meeting of the Acoustical Society of America

New Orleans, Louisiana

4-8 December 2017

Underwater Acoustics: Paper 4aUW2

Assessment of the proportion of anthropogenic underwater noise levels in passive acoustic monitoring

Mirko Mustonen
Department of Civil Engineering and Architecture, Tallinna Tehnikaulikool, Tallinn, Harjumaa, 19086, ESTONIA; mirkomustonen@gmail.com

Aleksander Klauson, Julia Berdnikova and Mihkel Tommingas
Tallinna Tehnikaulikool, Tallinn, Harjumaa, 19086, ESTONIA; aleksander.klauson@ttu.ee; julia.berdnikova@ttu.ee; mihke.tommingas@ttu.com

The marine environment faces a pressure from the increasing shipping intensity in the form of rising levels of continuous anthropogenic underwater noise. Current underwater noise monitoring guidelines advise to measure the long-term trends in the overall noise levels in the frequency bands where ship noise is most prevalent. However, the natural noise is omnipresent and prolongs the time period required for the detection of statistically significant trends in the overall noise. The monitoring efficiency can be improved by finding the proportions of the anthropogenic and the natural noise levels and by measuring the changes in the proportions over time. These proportions can be found by differentiating between the different types of ambient noise in the recordings according to both proximity of the ships and the variability of the environmental conditions. This is achieved by using the AIS ship traffic data along with the ship noise detection algorithms. The AIS data enables determination of the position of ships around a noise monitoring location and calibration of the ship noise detection algorithms. The results and the methods are presented for the passive acoustic monitoring in the Baltic Sea and applicability of the described methods are discussed.

1. INTRODUCTION

The anthropogenic underwater sound has been recognised as a possible threat to marine life in the Marine Strategy Framework Directive[1] (MSFD). In order to quantify this threat, the European Union member states are required to carry out the monitoring of the underwater sound levels. Long-term monitoring of the ambient sound can give some insight whether the measured sound levels are increasing, decreasing or staying the same. An increase in the long-term measured sound levels would indicate a possible deterioration of the marine habitats. The drawback in this reasoning is that long-term changes can take a long time to measure. According to Merchant *et al.*,[2] it would take as long as three decades to find a statistically significant trend of 3 dB per decade. Meanwhile, the long-term monitoring does not differentiate between the natural and the anthropogenic sound, and therefore any of the detected changes cannot be directly linked to changes in either of these categories.

The sources of natural underwater sound are mainly wind driven surface waves, rain, thunder, seismic activities, etc. An ensemble of their sounds covers a wide frequency range starting from 1-5 Hz for seismic events and up to 10 kHz for rain.[3] In the Baltic Sea, less frequently occurring natural sounds are the vocalizations of marine animals. The best known Baltic Sea vocalizing animals are mammals like harbour porpoise and seals. They mostly use higher frequencies that reach up to 5 kHz for ringed seals[4] and 130 kHz for porpoises.[5] Baltic Sea fishes - Atlantic herring and Atlantic cod - are also known to vocalize. The cod produces low frequency grunts between 45 to 90 Hz and click sounds at a peak frequency of 6 kHz. While the herring is known to produce a pulsed chirp with centroid frequencies ranging from 3 to 5.1 kHz.[4]

The main continuous anthropogenic underwater sound sources in the Baltic Sea are commercial maritime traffic and, in a lesser extent, offshore construction. Maritime traffic in shallow watered seas contributes most in the frequency range 40-200 Hz.[6] The MSFD requires to monitor the continuous underwater sound in two one-third octave bands with the center frequencies of 63 Hz and 125 Hz. These bands are considered good indicators for the abundance of shipping noise.[1]

The aim of this paper is to demonstrate detection algorithms based method for differentiating between the natural and the anthropogenic in the sound monitoring data. The differentiation enables the calculation of the increase in the median sound level due to the presence of ships. Measuring this increase over time might give a more meaningful and faster approach for the assessment of the pressure proposed by the continuous anthropogenic underwater noise. The differentiation might also help to determine the amount of ships in the monitoring area that do not use the Automatic Identification System (AIS). Estimating the number of these ships might help to make more precise sound maps in the future.

2. SOUND MONITORING LOCATIONS

A large sound monitoring effort in the Baltic Sea was launched in 2014 in cooperation with Sweden, Denmark, Germany, Poland, Estonia, and Finland. The monitoring was part of the Life+ project "Baltic Sea Information on the Acoustic Soundscape" (BIAS).[7] Each participating country was responsible for measuring the sound in a number of the total 36 locations for the whole year of 2014. This paper is based on the month of January data from four Estonian BIAS sound monitoring locations. Figure 1 shows these monitoring locations alongside the AIS based maritime traffic
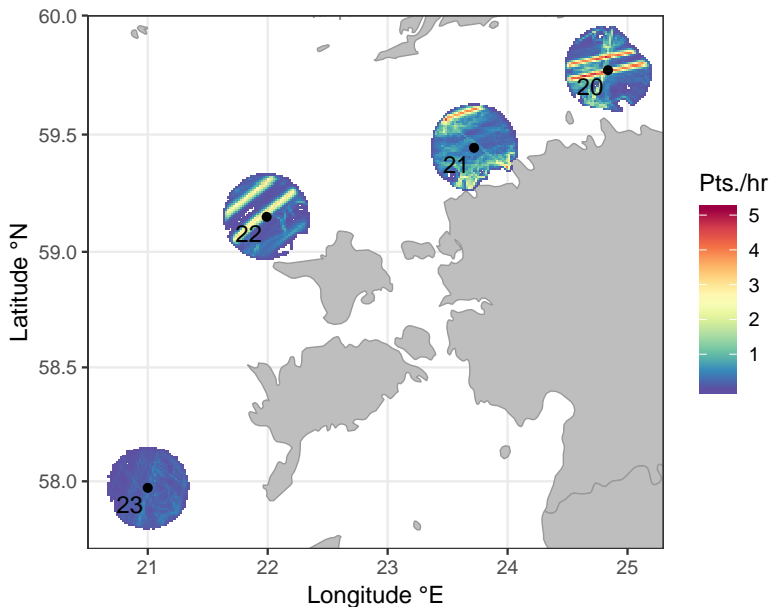
Figure 1: Mapped Estonian BIAS sound monitoring locations (20, 21,22, 23). The coloured circles show the averaged number of AIS based ship location points per hour in January 2014.

densities. The AIS position reporting is uneven in time and depends on the ship's speed, rate of turn and type of the onboard AIS transceiver. Therefore, the AIS position data was time regularized for better synchronisation with the other data. The ship traffic densities in Fig. 1 show the position of the main shipping lanes and the relative traffic intensity on these lanes. The sound monitoring location 20 had the most intense shipping traffic, followed by location 22. The maritime traffic was sparsest around the monitoring location 23. Therefore, according to the abundance of shipping, the expected proportion of anthropogenic noise should be highest in location 20 and lowest in location 23.

The sound monitoring locations 20 and 21 are situated in the Gulf of Finland and are in a more sheltered waters. In contrast, the Baltic Proper locations 22 and 23 are in a more open sea environment. This is confirmed by the long-term wave climate map of the Baltic Sea,[8] which shows higher long-term significant wave heights in locations 22 and 23 as compared to the Gulf of Finland locations. The natural ambient sound levels are known to be dependant on the wind speed.[6] Therefore, at a given time period, the wind speed data can be used as a proxy for the assessment of the natural sound levels. Figure 2 shows the wind roses based on SMHI MESAN data for the four monitoring locations during January 2014. The wind rose plots show that:

- the prevailing wind speeds in location 23 were likely the highest among the locations and prevailing wind direction was from the east-southeast direction,

- the most common sea state in location 23 was 5 on the Beaufort scale,
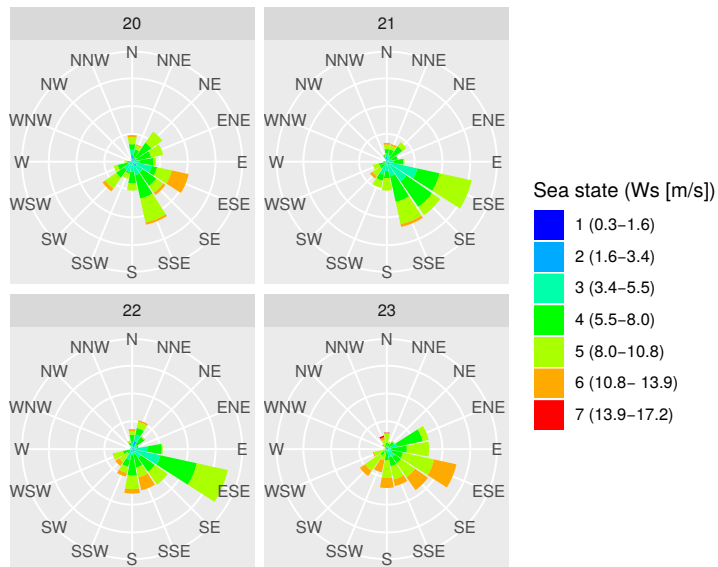
Figure 2: Wind rose plots for the four sound monitoring locations during January 2014. The modelled wind data is from Swedish Meteorological and Hydrological Institute (SMHI).

- according to the SMHI data, the lowest prevailing wind speeds occurred in location 21.

3. METHODS

The results of this paper are based on the analysis of the measured data obtained during the underwater sound monitoring. The setup of the Passive Acoustic Monitoring (PAM) rig is described in Ref 9. The rig had a Wildlife Acoustics SM2M[10] marine submersible recorder equipped with a omnidirectional hydrophone located at approximately 3 m from the sea bottom. The SM2M records all ambient sound including the natural and the anthropogenic component. Separation of the two in sound monitoring could help to assess the proportion of the anthropogenic noise that can adversely affect marine environment. This paper demonstrates several methods for this differentiation based on detection algorithms. Next, the applied detection algorithms are briefly described.

A. DETECTION USING AIS DATA

To differentiate the anthropogenic sound, the AIS ship positions data can be used. From the time regularised ship positions and the sound monitoring data, it is possible to estimate the audible distance of passing ships. The term 'audible distance' means the distance at which ships are audible in the sound recordings. If the audible distance is known, the sound data can be separated into time periods of the anthropogenic shipping sound or the natural sound according to the AIS data. However, this method has several drawbacks. One of them is the possibility of having
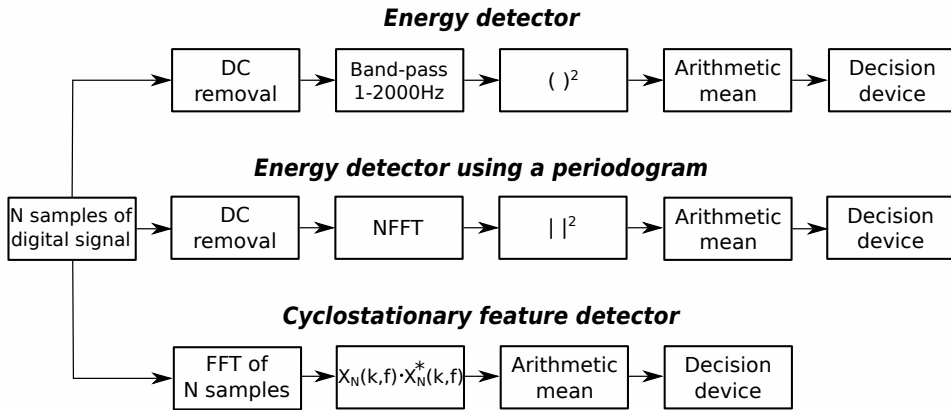
Figure 3: Block diagrams of the three anthropogenic sound detectors.

ships without AIS in some areas. In this case, some part of the anthropogenic sound would be incorrectly classified as natural. The second drawback is the difference in the source levels of ships, which makes the determination of the audible distance difficult. Another complicating aspect is the changing natural ambient sound level. An elevation in the sea state should bring about a higher natural ambient sound level and due to masking, a decrease in the audible distance of ships. Also, when the analysed time period extends over different seasons, the changes in the underwater sound propagation conditions have to be considered. As only the data from one month was analysed, the seasonal changes should not affect the presented results.

B. DETECTION USING SOUND MONITORING DATA

The long-term PAM produces large amounts of data that have to be stored and processed. The 1/3-octave band sound pressure level values required by the MSFD offer a good data compression when compared to the raw data. However, this compression can lead to the loss of some important information that could help to identify the anthropogenic noise. The following three signal detection methods are used: energy detector, energy detector using a periodogram, and cyclostationary feature detector. The three detectors were implemented and selected by M.Tomingas. The threshold selection process described in this paper was implemented by the main author.

i. Energy detector

This detector calculates the energy value associated with the recorded sound data over a chosen number of samples and frequency range. Figure 3 shows a block diagram with the main parts of the energy detector algorithm. The number of samples chosen for processing was N = 32000, which corresponded to 1 second of the recorded sound (sampling frequency was 32 kHz). At the next step, the DC bias of the N samples was removed and a band-pass filter for the frequency range 1-2000 Hz was applied. This range has been chosen as most representative for the broadband ship

noise. The arithmetic mean of the squared result is considered as the energy value of a 1 second length recorded signal. Therefore, the energy value is determined as the mean square of the 1-2000 Hz band-passed sound recording data. After the energy value for a 1 second of data is calculated, the outcome is compared with a threshold value. The setting of the threshold values is discussed later, similar to all the three detectors. According to the outcome of the comparison, the energy value is categorized as likely to be anthropogenic or natural.

### ii.   Energy detector using a periodogram

The energy detector using a periodogram is similar to the previous one; it differs by being implemented in the frequency domain, instead of the time domain. Diagrams in Fig. 3 show that the two methods formally differ only in two steps, the data sampling and the DC removal being the same for both of the detectors. Following the DC removal, the numerical fast Fourier transform (NFFT) was applied to the 1 second length recorded sound data. The outcome of the NFFT is N complex numbers; therefore, their modulus was found before squaring. The following steps are again identical to the previous detector.

iii.   Cyclostationary feature detector

This detector is intrinsically different from the others. The first two detectors are based on thresholding the intensity of the recorded sound within a chosen frequency band. The cyclostationarity feature values are related to the periodicities in the sound intensity instead of the intensity value itself. A ship propeller's cyclic movement creates a periodic cavitation process that has an amplitude modulated acoustic signature.[11] At the same time, the spectral content of the cavitation is broadband.[12] It can be assumed that the natural sources of an underwater sound will produce a stationary signal while ships produce predominantly a cyclostationary signal. Therefore, finding periodicities in the changes of the amplitude, i.e. the cyclostationary feature values of the recorded sound, is an attractive choice for the detection of ship noise. Figure 3 shows the block diagram of the implementation of the cyclostationary feature detector. Initially, the fast Fourier transform of N samples was performed. Thereafter, the N complex values from the Fourier transform were multiplied with their complex conjugates. These two steps are equivalent to the calculation of the Fourier transform of the signal's autocorrelation. Averaging this result gives the cyclostationarity value for a given time period of the recording.

iv.   Setting the thresholds

An important step in the implementation of the three detectors is to set their threshold values. This was done with the help of the AIS and SMHI modelled wind speed data. Time periods where no AIS signals were emitted at the audible distance from the monitoring location were used to calculate characteristic values attributable to the natural sound. The least squares method was used to fit a linear relationship between the wind speed and the logarithm of each calculated characteristic. The threshold values for a given wind speed were set as an exceedance of the linearly fitted value by two standard deviations. If the calculated characteristic value exceeds the threshold value, the recorded sound will be marked as anthropogenic. Figure 4 illustrates the wind dependance of the energy value and the setting of the threshold according to the linear least squares fit of the dependance. The peaks in the middle of this figure can be attributed to close passages
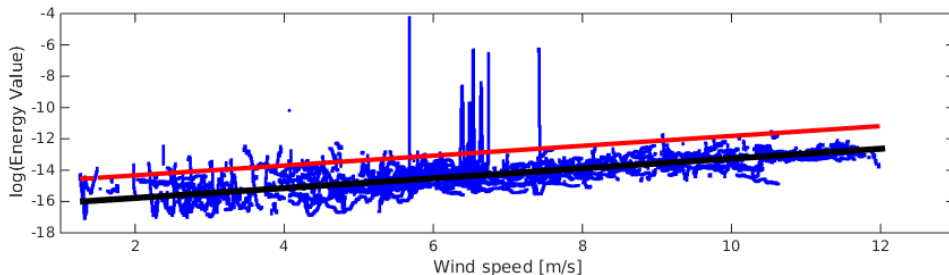
Figure 4: Setting the threshold for the calculated energy values (no AIS signal closer than 7.5 km) in location BIAS 20 January 2014. Blue dots represent the dependance between the modelled wind speed and the calculated energy values. The black line is the linear least squares fit for their dependance. Red line marks the calculated energy threshold values.

*Table 1: Detection score values and their corresponding sound categories.*

Detection score	Sound category
0,1	Natural
2	Mixed
3,4	Anthropogenic

of ships that did not use AIS. The exceedances of the threshold in lower wind speeds indicate that linear approximation might be not the model for lower sea states. Another interpretation of this exceedance can be related to the increase of the audible distance at the lower sea states.

C.   USING AIS DETECTION ALONG WITH SOUND DETECTION METHODS

As described earlier, the AIS detection has its faults. Also, the detection using only the sound monitoring data can yield false results due to the errors produced by setting the threshold. Therefore, it seems reasonable to use the ensemble of AIS detection along with the sound detection methods. All of the four detection methods were averaged to produce a binary detection value for every 20 seconds where zero corresponds to no detection (natural noise) and one to the detection of anthropogenic sound. The four different detection values were combined to give the overall detection score. Therefore, this score ranges from 0 to 4. According to the detection score, the recorded sound was categorized into three different groups (Table 1).

Table 1 shows the categorization for the different detection scores. If none or only one of the detectors marks the sound as anthropogenic, it is considered as natural sound. Sound is considered as anthropogenic in case at least three of the detectors show it. The mixed category is assigned when only half of the detectors sense the sound as anthropogenic. The chosen categorization should ensure with a high degree of certainty that no natural sound is categorized to be anthropogenic. Although it has to be stressed that the natural category might have anthropogenic components. This is due to the threshold for the anthropogenic noise detection being relatively high compared to the linear fit of the dependance between wind speeds and sound values.
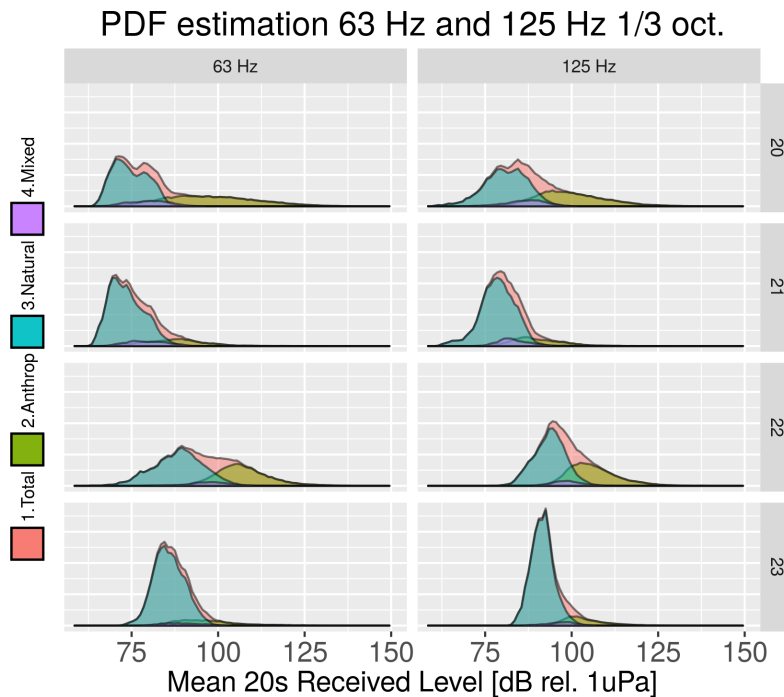
Figure 5: The estimated PDFs in the 63 Hz and 125 Hz 1/3-octave bands in the four sound monitoring locations and the decomposition of the PDF-s into different categories. The overall or total PDFs in the background are with pink color. The overall PDF is decomposed into the anthropogenic, natural and mixed categories. The anthropogenic is colored green, the natural - blue and the mixed - purple. The apparent difference in the decomposed areas indicates the proportions of the different categories.

4.   RESULTS

The detection methods were used to categorize each 20 second length of the recorded sound data. The categorization was applied to the 1/3-octave band SPL values in the four previously discussed monitoring locations. A concise presentation of the SPL values can be given by the estimated probability density function (PDF). The area under the PDF equals one and the ordinate values correspond to the likelihood of occurrence for the SPL values on the abscissa. The maximum of the PDF is the most frequently occuring SPL value, also known as the mode.

Figure 5 shows the decomposition of the sound pressure level PDFs in four sound monitoring locations. As expected, the sound levels categorized as "mixed" are located at the PDF just between the natural and the anthropogenic. It can be seen that sound categorized as "mixed" is considerably less frequent than the other two categories. The decomposition also reveals how the abundance of ships affects the monitored sound levels. The long right-sided tails of the overall sound level PDF show the presence of close passing ships and the thickness of the tail is dependant on the ship traffic

density. In location 22, the overall PDFs have bimodal shape with one of the modes attributable to the presence of ships. In location 20, the bimodality occurs in the natural sound levels. The PDF of the overall sound levels is closest to the natural category in location 23 that had the sparsest ship traffic.

Besides providing a good visual overview, the increase in the SPL values caused by the presence of ships can be quantified. The numerical increase is defined here as the difference between the median level of the decomposed natural and the overall SPL values. The increase of the median SPL value due to shipping was 1 dB in the sound monitoring locations 21 and 23 for both of the analysed 1/3-octave bands. The increase in the location 20 was estimated to be 5 dB. In location 22, the increase was estimated as 5 dB in the 63 Hz and 3 dB in the 125 Hz 1/3-octave band.

The decomposed natural sound levels of locations 20 and 21 are expectedly similar as they are situated in the same region. The highest natural sound levels were found in locations 22 and 23. The mean natural sound level and dispersion in location 22 were higher than in location 23, although the SMHI wind speed values in location 23 were higher.

5. DISCUSSION

It should be noted that the proposed method can still miscategorize some anthropogenic noise as natural. Also, calculating additionally the energy and the cyclostationarity values would have to be justified by significantly better differentiation when compared to using some of the already available 1/3-octave band values. In theory, the cyclostationary feature detector should yield significantly better results when compared to other detectors. Nevertheless, the cyclostationarity feature value was found to be dependent on the wind speed. This can be partly explained by the increase in the masking effect with increasing natural sound level. Another drawback of the cyclostationary feature detector was its slow calculation speed as compared to the other detectors.

6. CONCLUSIONS

The presented method demonstrates a potential for differentiating time periods in the sound monitoring with the prevailing natural or anthropogenic sounds. By application of the differentiation procedure, an increase in the median of the MSFD 1/3-octave bands due to the presence of ships close to busy shipping lanes was estimated to be in the order of 5 dB and 1 dB in the locations with distant or sparse ship traffic. The true value of the increase of median SPL might be even higher with the improved detection of time periods with natural sound. Also, the estimated natural sound levels were found to be similar in areas with similar wave climate.

ACKNOWLEDGMENTS

REFERENCES

[1] Commission Decision (EU) 2017/848 of 17 May 2017

[2] Merchant, Nathan D. and Brookes, Kate L. and Faulkner, Rebecca C. and Bicknell, Anthony WJ and Godley, Brendan J. and Witt, Matthew J. "Underwater noise levels in UK waters," *Scientific Reports* **6**, (2016).

[3] Wenz, Gordon M., "Acoustic ambient noise in the ocean: spectra and sources," *The Journal of the Acoustical Society of America*, **34**, 1936–1956, (1962)

[4] HELCOM, "Noise Sensitivity of Animals in the Baltic Sea," 76, (2016)

[5] Clausen, Karin Tubbert and Wahlberg, Magnus and Beedholm, Kristian and Deruiter, Stacy and Madsen, Peter Teglberg, "Click communication in harbour porpoises Phocoena phocoena," *Bioacoustics*, **20**, 1–28, (2011)

[6] Carey, William M. and Evans, Richard B., "Ocean ambient noise: Measurement and theory," *Springer Science & Business Media*, (2011)

[7] Sigray, Peter and Andersson, Mathias and Pajala, Jukka and Laanearu, Janek and Klauson, Aleksander and Tegowski, Jaroslaw and Boethling, Maria and Fischer, Jens and Tougaard, Jakob and Wahlberg, Magnus and others, "A Regional Management of Underwater Sound in the Baltic Sea," *The Effects of Noise on Aquatic Life II*, 1015–1023, (2016)

[8] Räämet, Andrus and Soomere, Tarmo, "The wave climate and its seasonal variability in the northeastern Baltic Sea," *Estonian Journal of Earth Sciences*, **59**, 100–113, (2010)

[9] Verfuß, U. K. and Andersson, M. and Folegot, T. and Laanearu, J. and Matuschek, R. and Pajala, J. and Sigray, P. and Tegowski, J. and Tougaard, J., "BIAS Standards for noise measurements – Background information, Guidelines and Quality Assurance," (2014)

[10] Wildlife Acoustics, "Product User Guides and Supplements," URL: https://www.wildlifeacoustics.com/support/documentation

[11] Da Costa, Evandro L., "Detection and Identification of Cyclostationary Signals," Naval Postgraduate School Monterey CA, (1996)

[12] Hanson, David and Antoni, Jerome and Brown, Graham and Emslie, Ross, "Cyclostationarity for ship detection using passive sonar: progress towards a detection and identification framework," *Proceedings of Acoustics*, (2009)

Publication IV

SCIENTIFIC REPORTS

natureresearch

OPEN

# Spatial and Temporal Variability of Ambient Underwater Sound in the Baltic Sea

Mirko Mustonen [1], Aleksander Klauson[1], Mathias Andersson[2], Dominique Clorennec[3], Thomas Folegot[3], Radomił Koza[5], Jukka Pajala[4], Leif Persson[2], Jarosław Tegowski[5], Jakob Tougaard [6], Magnus Wahlberg[7] & Peter Sigray[2]

During last decades, anthropogenic underwater sound and its chronic impact on marine species have been recognised as an environmental protection challenge. At the same time, studies on the spatial and temporal variability of ambient sound, and how it is affected by biotic, abiotic and anthropogenic factors are lacking. This paper presents analysis of a large-scale and long-term underwater sound monitoring in the Baltic Sea. Throughout the year 2014, sound was monitored in 36 Baltic Sea locations. Selected locations covered different natural conditions and ship traffic intensities. The 63 Hz, 125 Hz and 2 kHz one-third octave band sound pressure levels were calculated and analysed. The levels varied significantly from one monitoring location to another. The annual median sound pressure level of the quietest and the loudest location differed almost 50 dB in the 63 Hz one-third octave band. Largest difference in the monthly medians was 15 dB in 63 Hz one-third octave band. The same monitoring locations annual estimated probability density functions for two yearly periods show strong similarity. The data variability grows as the averaging time period is reduced. Maritime traffic elevates the ambient sound levels in many areas of the Baltic Sea during extensive time periods.

The influence of the sounds from increasing human activities pose considerable risks for the overall health of our seas. Anthropogenic underwater sound is recognized as a pollutant that may have long-term detrimental effects on marine ecosystems. Among these effects are the reduction of communication space[1–3], increase in stress levels and perturbation of development of marine species[4]. At the same time, the list of marine animals known to be sensitive to sound has been ever extending. Now it is ranging from marine mammals and fishes to crustaceans and invertebrates. As an example, cod can perceive noise generated within a frequency range of 100–1000 Hz and display a heightened cortisol plasma level with the potential negative impacts on their spawning performance[5]. Another recent study demonstrated reduced foraging in harbour porpoises caused by loud ship noise[6].

EU's Marine Strategy Framework Directive (MSFD) was adopted in June 2008 with the aim to achieve Good Environmental Status (GES) and maintaining the marine biodiversity of European marine habitats by the year 2020[7]. The directive sets qualitative descriptors for GES. Among these, Descriptor 11 (D11) concerns energy introduced into the marine environment, including underwater sound, which should be at levels that do not adversely affect the marine environment. The Technical Sub-Group on Underwater Noise (TSG Noise) issued a set of recommendations[8] and monitoring guidance specifications[9]. Another monitoring guide has been issued by NPL[10]. Concerning the criterion for the continuous low-frequency underwater sound, it is stated that it should be monitored in two one-third octave bands (here and after base 2) with the center frequencies of 63 Hz and 125 Hz[11]. The sound pressure level (SPL) of these frequency bands has been chosen due to being a proxy for the abundance of the continuous low-frequency anthropogenic sound, mostly generated by commercial vessels.

[1]Tallinn University of Technology, School of Engineering, Tallinn, 19086, Estonia. [2]Swedish Defence Research Agency, Stockholm, SE-164 90, Sweden. [3]Quiet-Oceans, Plouzané, 29280, France. [4]Finnish Environment Institute, Helsinki, FI-00251, Finland. [5]University of Gdansk, Institute of Oceanography, Gdynia, 81-378, Poland. [6]Aarhus University, Department of Bioscience, Roskilde, 4000, Denmark. [7]University of Southern Denmark, Department of Biology, Odense M, 5230, Denmark. Mathias Andersson, Radomił Koza, Leif Persson and Jarosław Tegowski contributed equally. Correspondence and requests for materials should be addressed to M.M. (email: mirko. mustonen@ttu.ee)
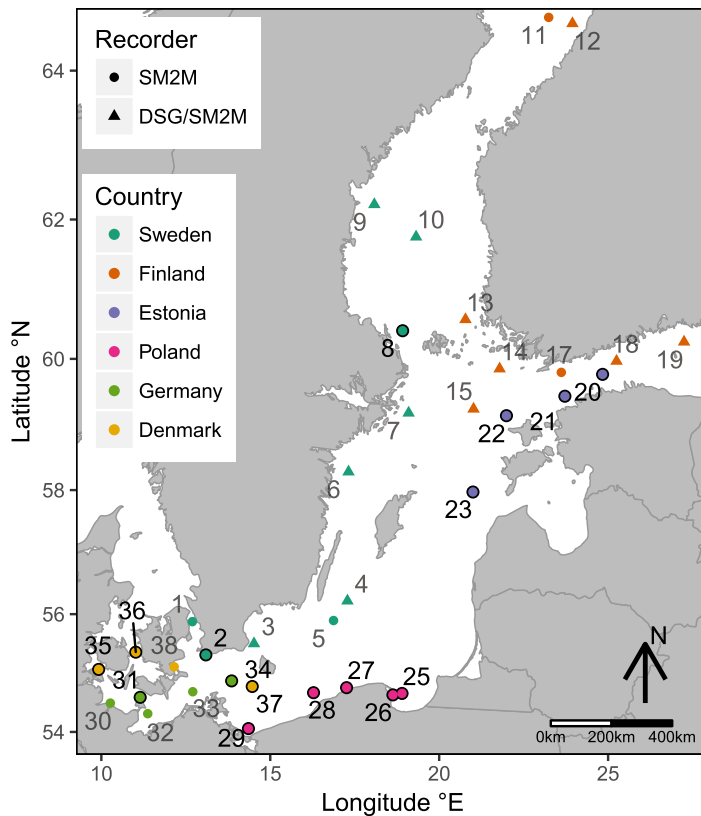
Figure 1. Underwater sound monitoring locations of the BIAS-project. The locations where SM2M marine submersible recorder was used throughout the sound monitoring are depicted with a circular marker and locations with alternate deployments of the DSG Ocean recorder with triangular markers. More details on the measurement equipment can be found in the methods section of this paper. The numbers of the monitoring locations analysed in this paper are highlighted with a darker colour.

Setting up sound monitoring programmes is the first step in the assessment of the levels of anthropogenic underwater sound in marine habitats. Initially, they help to establish the baseline levels of sound. Both deep-ocean observatories[12,13] and autonomous recording systems[14–16] have been used for monitoring. Ideally the monitoring of underwater sound can be imagined to be a network of cabled monitoring stations that sufficiently cover a given marine area. However, costs limit this kind of ambition and a realistic monitoring programme will entail only a few monitoring locations. This has the drawback of not being representative of the whole marine area. In order to circumvent this limitation, sound propagation modelling is commonly used in combination with the monitoring. Modelling helps to estimate the spatial extent of sounds from various anthropogenic sources (mainly ships) in a given marine environment[17,18].

In order to assess the levels of underwater sound in a big marine area that is the Baltic Sea a joint international cross-bordering effort is needed. First project of this kind was Life+ "Baltic Sea Information on the Acoustic Soundscape" (BIAS) launched in 2012[19]. The main aim of the BIAS project was the characterisation of the Baltic Sea soundscape. The modeled soundscape was mapped and a planning tool for using the maps developed[20]. Therefore, the monitored sound data was primarily used to calibrate and ground truth the sound propagation modelling. Although the modelling provides information about spatial sound level distribution, the data gathered during a sound monitoring programme are potentially a valuable source of additional information. When compared to modelling, it possesses higher resolution and is the most accurate representation of the actual sound levels in a location. Therefore, the data from sound monitoring in a marine area are worthy of being analysed separately and more thoroughly. There is a large number of open questions related to long-term monitoring of sound that need to be answered. Consequently, this paper aims to provide a detailed analysis of the extensive BIAS sound monitoring data. Moreover, the recorded data can serve as a baseline of the Baltic Sea underwater ambient sound that can be used for tracking changes in the following years.

No.	Country, Loc. Name	Lat.°N	Lon.°E	Depth [m], Seabed Substrate
2	SWE-Trelleborg	55.3210	13.0950	23, Coarse substrate
8*	SWE-Sea of Åland	60.4158	18.9183	45, Mixed Sediment
20	EST-GoF, Tallinn	59.7715	24.8397	75, Mud to Muddy Sand
21	EST-GoF, Paldiski	59.4416	23.7276	89, Mud to Muddy Sand
22	EST-Hiiumaa	59.1499	21.9901	70, Mud to Muddy Sand
23	EST-Saaremaa	57.9689	21.0035	88, Mud to Muddy Sand
25	POL-Gulf of Gdansk	54.6665	18.9001	80, Mud to Muddy Sand
26	POL-Puck Bay	54.6413	18.6310	30, Mud to Muddy Sand
27	POL-Łeba & Rowy	54.7649	17.2589	18, Sand
28	POL-Darłowo-Ustka	54.6793	16.2813	41, Coarse substrate
29	POL-Świnoujście	54.0602	14.3549	12, Sand
31	GER-Fehmarn Belt	54.5997	11.1497	27, Sand/Mud to M-Sand
34	GER-Arkona Basin	54.8803	13.8574	44, Mud to Muddy Sand
35	DNK-Little Belt	55.0755	9.92133	30, Mud to Muddy Sand
36	DNK-Great Belt	55.3672	11.0193	27, Mixed/Mud to M-Sand
37	DNK-Rønne Banke	54.7853	14.4673	20, Sand/Coarse substrate

Table 1. Selected monitoring locations from the BIAS-project. Seabed substrate data originates from EMODnet (http://www.emodnet-geology.eu/). The asterisk behind location 8 is to point out significantly lower data coverage (May to December 2014, coverage 64% against 88–100% for the other locations).

BIAS-project and Sound Monitoring Locations

An extensive BIAS sound monitoring programme was launched by the joint effort of scientists from six Baltic Sea countries - Sweden, Denmark, Germany, Poland, Estonia, and Finland. In shallow watered seas this programme stands out for its longevity and spatial coverage. Figure 1 shows the sound monitoring locations of the BIAS-project. The locations were chosen to cover different depths, seabed substrates and ship traffic intensities. The numbering of the monitoring locations follows a clockwise direction around the coast of the Baltic Sea. The numbering starts in the Øresund Strait near the coast of southern Sweden and finishes with location number 38 in the Faxe Bay, Denmark. A large amount of data has been collected from all these measurement locations during the period from 1 January 2014 to 31 December 2014. For the sake of brevity we will restrict the discussion and analysis to the data from some specific but spatially representative monitoring locations listed in Table 1. This table shows that the water depth of the locations varies from 12 m to 89 m and a variety of seabed substrates. Ice cover did not occur in the selected monitoring locations during the winter of 2014. This was affirmed by the SMHI open-access data from HIROMB BS01 oceanographic forecast model.

The distance to the closest shipping lane as well as the intensity of ship traffic are two important parameters that affect the continuous low frequency anthropogenic sound levels. The proxy of the shipping intensity was taken to be the normalised number of time regularised automatic identification system (AIS) ship distances from the monitoring location. The AIS data for the BIAS project was provided by the Helsinki Commission (HELCOM). The time regularisation of the AIS data was necessary as the intervals for the systems location reporting are irregular in time. The reporting frequency is dependant on the rate of turn and speed of the ships as well as the class of AIS transceiver. The time regularised AIS ship distances were normalised to give the mean number of ships most likely to be present at any time during 2014. Figure 2 shows the differences in the mean number of ships near monitoring locations. Locations 37 (Rønne Banke) and 23 (Saaremaa) stand out as having the lowest shipping intensities in the radius of 20 km where on average only one vessel was present. Figure 2 also shows that in location 37 most of the ships occured in the distance interval 15–20 km. In contrast location 31 (Fehmarn Belt), was exposed to the most intensive shipping. In this location, on average two vessels were present at any given time within 5 km and more than eleven vessels within 20 km. Besides the shipping no other significant anthropogenic sound sources that could have affected the long-term sound levels were present during the monitoring in the selected locations.

Results

Analysis of spatial ambient noise variability. Analysis of the spatial variability of ambient noise is based on the sound measurements in the selected BIAS sound monitoring locations. The underwater ambient sound was expected to be a mixture of the natural sounds, mostly caused by wind driven waves, and the anthropogenic sounds, mostly produced by commercial ship traffic. The spatial variability of the ambient sound arises from the spatial variability of the dominant sound sources as well as from the sound propagation conditions that are dependant on the water column properties, changing bathymetry and seabed substrates. As the Baltic is a shallow sea with average depth of 55 meters its temporal and spatial variability in the sound pressure level is expected to be larger than in the deep water. Also it is expected the high frequency sound contribution should be proportionally more important than in the deep water. The latter is explained by the cut-off phenomena reducing sound propagation in the lower frequencies[21,22]. In the Baltic Sea, the spatial variation is also caused by the occurrence of ice. While the Southern Baltic Sea is rarely frozen, the Bay of Bothnia and various other sea areas freeze annually. The extent of the ice cover can vary greatly with each year. The soundscape of the sea when covered with ice is
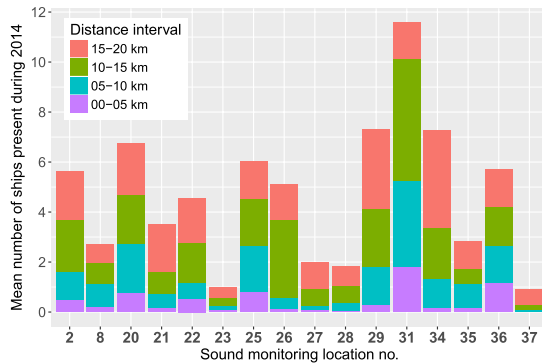
Figure 2. Average ship traffic intensity at different distance intervals within 20 km maximum range from the monitoring locations in 2014. The intensity calculation is based on 20 second time-regularised ship location data from the automatic identification system (AIS). The mean number of ships corresponds to the most likely number of ships within a distance interval at a randomly selected time during 2014.

expected to be very different when compared to the period when the sea is open[23]. This change was recorded in the middle of the Bay of Bothnia in the BIAS sound monitoring location 11 during the winter of 2016. Figure 3 shows 10 dB decrease in the SPL in the 2 kHz one-third octave band with the growing ice cover. The true decrease might be even higher as the recorders self-noise level restricted measuring the SPL lower than 70 dB re 1 μPa in this one-third octave band. The self-noise levels of the recorder are presented the methods section in Table 2. The presented ice cover data originated from the The Finnish meteorological Institute.

The tides are known to be a source of 'pseudo-noise' caused by turbulence around the hydrophone during tidal flow that contributes significantly at lower frequencies[16,24]. The Baltic Sea is shallow with brackish water and has been called a practically non-tidal sea by some authors[25] and thus the pseudo-noise is not expected to occur. Another important part of the underwater soundscape is often contributed by marine animals. A well-known example in warm coastal waters is the impulsive biological noise produced by the snapping shrimp[26]. The biological contribution in the Baltic Sea long-term sound monitoring is expected to be mostly negligible, especially in its northern parts.

The annual underwater SPL values in different locations are concisely presentable by the estimated probability density function (PDF). A good way to compare different probability density functions of the one-third octave band SPL values is to compile them in the form of violin plots. As common for probability density functions, the area of each violin plot equals unity. The abscissa of the plots shows the probability for the occurrence of the SPL value displayed on the vertical axis. Various statistical measures are added to the violin plots for making them visually comparable and readable. The added statistical measures are the geometric mean (GM) and exceedance levels L5, L10, L25, L50, L75, L90, and L95. In the case of sound monitoring, exceedance level L95 is a low SPL value that is exceeded 95% of the time. Therefore, L95 can be related to the infrequent quieter natural sound levels. The exceedance level L5 is the SPL value that is exceeded only 5% of the time. In most cases it is related to occasional louder events when vessels pass close by the monitoring location. The statistical analysis presented hereafter was performed using bespoke software written in the programming language R[27].

Figures 4–6 show the annual estimated PDFs as the violin plots for the selected monitoring locations and frequency bands. The SPL values in the two lower one-third octave bands lie mostly between 65 and 115 dB, while the 2 kHz one-third octave band SPL values are mostly between 70 and 100 dB re 1 μPa. In 63 Hz and 125 Hz one-third octave bands (Figs 4 and 5), the measured SPL values are highly dependent on the sound monitoring location. The difference between the median SPL values of the quietest location, no. 8 (Sea of Åland) and the loudest location, no. 31 (Fehmarn Belt), is around 50 dB for the 63 Hz one-third octave band and 40 dB for the 125 Hz one-third octave band. This observation confirms the prediction made by Urick[21] about the expected large spatial variability of the low frequency sound levels in the shallow seas. Figure 6 shows that the spatial variability is much lower for the 2 kHz one-third octave band. The difference in the median SPL values within this one-third octave band when comparing locations 26 (Puck Bay) and 31 (Fehmarn Belt) is around 15 dB. At this higher frequency band, the natural sources, i.e., wind and surface waves, dominate over the shipping noise. The difference in the dominant sources is also indicated by the fact that the lowest median SPL value was in a different location for the 2 kHz one-third octave band when compared with the lower frequency bands. However, the monitoring locations where the shipping is intense, the 2 kHz one-third octave band levels are visibly higher (31, 34 and 36).

Most of the probability density functions do not follow a normal distribution. This is confirmed by the Shapiro-Wilk test of normality[28]. According to this test, the estimated PDFs of the 63 Hz one-third octave band SPL values (Fig. 4) from locations 27, 28, 31 are the closest to a normal distribution. For the 125 Hz one-third octave band SPL values (Fig. 5), only the PDF of location 31 is close to a normal distribution. In the absence of shipping, the non-normality of the PDFs can be anticipated as the wind speeds and significant wave heights usually follow a Weibull distribution[29,30].
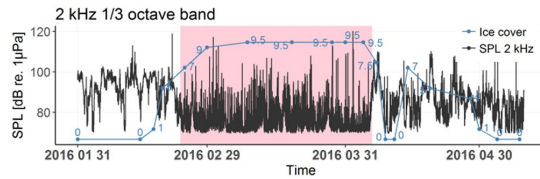
Figure 3. The effect of ice on the measured 2 kHz one-third octave band SPL in the Bothnian Bay BIAS sound monitoring location 11. The ice concentration is a fraction that expresses the sea surface ice cover in one-tenths (1/10). The complete coverage by ice corresponds to 10/10. The pink background highlights the time period when the ice concentration seems to affect the measured sound levels the most. During ice cover a wide selection of ice dynamics driven impulsive sounds is apparent. In this location the ship traffic intensity was relatively low but the recordings still contain the sounds of some ships breaking through ice.
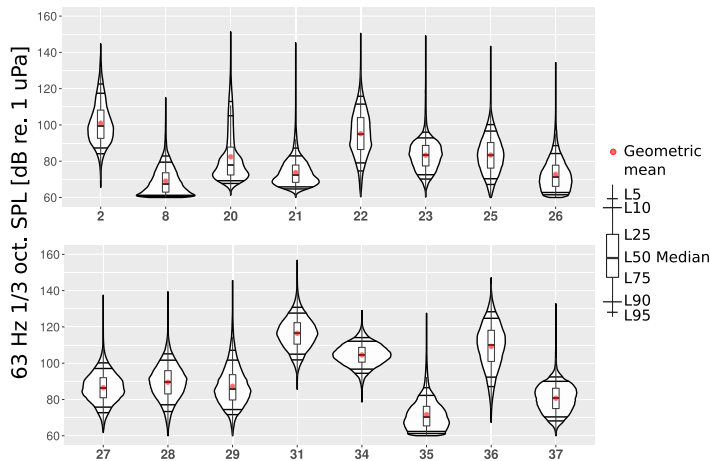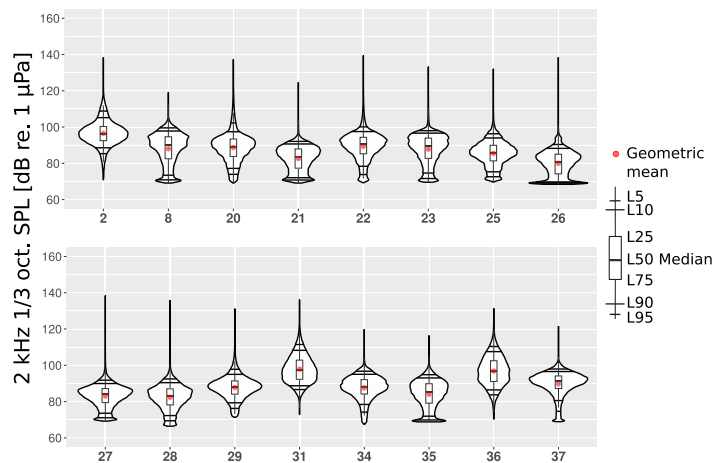

Figure 4. The estimated probability density functions of the measured SPL in sixteen different locations in the 63 Hz one-third octave band measured during the year 2014. The horizontal black lines represent L95, L90, L10, L5; the red dot marks the geometric mean (GM); the upper and the lower lines of the boxplot mark L25, L75; the thicker black line in the middle of the boxplot marks the median of the data.

Figure 4 shows that half of the 63 Hz one-third octave band PDF-s (locations 2, 8, 20, 21, 22, 26, 29, 35) are asymmetric and visibly positively skewed as they have long thin upper tail and fatter lower tail. Only one PDF (location 36) has a visibly longer lower tail. Figure 5 shows that the 125 Hz one-third octave band PDFs are more symmetric when compared to the 63 Hz one-third octave band. In this octave band, the PDFs are still mostly positively skewed. The PDF of location 37 shows the largest negative skewness in the 125 Hz one-third octave band. The long and thin upper tails of the PDF plots are related to the rarely occurring loud events that in most cases are close passages of vessels. The differences in the upper ends of the tails indicate that the recorders were not subject to significant clipping. This was also confirmed by the clipping tests performed on the data during the processing. In contrast to the lower frequency bands, the 2 kHz one-third octave band PDFs in Fig. 6 show an average negative skew. This negative skew is largest for the PDF of monitoring location 37 where the ship traffic intensity is the lowest (Fig. 2). Figure 6 also shows that the largest positive skew is in location 31 that had the highest ship traffic intensity. The overall negative skew of the 2 kHz one-third octave band indicates the dominance of natural sound sources in this frequency range.

The lower tails of the violin plots are bounded by the limit imposed by the self-noise level of the SM2M recorder standard hydrophone with no gain (Table 2). In monitoring locations 8, 26 and 35, there might have occurred relatively low SPL values, often well below the self-noise level. These low levels could not have been recorded, instead, they were replaced by the recorders self-noise values. An example of a time series of the SPL values where the noise floor was reached is presented in Fig. 3. This "piling up" of self-noise values seems to cause the local maxima apparent in lower tails of the PDFs. The SPL values that are below the self-noise can be related to the lower sea states in sheltered waters. In order to avoid hitting the noise floor equipment with lower self-noise should be used. It is important to note that while the geometric mean values are affected by occurrence of self-noise, the median or exceedance levels L5, L10, L25 remain unaffected. When the effect of the self-noise level on the violin plots is acknowledged, they are still very useful for interpreting the soundscape at a specific location.
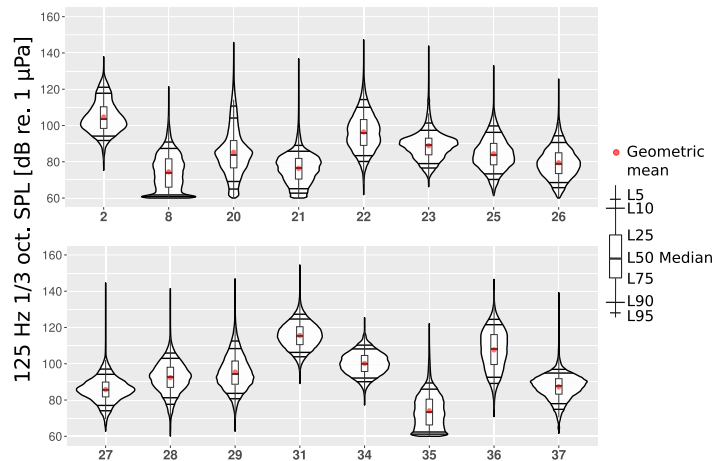
Figure 5. The annual estimated probability density functions of the SPL measured in sixteen different locations in the 125 Hz one-third octave band during the year 2014.

Figure 6. The annual estimated probability density functions of the SPL measured in sixteen different locations in the 2 kHz one-third octave band during the year 2014.

In spite of the apparent variability, some similarities in the PDFs can be found, mostly by regions and by similar conditions:

1. The highest annual SPL values in all the one-third octave bands were recorded near the Danish straits (locations 31, 36). This was somewhat expected, as Fig. 2 shows that these locations had also the highest shipping intensities among the monitoring locations. The depth at both of these monitoring locations was 27 meters. These monitoring locations were situated in the straits called Great Belt and Fehmarn Belt, which are frequently crossed by ferry-boats. Also, numerous cargo ships, tankers, including the largest ships, go through this deeper-watered route into the Baltic Proper. On top of that, seasonally, there is a high number of sailing and leisure boats.

2. The quietest locations with the lowest annual SPL values are more difficult to analyze when compared to the loudest. This is due to the aforementioned self-noise that limits the measurement of low sea state SPL values in the quietest locations. The sheltered location 26 is in the Bay of Puck (Poland) that is separated from the open sea by the Hel Peninsula. Location 35 was in a winding Danish strait the Little Belt. Although the annual 63 Hz and 2 kHz one-third octave band SPL values from these locations have relatively similar PDFs, they differ considerably in the 125 Hz one-third octave band. The quietest within the two
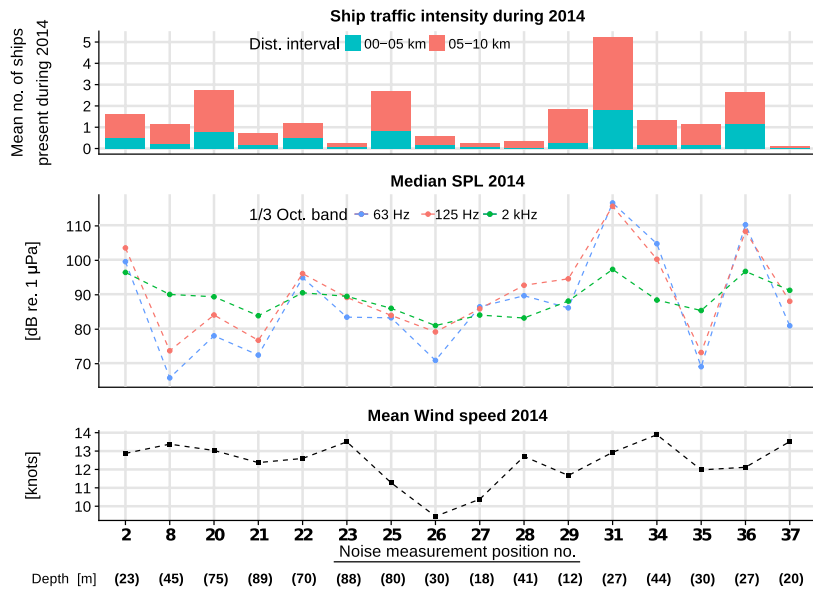
Figure 7. Median SPL one-third octave band levels at all monitoring locations in the middle along with the mean values of the ship traffic intensity on the top, mean wind speeds and the water depths in the bottom. The dashed lines joining the points are to be considered as aids for visualising the data and not as indicating the intermediate values between the locations. The wind speed data originates is the SMHI open-access data from MESAN weather analysis model.

lower frequency bands was location 8 (Sea of Åland). This does not follow any of the simple patterns as it is neither in sheltered waters nor with the lowest shipping intensity. The lowest levels in this location can partly be explained by the different data coverage, as the recordings are not available during the first four months of the year. Due to seasonal changes, these months are known to be the loudest ones. Still location 8 was the quietest when comparing the median SPL of the locations on monthly basis.

3. The locations in the Gulf of Finland (20 and 21) have similar annual PDFs for the SPL values. The waters are known to be mostly calmer than in the Baltic Proper, being protected from the South-Westward winds. Therefore, it is anticipated that the natural ambient SPL values are lower than in the Baltic Proper but higher than in sheltered waters. Locations 20 and 21 differ by the annual mean wind speed, which is lower in location 21. Also, they differ by their ship traffic intensity, which is higher in location 20, situated near busy crossing shipping lanes. Therefore, the annual SPL values at location 20 at all the frequency bands are expectedly higher when compared to location 21. The higher shipping intensity manifests itself as a longer and fatter upper tail and higher L5, L10 values in the PDFs for location 20.

4. The SPL levels in all the frequency bands for the monitoring locations in the Baltic Proper open sea conditions (2, 22, 23, 25, 27, 28, 29, 34, 37) have some considerable similarities and differences.

(a) In the Baltic Proper locations 37 and 23, overall ship traffic was lowest and the recorded sound may be considered mostly natural. The mean annual wind speed in these locations is almost the same, resulting in very similar PDFs.

(b) Locations 25, 27, 28 and 29 at the coast of Poland have quite similar PDFs. The differences in the PDFs follow loosely the differences in shipping intensities, wind speeds and depths. Locations 27 and 28 have both very low shipping intensities. The annual mean wind speed is higher and water is deeper in location 28. This anticipates the higher SPL values. When comparing location 29 with the previous locations, the shipping intensity is considerably higher, which means higher SPL levels in the 125 Hz and 2 kHz one-third octave bands. The very shallow depth of this location (12 meters) has probably constrained the higher SPL values due to the cut-off effect.

(c) Locations 2 and 22 had similar PDFs, both affected by higher annual mean wind speeds and higher intensities of shipping.

Similarities of the annual sound pressure level PDFs by regions have been presented previously in a study about the UK waters[16]. This study presented the 125 Hz one-third octave band PDFs of shorter deployments from ten monitoring locations in the North Sea.

For a better overview of the ensemble of the monitoring locations, Fig. 7 presents the annual median results for all one-third octave bands together with the depths, annually averaged shipping intensity and wind speeds. Comparison of the graphs shows the following:

- The annual median SPL values of 63 Hz and 125 Hz one-third octave bands have strong correlation. The 125 Hz one-third octave band annual median SPL values in monitoring locations are on average 3 dB higher.
- The 2 kHz one-third octave band annual median SPL values correlate weakly with the lower frequency octave bands.
- Some patterns can be noted, when looking at which of the annual median one-third octave band SPL value was highest in a monitoring location. For half of the locations (8, 20, 21, 23, 25, 26, 35, 37), the highest annual median SPL value is in the 2 kHz one-third octave band, followed by the 125 Hz and 63 Hz one-third octave bands. This order was reversed in three locations (31, 34, 36). The reversal hints at some significant differences in the overall recorded sounds spectra in locations where ship traffic is very intense.
- As expected, the two lower frequency band median SPL values seem to be more affected by the ship traffic intensity than is the 2 kHz one-third octave band.
- The median 2 kHz one-third octave band values in locations with very intense traffic are higher. Otherwise, some dependence on mean wind speeds can be noted.

Analysis of Temporal Variability in Ambient Noise

The temporal variability in the ambient noise of the Baltic Sea is known to be periodic at different time scales. Diel variations have been measured that were related to vertical migration of marine organisms in the southern part of the Baltic Sea[31]. Simultaneously AIS data analysis has shown that some shipping activities have also diel patterns. This is understandable, as ferry boats have daily schedules, fishing boats have their daily routines and so do the leisure boats and sailing ships. Preliminary analysis of our data has shown significant diel variations in the SPL values. In locations with more intense ship traffic these variations coincided with the diel changes in the number of ships present around a monitoring location.

The seasonal variability of the recorded sound is mostly related to the periodic variations in the sound speed profile of the water column. The upper layers of the water column get warmer during summer months. As a result, the sound waves refract downwards and reach the bottom, causing faster loss of the propagating acoustic energy[32]. The wind speeds and wave heights in the Baltic Sea are also known to have a seasonal periodicity, both being higher during the winter months[33]. Besides the natural sources of seasonality, some ship types have also seasonal occurrence patterns.

The seasonal variability in SPL values in the southern Baltic Sea has been measured to be in the range of 12 dB[34], or 10–15 dB[31] with greater levels during the winter. For the seasonal variability, the monthly median SPL values in all the selected monitoring locations and frequency bands were calculated and compared. As was expected, the highest monthly medians were recorded during the winter and the lowest in the summer months. The minimum in the monthly medians for all the one-third octave bands in most positions was recorded in July. The month with the highest median varied according to the frequency band. In the 63 Hz and 2 kHz one-third octave bands, the loudest month in most locations was December. As for the 125 Hz one-third octave band, in most locations, the loudest months were January and February. The difference between the medians of the loudest and the quietest was on average 10 dB. In the monitoring locations with intense shipping, the monthly medians changed less throughout the year when compared to other locations. For example, location 31 with most intense shipping had only 2 dB seasonal difference in the 63 Hz one-third octave band, 3 dB in the 125 Hz one-third octave band and 6 dB in the 2 kHz one-third octave band.

Comparison of two years of sound monitoring results in a location has the potential to estimate the plausibility of finding long-term trends. In some of the selected monitoring locations, the deployments continued after the end of the BIAS project. Two of these were locations 20 and 26. Location 20 is in the Gulf of Finland near the intersection of busy eastward shipping lane to St Petersbourg and northward ferry route between Tallinn and Helsinki. After 2014, the next yearly monitoring in this location was performed from November 2015 until October 2016. Location 26 is in the sheltered Polish waters of the Bay of Puck over 10 km to the north from the port of Gdynia.

Figure 8 presents the comparison of two years of sound monitoring results in locations 20 and 26. As can be seen, the results of two consecutive annual periods are similar for all three frequency bands. This hints that the yearly averaged soundscape in a given location remains relatively unchanged. Even if the seasonal variability of noise is high, the overall annual values are similarly distributed from one year to another. This implies that sound monitoring has to cover most of the year to give a representative estimate to the prevailing SPL values in a location. The yearly SPL values serve as a baseline for this location, against which to compare any measurements in the same location in the following years. The results of comparing the two years with the Mann-Whitney U test (significant if p-value < 0.05) are as follows:

- In location 20, the 63 Hz one-third octave band had no statistically significant change in the annual SPL values, while in the 125 Hz and 2 kHz one-third octave bands there was a statistically significant increase in the SPL values. The annual median value in the 125 Hz one-third and 2 kHz octave bands was about 1.7 dB higher in the second monitoring period.
- In location 26 for all the one-third octave bands, there was no significant change in the annual SPL values. The difference in the medians between the two monitoring periods was less than 0.25 dB.
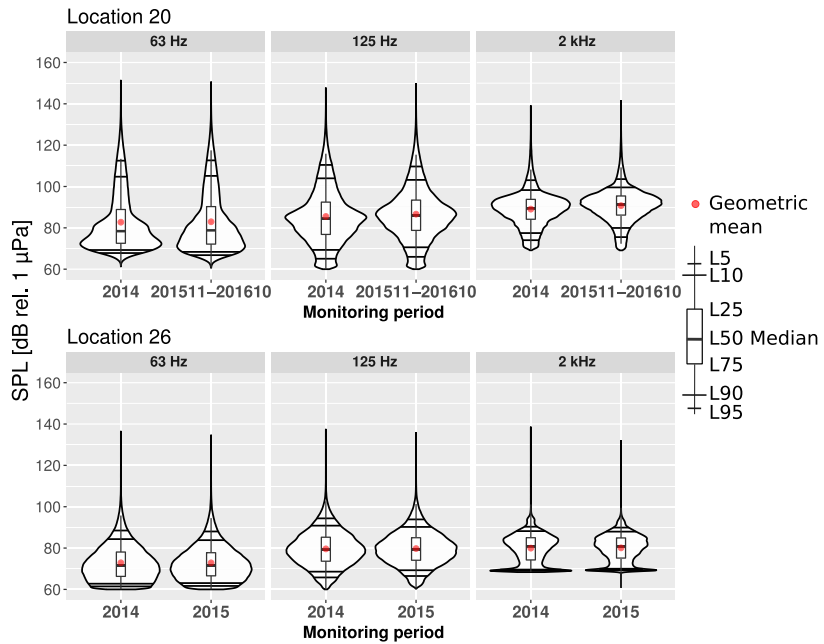
Figure 8. Estimated probability density functions of the measured SPL at three different one-third octave bands for the measurement location 20 (Tallinn, EST) and location 26 (Puck Bay, POL) for two monitoring periods.
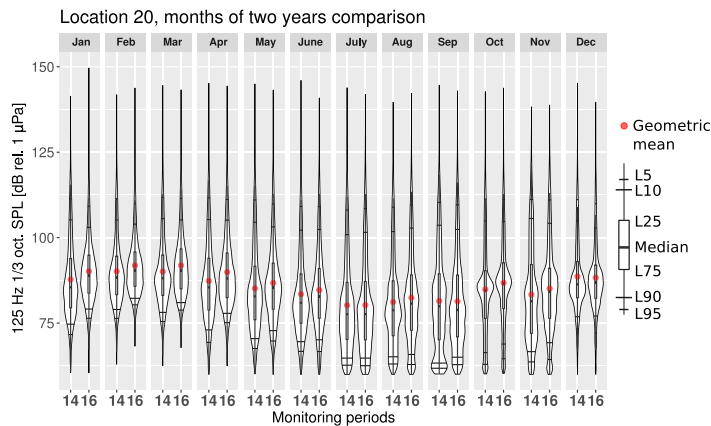
Figure 9. Comparison between monthly estimated PDFs from two separate monitoring periods in the 125 Hz one-third octave band for the measurement location 20 (Tallinn). The number 14 on the x-axis marks the monitoring period from from 1 January 2014 to 31 December 2014 and the number 16 marks monitoring period from from 1 November 2015 to 31 October 2016.

Similar low interannual variability has been previously observed at some monitoring locations in the North Sea[16].

The differences in the seasonal changes of the SPL values between the two years can be better exemplified by comparing the monthly estimated PDFs. Figure 9 shows that the monthly SPL values from two different monitoring periods recorded in one location have similar distributions. For most of the months, the second monitoring period has higher median SPL values. Although the loudest month remained unchanged, being still February, the median value was higher in the second monitoring period. Figure 9 also shows that during the winter months, the lower SPL values were above the self-noise level of the marine recorder. From June to November, the SPL values seem to have been occasionally below the self-noise level. Thus, due to seasonality, the previously discussed effect

of self-noise "piling up" in the lower tails of the PDFs is more likely present in the summer months. Interannual comparison on the monthly basis reaffirms that the variability is growing with the reduction of the averaging time period.

Conclusions

Baltic Sea underwater ambient sound pressure levels were measured in monitoring programmes running since 2014. These monitoring programmes have been pioneering in terms of their coordinated cross-bordering effort, longevity and spatial coverage. The collected data offer an opportunity to analyse the spatial and temporal variability of the sound. Analysis was restricted to 16 selected monitoring locations out of the total 36 in the BIAS-project. The choice was made due to the annual data coverage and the aim to represent different natural conditions and ship traffic intensities in the Baltic Sea. The presented analysis also revealed that any future monitoring of noise in calm sheltered waters should consider the use of recording equipment with lower self-noise.

The annual SPL values from the different monitoring locations show high variability with some clear regional similarities. The difference between the loudest and quietest location was almost 50 dB in 63 Hz one-third octave band and 40 dB in 125 Hz one-third octave band. The locations with the lowest recorded annual median SPL were recorded in calm sheltered waters, while the highest annual median SPL values were in the Danish straits where a lot of vessels are present at any given time. The annual estimated probability density functions (PDFs) of the two lower frequency bands were often positively skewed, especially for the locations with low median SPL values. For most of the locations, the recorded SPL had clear relation with prevailing wave/wind weather and shipping intensity. However, in some locations, the relation was not so clear and the interplay of the sound propagation conditions along with sound sources should be further investigated.

When monitoring noise at the same locations for two yearly periods, the overall sound levels of the two periods were found to be very similar. This was confirmed in two separate locations, one in the Gulf of Finland and another in the Bay of Puck. The temporal variability was shown to be highly dependent on the time scale. This was illustrated by the different monthly SPL values for two consecutive annual periods contrasting with the similar annual values. This shows the decrease of variability with the increase of averaging time period. This low variability of the annual PDFs indicates that it is a good measure of the baseline SPL values at a given location. The seasonal variations of sound pressure levels were found to be in the range of 10 dB with lower variation in locations with a heavier traffic. This indicates that in many areas of the Baltic Sea shipping already contributes significantly to the prevailing ambient sound levels. However, more effort should be made for better assessing the contributions made by ships by differentiating between monitored sound levels in presence and absence of ships.

Methods

Sound pressure monitoring technique. The presented measurements were performed following the measurement and signal processing standards developed for the BIAS-project[35,36]. In order to assure the comparability between different countries the use of standards in measurements was essential. In the BIAS-project, two different autonomous recording systems were used for monitoring the continuous underwater sound: the DSG Ocean marine recorder manufactured by Loggerhead Instruments and the SM2M manufactured by Wildlife Acoustics[37]. Figure 10 presents the setups of the standard measurement rigs. The DSG Ocean marine recorder was used in the rig design marked with letter **A**. This design was deployed for some periods in sound monitoring locations marked with the triangular markers in Fig. 1. Letter **B** in Fig. 10 marks the most used rig design with the SM2M recorder. The exceptions were the rigs deployed in the Polish waters which had an alternative design marked with **C**. The probability of losing the rig due to trawling was high there and additional protection was needed. In the alternative rig-design, the hydrophone is located 1 m above the seafloor instead of 3 m. The recording system is surrounded by a protective structure made up of pyramid-shaped steel frame. This configuration allows the sensor pod to tilt and the trawl net to slip over the rig. A plastic tube serves as a housing that protects the recorder, acoustic releaser and rope container against direct impact from trawls[35]. The presented rig designs proved suitable for monitoring in the Baltic Sea. Although it must be noted that they may not be optimal for locations with high tidal flow.

In all the monitoring locations chosen for this study, the ambient sound was recorded during the whole year of 2014 and therefore, the annual data are comparable. Duty cycles in the different monitoring locations varied from 20 to 59 minutes per hour. Data exclusion tests with the 59 minute duty cycle recordings did not indicate to any significant effect on the long term monitoring results. The standard SM2M marine recorder allows measurements with sampling frequencies from 4 kHz to 96 kHz and a bit depth of 16-bits. Most of the measurements were made with a sampling frequency $f_s = 32$ kHz. In addition to the indicator one-third octave bands, centered at 63 Hz and 125 Hz, a one-third octave band centered at 2 kHz and a broadband 10 Hz–10 kHz were monitored in the BIAS-project. The 2 kHz one-third octave band was added as it is more relevant for marine mammals, which have poor hearing abilities at lower frequencies.

The frequency response of the SM2M can be considered to be relatively flat, being $+/-2$ dB of the rated sensitivity in the frequency range that spans all the one-third octave bands of interest. This enables the sensitivity M_f of the instrument to be handled as a single number. All acoustic recorders were point calibrated (frequency 250 Hz) with a pistophone before the first deployment and after the last retrieval. Within the range of $+/-1$ dB, no significant change in sensitivities was observed. Table 2 lists the evaluated self-noise of the SM2M recorder in the one-third octave bands.

Recorded sound pressure data processing. The Good Practice Guide for Underwater Noise Measurement[10] states that: "The metric most suitable for quantifying the continuous sounds, is the Sound Pressure Level (SPL)". The SPL is defined among other entities in the ISO standard[38] as
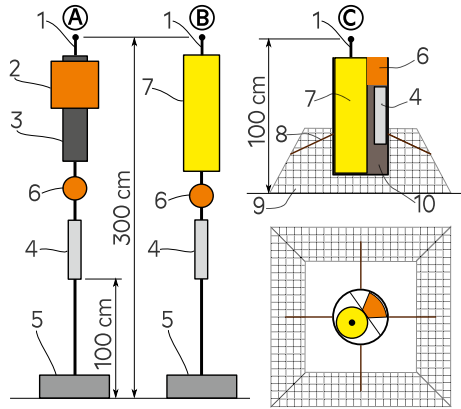
Figure 10. Sketch of the three BIAS standard rigs marked with letters A,B,C; 1-hydrophone, 2-extra buoyancy, 3-DSG Ocean recorder, 4-acoustic releaser, 5-ballast (min 20 kg wet weight), 6-buoy, 7-SM2M recorder, 8-rope, 9-steel grid cage, 10-rope container[35].

One-third Octave central freq.	63 Hz	125 Hz	2 kHz
Self-noise [dB re 1 μPa]	63	65	70
Spectral density [dB re 1 μPa²/Hz]	51	50	43

Table 2. Evaluated self-noise and spectral densities of the SM2M recorder in the one-third octave bands 63 Hz, 125 Hz and 2 kHz.

$$L_p = 10\log_{10}\frac{\hat{p}^2}{p_0^2},$$

where p_0 is the reference value of sound pressure which in water is $p_0 = 1\,\mu$Pa. The $\hat{p}^2$ is the mean-square sound pressure that is defined as

$$\hat{p} = \frac{1}{t_2 - t_1}\int_{t_1}^{t_2} p^2(t)\,dt$$

where $p(t)$ is the sound pressure, and t_1 and t_2 are the start and end times, respectively. As already addressed in the introduction, the indicator D11 criterion for continuous low-frequency sound[11] specifies that the average sound level (re 1 μPa root-mean-square RMS) should be presented in the one-third octave bands with center frequencies of 63 Hz and 125 Hz. In the BIAS-project, the average of the sound level in the one-third octave band was determined as the geometric mean of 20 consecutive one-second averaged one-third octave band root-mean-square sound pressure levels, i.e. computationally approximately equivalent to RMS-average over the 20 seconds. The reason behind this granularity in the data resolution was the consideration of making the data publicly shareable. Some national authorities considered a finer resolution to compromise their national security interests.

The SM2M and DSG recorders, as various other marine submersible recorders, digitise the measured sound pressure and store it as discrete values in .*wav*-file format. As an initial step, the discrete 16-bit values are scaled to volts. The root-mean-square of discrete values is calculated with the following formula:

$$\hat{x} = \sqrt{\frac{1}{N}\sum_{n=1}^{N} x^2[n]}\,.$$

This can be rewritten by applying the Parseval's theorem. For a sampled value $x[n] = x[t = NT]$, where T is the sampling period (equal to the reciprocal of the sampling frequency)

$$\sum_{n=1}^{N} x^2[n] = \frac{1}{N}\sum_{m=1}^{N} |X[m]|^2,$$

where $X[m]$ is the Discrete Fourier Transform (DFT) of $x[n]$, N is the number of samples and DFT coefficients. In practice, the root-mean-square of the discrete samples can be obtained from the sum of the frequency amplitude spectrum. Therefore, the root-mean-square of a discrete valued variable can be calculated from

$$\hat{x} = \sqrt{\frac{1}{N^2}\sum_{m=1}^{N}|X[m]|^2}$$

No window functions were applied to the data prior to the estimation of the DFT since it did not improve the statistical estimates. If the sensitivity $|M_h|$ of the measurement system is known (the gain was $G = 1$ and the discrete voltage values $v[n]$ were also known from scaling) the SPL was calculated from the recorded bits as

$$L_p = |M_h| + 10\log_{10}\hat{v}^2 = |M_h| + 10\log_{10}\left(\frac{1}{N^2}\sum_{m=1}^{N}|V[m]|^2\right),$$

where $\hat{v}$ is the RMS voltage of N samples and $V[m]$ the FFT of $v[n]$. If the one-third octave band SPL values are calculated, the last expression becomes

$$L_{p_{1/3}} = |M_h| + 10\log_{10}\left(\frac{1}{N^2}\sum_{m=k_1}^{k_2}|V[m]|^2\right),$$

where k_1 and k_2 are the indices corresponding to a given one-third octave bands lower and upper frequencies.

The BIAS-project established Quality Assurance (QA) in order to assure equal data quality among the BIAS partners. An inter-comparative analysis, "ring-test", was carried out among all the participating countries. Identical sound samples were processed by all beneficiaries and the results compared. The sample data were processed by the named experts from each of the participating countries. The test checked the sample length, portion of clipping and SPL values in all the monitored frequency bands. The ring tests were found to be a useful tool for the QA. All discrepancies were investigated and at the end of the testing, the results of all the six countries were in agreement with one another.

Data Availability

The one-third octave band SPL values, AIS data and other datasets analysed during the current study are available from the corresponding author on reasonable request. The recorded raw data are not publicly available due to confidentiality reasons.

References
1. Payne, R. & Webb, D. Orientation by means of long range acoustic signaling in baleen whales. *Annals New York Acad. Sci.* **188**, 110–141 (1971).
2. Clark, C. W. *et al.* Acoustic masking in marine ecosystems: intuitions, analysis, and implication. *Mar. Ecol. Prog. Ser.* **395**, 201–222 (2009).
3. Jensen, F. H. *et al.* Vessel noise effects on delphinid communication. *Mar. Ecol. Prog. Ser.* **395**, 161–175, http://www.jstor.org/stable/24874248 (2009).
4. Williams, R. *et al.* Impacts of anthropogenic noise on marine life: publication patterns, new discoveries, and future directions in research and management. *Ocean. & Coast. Manag.* **115**, 17–24 (2015).
5. Sierra-Flores, R., Atack, T., Migaud, H. & Davie, A. Stress response to anthropogenic noise in Atlantic cod Gadus morhua L. *Aquac. engineering* **67**, 67–76 (2015).
6. Wisniewska, D. M. *et al.* High rates of vessel noise disrupt foraging in wild harbour porpoises (Phocoena phocoena). In *Proc. R. Soc. B*, vol. 285, 20172314 (The Royal Society, 2018).
7. Directive, M. S. F. Directive 2008/56/EC of the European Parliament and of the Council of 17 June 2008 establishing a framework for community action in the field of marine environmental policy. *Off. J. Eur. Union L* **164**, 19–40, http://eur-lex.europa.eu/LexUriServ/LexUriServ.do?uri=OJ:L:2008:164:0019:0040:EN:PDF (2008).
8. Tasker, M. L. *et al.* Marine Strategy Framework Directive – Task Group 11 Report. Underwater Noise and Other Forms of Energy. *JRC Sci. Policy Rep. EUR 24341 EN, Publ. Off. Eur. Union, Luxemb* (2010).
9. Dekeling, R. P. A. *et al.* Monitoring guidance for underwater noise in European seas. *JRC Sci. Policy Rep. EUR 26557 EN, Publ. Off. Eur. Union, Luxemb* (2014).
10. Robinson, S. P., Lepper, P. A. & Hazelwood, R. A. Good Practice Guide for Underwater Noise Measurement. NPL Good Practice Guide No. 133/National Measurement Office, Marine Scotland. *The Crown Estate* (2014).
11. Decision, E. C. Decision 2017/848/EC of the European Commission of 17 May 2017 laying down criteria and methodological standards on good environmental status of marine waters and specifications and standardised methods for monitoring and assessment, and repealing. *Off. J. Eur. Union L* **125**, 43–74 (2017).
12. van der Schaar, M., Ainslie, M. A., Robinson, S. P., Prior, M. K. & André, M. Changes in 63 Hz third-octave band sound levels over 42 months recorded at four deep-ocean observatories. *J. Mar. Syst.* **130**, 4–11 (2014).
13. Viola, S. *et al.* Continuous monitoring of noise levels in the Gulf of Catania (Ionian Sea). Study of correlation with ship traffic. *Mar. pollution bulletin* **121**, 97–103 (2017).
14. Merchant, N. D., Witt, M. J., Blondel, P., Godley, B. J. & Smith, G. H. Assessing sound exposure from shipping in coastal waters using a single hydrophone and Automatic Identification System (AIS) data. *Mar. Pollut. Bull.* **64**, 1320–1329, https://doi.org/10.1016/j.marpolbul.2012.05.004 (2012).
15. Merchant, N. D. *et al.* Measuring acoustic habitats. *Methods Ecol. Evol.* **6**, 257–265 (2015).
16. Merchant, N. D. *et al.* Underwater noise levels in UK waters. *Sci. Reports* **6** https://www.ncbi.nlm.nih.gov/pmc/articles/PMC5103265/ (2016).
17. Hatch, L. *et al.* Characterizing the relative contributions of large vessels to total ocean noise fields: a case study using the Gerry E. Studds Stellwagen Bank National Marine Sanctuary. *Environ. management* **42**, 735–752 (2008).
18. Erbe, C., MacGillivray, A. & Williams, R. Mapping cumulative noise from shipping to inform marine spatial planning. *The J. Acoust. Soc. Am.* **132**, EL423–EL428 (2012).
19. Sigray, P. *et al.* BIAS: A Regional Management of Underwater Sound in the Baltic Sea. In *The Effects of Noise on Aquatic Life II*, 1015–1023 https://doi.org/10.1007/978-1-4939-2981-8_126 (Springer, 2016).

20. Nikolopoulos, A., Sigray, P., Andersson, M., Carlström, J. & Lalander, E. *BIAS Implementation Plan: Monitoring and assessment guidance for continuous low frequency sound in the Baltic Sea*, http://www.diva-portal.org/smash/record.jsf?pid=diva2:1072183 (BIAS LIFE11 ENV/SE/841, 2016).
21. Urick, R. J. *Principles of Underwater Sound 3rd Edition* (Peninsula Pub, Los Altos, Calif, 1996), originated 1983 edition edn.
22. Garrett, J. K. *et al.* Long-term underwater sound measurements in the shipping noise indicator bands 63 Hz and 125 Hz from the port of Falmouth Bay, UK. *Mar. Pollut. Bull.* **110**, 438–448 (2016).
23. Roth, E. H., Hildebrand, J. A., Wiggins, S. M. & Ross, D. Underwater ambient noise on the Chukchi Sea continental slope from 2006–2009. *The J. Acoust. Soc. Am.* **131**, 104–110 (2012).
24. Kinda, G. B., Le Courtois, F. & Stéphan, Y. Ambient noise dynamics in a heavy shipping area. *Mar. pollution bulletin* **124**, 535–546 (2017).
25. Alenius, P., Myrberg, K. & Nekrasov, A. The physical oceanography of the Gulf of Finland: a review. *Boreal Environ. Res.* **3**, 97–125 (1998).
26. Johnson, M. W., Everest, F. A. & Young, R. W. The role of snapping shrimp (Crangon and Synalpheus) in the production of underwater noise in the sea. *The Biol. Bull.* **93**, 122–138 (1947).
27. Team, R. C. R: *A language and environment for statistical computing. Vienna, Austria: R Foundation for Statistical Computing; 2014* (2014).
28. Royston, J. P. An extension of Shapiro and Wilk's W test for normality to large samples. *Appl. statistics* 115–124 (1982).
29. Battjes, J. A. Long-term wave height distributions at seven stations around the British Isles. *Deutsche Hydrografische Zeitschrift* **25**, 179–189, https://doi.org/10.1007/BF02312702 (1972).
30. Conradsen, K., Nielsen, L. B. & Prahm, L. P. Review of Weibull statistics for estimation of wind speed distributions. *J. climate Appl. Meteorol.* **23**, 1173–1183 (1984).
31. Klusek, Z. & Lisimenka, A. Seasonal and diel variability of the underwater noise in the Baltic Sea. *The J. Acoust. Soc. Am.* **139**, 1537–1547 (2016).
32. Brekhovskikh, L. M. & Lysanov, Y. P. *Fundamentals of Ocean Acoustics*. Modern Acoustics and Signal Processing (Springer-Verlag, New York, 2003), 3 edn. www.springer.com/us/book/9780387954677.
33. Räämet, A. & Soomere, T. The wave climate and its seasonal variability in the northeastern Baltic Sea. *Estonian J. Earth Sci.* **59** (2010).
34. Wagstaff, R. A. & Newcomb, J. Omnidirectional ambient noise measurements in the southern Baltic Sea during summer and winter. In *Progress in Underwater Acoustics*, 445–452 (Springer, 1987).
35. Verfuß, U. K. *et al.* BIAS Standards for noise measurements. Background information, guidelines and quality assurance, https://biasproject.files.wordpress.com/2016/04/bias_standards_v5_final.pdf (2014).
36. Betke, K. *et al.* BIAS Standards for Signal Processing. Aims, Processes and Recommendations. Amended version, https://biasproject.files.wordpress.com/2016/01/bias_sigproc_standards_v5_final.pdf (2015).
37. WildlifeAcoustics. User Manual Supplement SM2m+, https://www.wildlifeacoustics.com/images/documentation/SM2M-User-Manual.pdf.
38. ISO 18405:2017 - Underwater acoustics – Terminology, https://www.iso.org/standard/62406.html.

Acknowledgements

Author Contributions

M.M. and A.K. wrote the main manuscript text. M.M. prepared all the figures and tables. J.P. provided the data and text about the effect of ice and text about the Quality Assurance in the BIAS project. R.K. provided the Puck Bay sound monitoring results for the year 2016 in Figure 8. All authors reviewed and made contributions in writing the manuscript.

Additional Information

Competing Interests: The authors declare no competing interests.

Publisher's note: Springer Nature remains neutral with regard to jurisdictional claims in published maps and institutional affiliations.

Publication V

Natural sound estimation in shallow water near shipping lanes

Mirko Mustonen,[1,a)] Aleksander Klauson,[1,b)] Thomas Folégot,[2,c)]
and Dominique Clorennec[2]

[1]*Civil Engineering and Architecture, Tallinn University of Technology, Tallinn, 19086, Estonia*
[2]*Quiet-Oceans, Plouzané, Brittany, 29280, France*
mirko.mustonen@taltech.ee, aleksander.klauson@taltech.ee, thomas.folegot@quiet-oceans.com,
dominique.clorennec@quiet-oceans.com

Abstract: Underwater ambient sound has been recently re-addressed in regard to the impact of anthropogenic sound from commercial shipping on marine life. Passive acoustic monitoring provides the overall ambient sound levels at a given location and is often used to calibrate the sound propagation modeling for assessing ambient sound levels in larger marine areas. To quantify the pressure on the environment, the proportion of the anthropogenic component in the total measured levels of the monitored sound should be properly assessed. The present paper addresses the methodology for categorisation of the measured sound into its wind-driven natural and anthropogenic components.
© 2020 Acoustical Society of America

1. Introduction

Underwater ambient sound has been an important research subject in underwater acoustics. Developments in this field have mainly been driven by the need to predict the signal-to-noise ratios of underwater sound measuring equipment. Pioneering studies were published by Knudsen *et al.* (1948) and by Wenz (1962). Ambient noise measurements and its characteristics are described in detail in Carey and Evans (2011), Hildebrand (2009), Urick and Kuperman (1989), and Urick (1967). The underwater ambient sound is generally categorised as anthropogenic and natural, which includes a biological component. Most of the omnipresent non-biological natural sound comes from the wind-driven sea-surface agitation, but also from precipitation [mostly rain (Nystuen *et al.*, 2010) as well as hail and snow (Scrimger *et al.*, 1987)] and from processes related to the ice cover during the winter months (Menze *et al.*, 2017). The most widespread anthropogenic underwater sound is related to commercial shipping (Hildebrand, 2009).

  The continuous anthropogenic noise can have adverse effects on marine life by causing the reduction of listening and communication space (Pine *et al.*, 2018; Putland *et al.*, 2018) and an increase in stress levels (Nichols *et al.*, 2015). Masking of the vital components of soundscapes can have consequences for marine mammals' and fishes' energy budget (Wright *et al.*, 2007) or disorientation of larvae (Simpson *et al.*, 2016). In the EU, human-induced underwater noise is included among the indicators for Good Environmental Status (GES) in the Marine Strategy Framework Directive (MSFD) (Decision, 2017) whereby Member States have to take steps for ensuring the noise is at levels that do not adversely affect the marine environment. In the MSFD, sound pressure levels (SPL) in one-third octave bands (TOBs) centered around 63 and 125 Hz have been suggested as the proxies for the continuous anthropogenic sound.

  Since the anthropogenic sound contributes to the total ambient sound, a simple and efficient method is needed to evaluate the proportion of the anthropogenic component in the overall sound. The anthropogenic sound in the recordings can be detected (Mustonen *et al.*, 2017), but such an approach can be computationally expensive and its detection threshold values vary with natural ambient sound levels. In contrast, the approach presented in this paper focuses on the readily available 63 and 125 Hz TOB SPL values from the ambient sound monitoring required by the MSFD. In the assessment of the ambient sound level, we took into account that no ice cover was present near the monitoring locations during 2014. The sound level for the highest

recorded rain rates (< 14 mm/h) exhibited no increase in the low frequency TOBs. Consequently, for the frequency bands chosen, the natural sound levels were estimated based only on the wind speed data. In order to estimate the wind-driven sound levels, it is required to establish their dependence on the wind speed. This task can be solved easily by ambient sound monitoring in a location unexposed to anthropogenic sounds. However, recording in locations without anthropogenic components conflicts with the aim of anthropogenic sound monitoring. Additionally, the wind-dependency of the MSFD indicator TOBs is known to be rather weak (Vagle *et al.*, 1990). It is generally accepted that wind-driven sound is an important contributor to ambient noise in frequency bands above 200 Hz (McDonald *et al.*, 2006). Therefore, the key question is to estimate the dependence of the natural ambient sound level on the wind speed in the TOBs 63 and 125 Hz in a robust and reliable way in monitoring locations exposed to marine traffic noise.

2. Methods

2.1 Empirical models of wind speed dependency

The dependence of the natural sound level on the wind speed is variable across different frequency ranges (Wenz, 1962). Piggott (1964) has suggested that in the lower frequency bands, the noise level tends to be a result of a wind independent background and a wind dependent component. According to Piggott, within certain wind speed ranges, the noise level increases linearly with the logarithm of the wind speed,

$$L(f, u) = S_1(f) + 20\, n(f)\, \log_{10}(u),\qquad(1)$$

where L is the ambient sound spectrum level at frequency f, $S_1(f)$ is the sound level at a unit wind speed, $n(f)$ is a fitted coefficient, and u the wind speed at 10 m above the sea surface (Klusek and Lisimenka, 2016). Equation (1) models the wind dependent regime, under the consideration that the wind independent component is exceeded. For modeling low wind speed conditions, Poikonen (2012) used a logarithmic model based on three parameters that describe the two regimes of the wind-driven ambient sound

$$L(f, u) = S_0(f) + 10\, \log_{10}\left[1 + \left(\frac{u}{u_c(f)}\right)^{k(f)}\right],\qquad(2)$$

where S_0 is the spectrum level of the wind independent background, u_c is the critical wind speed below which background dominates over the wind dependent component, and k is the wind speed dependence factor. Above some critical wind speed, higher sound attenuation takes place due to the presence of dense bubble clouds and persistent bubble layers (Poikonen, 2012). Therefore, there exists a maximum wind speed above which Eq. (2) does not hold. However, such high wind speeds were rare in the Baltic Sea during the monitoring period.

2.2 Wind-noise model

The results presented are based on the sound pressure data measured and processed, following the relevant standards of the BIAS-project (Betke *et al.*, 2015; VerfuSS *et al.*, 2014). We used the Wildlife Acoustics SM2M sound recorder with standard hydrophone (WildlifeAcoustics, 2013) for our measurements. Figure 1(A) shows a sketch of the bottom mounted rig design. Measurements were carried out during 2014 almost continuously, with minor gaps between deployments of which the longest was two weeks. The recording duty cycle varied from 20 to 59 min per hour. Figure 1(B) displays the map with four sound monitoring locations that were chosen to cover different propagation conditions and distances to shipping lanes (Dekeling *et al.*, 2014). Figure 1(B) shows the time-synchronised averaged AIS-based ship densities (number of ships per hour per square km) within 20 km radius from each measurement location. displays a stacked barplot that shows the averaged AIS-based number of vessels likely to be present at any given time. For example, at location 20, the expectation during 2014 was to find 1 vessel closer than 5 km and 3 vessels closer than 10 km from the monitoring location at any time. It can be seen that exposure to shipping noise in each location was different. While locations 20 and 22 are situated close to busy shipping lanes, locations 21 and 23 are mostly exposed to distant traffic noise.

As the wind speed was not directly measured for this study, and existing weather stations were far from the monitoring locations, the wind speed data of SMHI mesoscale analysis system MESAN (Häggmark *et al.*, 2000) was used. The closest grid node to each location typically at distances around 7–13 km. The sample interval of the wind data was 1 h.

The main assumption behind the wind generated noise model is that between passing ships the ambient sound returns to the natural level. If a relatively stable wind speed dependence exists, it can be approximated from the natural sound levels and known wind speeds.
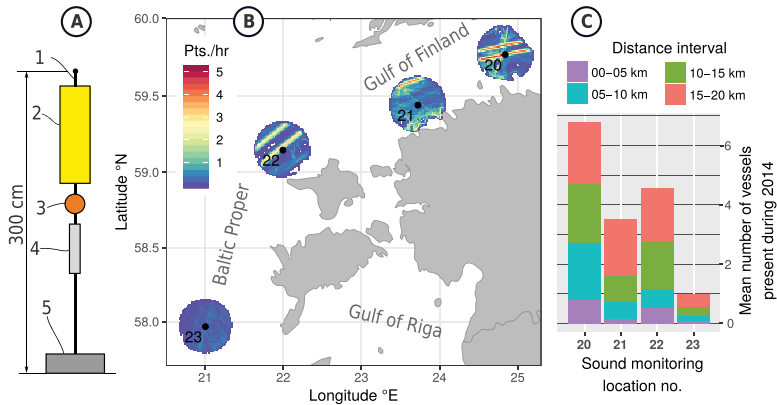
Fig. 1. (Color online) (A) Sketch of the monitoring rig: 1—hydrophone, 2—recorder, 3—extra buoyancy, 4—acoustic release, 5—ballast weight (min 20 kg wet weight). (B) Map with the Estonian BIAS sound monitoring locations (20, 21, 22, 23) with the depths, respectively 75, 89, 70, and 70 m. The coloured circles show the time-regularised averaged number of AIS based ship location points in regular 1 km² squares per hour in January 2014. (C) AIS based averaged vessel presence expected at different ranges from the monitoring location in 2014.

To demonstrate the validity of this assumption, Figs. 2(a) and 2(b) show 20-day long TOB 63 Hz SPL values recorded in monitoring location 23 between 10th and 30th of September 2014. The highest narrow peaks visible in these figures correspond to the closest passes of ships. Figure 2(a) shows recorded SPL values in 63 Hz TOB plotted against the wind speed. On this plot, a distinct wind-dependence of the lower bound can be observed for wind speeds higher than 6 m/s. The lower bound was first extracted by finding lower percentile values of the recorded SPL within fixed width ranges of wind speed. The uniformly distributed extracted data points are shown in
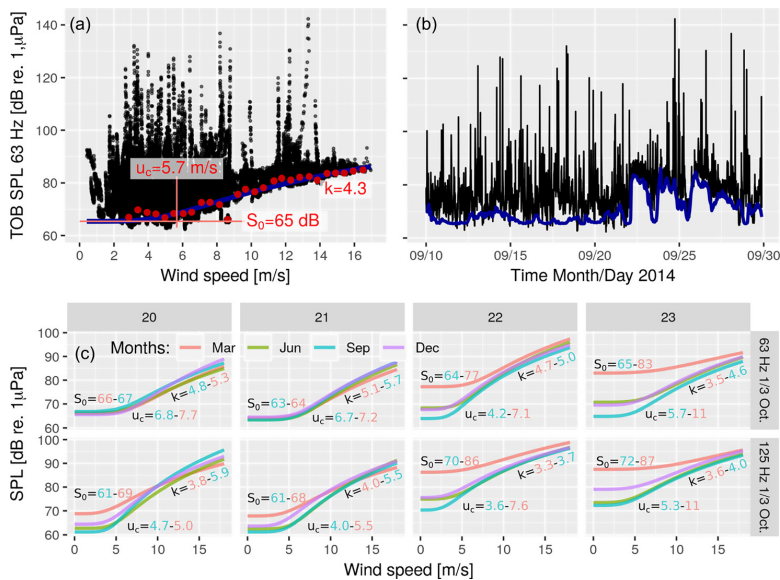
Fig. 2. (Color online) Data recorded in sound monitoring location 23: (a) Black dots are the recorded SPL values plotted against MESAN wind speeds. Red dots represent 10th percentile values of 0.5 m/s wide wind speed ranges. The blue line shows the model fit with the parameters $S_0 = 65$ dB, $u_c = 5.7$ m/s, and $k = 4.3$. (b) The black line shows the time series of the 63 Hz TOB SPL. The blue line presents predicted wind-driven ambient sound values. (c) The fitted averaged wind dependencies of the natural ambient sound for four months of the year (March, June, September, and December) in the four monitoring locations and two TOBs. The fitted parameter S_0, u_c, and k values for the noisiest (March) and the quietest (September) months are listed with red and blue coloured numbers accordingly.

Fig. 2(a) by red dots. These data points were found to follow the model given by Eq. (2). Fitting with the model gave estimates for the parameters S_0, u_c, and k. The resulting fit is shown on the same plot with a blue line.

Fitted wind dependencies for different seasons, locations and frequency bands are shown in Fig. 2(c). It can be seen that seasonal variability is larger in the Baltic Proper and in the higher frequency band. The seasonal variation of the fitted parameters is largest in location 23 where the parameter S_0, marking the level of the wind independent background, varies between March and September up to 18 dB. A study of the Baltic Sea ambient sound (Mustonen et al., 2019) has shown that the seasonal variation of the sound pressure levels can exceed 10 dB in the analysed low frequency bands. This can be attributed to the seasonal changes in the sound speed profile. During the summer months, the rising temperature of mixed layers causes downward refraction and larger propagation losses. According to some researchers changes in the water temperature and salinity can affect the bubble density and size (Pounder, 1986) that may be linked to the level of the wind-driven ambient sound (Prosperetti, 1985). Therefore, the choice of a time window is crucial for the proposed method: time period for fitting has to be long enough to cover a variety of different wind speeds while not too long to minimise the effect of seasonal changes. For this reason, three different length rolling time windows (10, 15, 30 days) were used to find statistically significant fits for the parameters throughout the year. The shorter time window of 10 days sufficed for periods with highly variable wind speeds. It has to be noted that in the case of dense ship traffic, the time intervals when the sound level returns to the natural level are scarce. In most cases if the rolling time window exceeded 30 days the seasonal changes made finding a significant fit difficult. Besides seasonality, the noise floor of the sound recorder has to be considered. In some locations, from June to November, the ambient sound level was below the self-noise level of the measurement instrument. The upper limit for the self-noise levels for the TOB 63 and 125 Hz is around 63 and 65 dB respectively.

3. Extraction of anthropogenic sound and discussion

The described method allows estimating the wind-dependent component of the recorded TOB sound pressure levels. However, it is quite complicated to determine the exact bound between the natural and the anthropogenic sound. Therefore, after inspection of the data, it was assumed that when the recorded levels exceed the estimated wind dependent levels by 4 dB, they mostly correspond to the anthropogenic sound. This assumption enabled the division of the measured SPL values into the natural and anthropogenic components accordingly. The outcome of the division is demonstrated in Fig. 3 with an overview of the annual 2014 SPL time series and their empirical probability density functions (PDFs). Presented time series show the different extent of the seasonal changes. Thus, very low seasonal variations for 63 Hz TOB SPL values are apparent
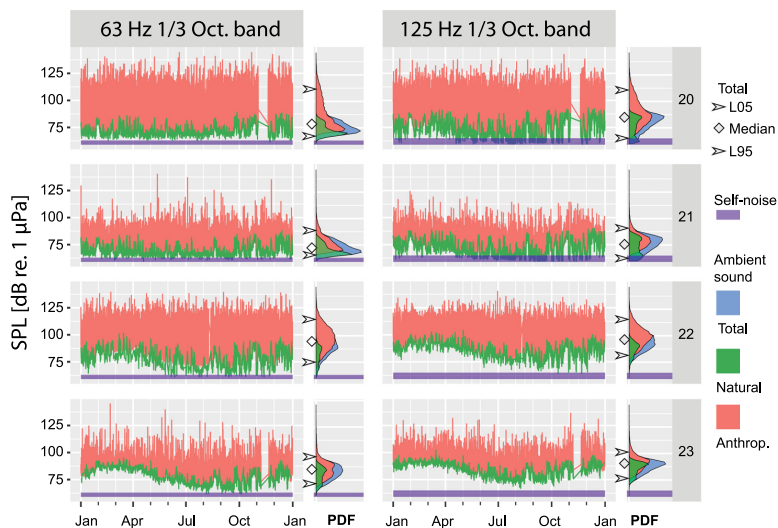

Fig. 3. (Color online) Estimated decompositions of time series and the probability density functions (PDFs) of 2014 recorded SPL values in four different monitoring locations (20, 21, 22, and 23) for two TOBs (63 and 125 Hz).

Table 1. Estimated natural sound level (Nat) and recorded total (Tot) values with the added excess levels (Ex) in four different monitoring locations for two TOBs. The BSN marks that the value was below the self-noise limit of the SM2M data logger and therefore no reliable comparison can be made.

TOB	63 Hz [dB re 1 μPa]									125 Hz [dB re 1 μPa]								
Exceedance	L95			L50			L05			L95			L50			L05		
Mon locs\Val	Nat	Tot	Ex	Nat	Tot	Ex	Nat	Tot	Ex	Nat	Tot	Ex	Nat	Tot	Ex	Nat	Tot	Ex
20, Tallinn	66	68	2	68	79	11	79	112	33	BSN	65	4	72	85	13	85	110	25
21, Paldiski	63	65	2	66	73	7	77	88	11	BSN			70	77	7	82	89	7
22, Hiiumaa	65	75	10	75	94	19	88	116	28	73	80	7	83	96	13	93	114	21
23, Saaremaa	65	70	5	76	84	8	87	96	9	73	77	4	84	90	6	91	101	10

in monitoring locations 20 and 21. Although some seasonality is apparent in these locations for the 125 Hz TOB, it can hardly be quantified due to the self-noise limit being reached from May until November. The noise floor for each TOB is indicated by transparent horizontal violet bands. In locations 22 and 23, the effect of the seasonal change is clearly visible in both TOBs.

The PDFs in Fig. 3 demonstrate the prevalence of the measured sound levels by the frequency bands and locations. The total PDFs (blue) are presented with the superimposed wind-driven natural (green) and anthropogenic (red) components. Exceedance levels L05, L95, and median (L50) of the total PDFs are shown by arrows and diamond marks accordingly. The L95 exceedance level corresponds to SPL that is exceeded 95% of the time. The depicted categorisation enables us to draw several conclusions.

(a) Gulf of Finland (GoF) (locations 20 and 21). The estimated natural sound levels are relatively similar being slightly quieter in the more harbored location 21. This observation is confirmed by median wind speeds that were 6.5 and 6.1 m/s in locations 20 and 21 accordingly.

The estimated anthropogenic component is significantly higher in monitoring location 20 than in location 21. This difference is caused by the proximity of busy shipping lanes in location 20. The differences in shipping intensity are shown in Fig. 1(C), where within the distance of 10 km at any given time, on average two more vessels are present in location 20 than in location 21.

(b) Baltic Proper (BP) (locations 22 and 23). Wind-driven sound is often represented by sources in a layer that is assumed to exist just below the sea surface (Kuperman and Ingenito, 1980). Apparently, with the formation of thermocline during the summer period, the distant natural ambient sound sources contribute less in low frequency bands, as their generated sound is downward refracted, causing comparatively higher propagation loss. As a result, the seasonal variation of the lower bound values in Fig. 3 BP locations is clearly visible.

As compared to the GoF locations, the median natural ambient sound levels are around 10 dB higher. Comparing the medians of the estimated natural SPLs in the BP locations, the median levels in location 23 are only slightly higher. The yearly median wind speed was 6.0 m/s in location 22 and 6.8 m/s in location 23.

It can be seen from the categorisation of the PDFs in locations 22 and 23 that the geographical proximity can lead to considerable similarities in the PDFs of the natural sound.

The anthropogenic component is contrastingly different for the BP locations. This was expected as location 22 is exposed to widely different shipping intensity compared to location 23, as shown in Fig. 1(C).

Numerical values of the total exceedance levels from Fig. 3 along with estimated natural exceedance levels are listed in Table 1.

4. Conclusion

A method for separating the anthropogenic component of the measured ambient sound for the ship noise indicator at low frequency bands is presented. The method is based on the fitting of the dependence of the empirical natural sound level on the wind speed and consequent extraction of the wind-driven sound from the recorded data. The method is demonstrated on the annual ambient sound monitoring data at four monitoring stations in the Baltic Sea but it can be applied to the assessment period of any duration provided that the wind speed data is available. The accuracy of the method is essentially influenced by the accuracy of the wind speed data and the sensitivity of the recorders. There will always be uncertainty in distinguishing low anthropogenic sound levels from the natural background, but such low levels are less likely to produce adverse effects in marine organisms. On the other hand, the quality of fitting will depend on the

J. Acoust. Soc. Am. **147** (2), February 2020

Mustonen *et al.*   EL181

choice of the appropriate length of the time window. The proposed method for the characterisation of the ambient sound can be used to assess the proportion of anthropogenic sound in the recorded data by the determination of excess levels over the natural sound level. Excess levels can be used as a basis of the assessment of the anthropogenic pressure on marine wildlife.

Acknowledgments

References and links

Betke, K., Folegot, T., Matuschek, R., Pajala, J., Persson, L., Tegowski, J., and Wahlberg, M. (**2015**). "BIAS Standards for Signal Processing. Aims, Processes and Recommendations. Amended version," https://biasproject.files.wordpress.com/2016/01/bias_sigproc_standards_v5_final.pdf (Last viewed 02/13/2020).

Carey, W. M., and Evans, R. B. (**2011**). *Ocean Ambient Noise: Measurement and Theory* (Springer Science & Business Media, New York).

Decision, E. C. (**2017**). "Decision 2017/848/EC of the European Commission of 17 May 2017 laying down criteria and methodological standards on good environmental status of marine waters and specifications and standardised methods for monitoring and assessment, and repealing Decision 2010/477/EU," Off. J. Eur. Union L **125**, 43–74.

Dekeling, R., Tasker, M., Van der Graaf, A. J., Ainslie, M. A., Andersson, M. H., André, M., Borsani, J. F., Brensing, K., Castellote, M., and Cronin, D. (**2014**). "Monitoring guidance for underwater noise in European seas-part II: Monitoring guidance specifications," JRC Scientific and Policy Report UR No. 26555.

Häggmark, L., Ivarsson, K.-I., Gollvik, S., and Olofsson, P.-O. (**2000**). "Mesan, an operational mesoscale analysis system," Tellus A: Dyn. Meteorol. Oceanogr. **52**(1), 2–20.

Hildebrand, J. A. (**2009**). "Anthropogenic and natural sources of ambient noise in the ocean," Marine Ecol. Prog. Ser. **395**, 5–20.

Klusek, Z., and Lisimenka, A. (**2016**). "Seasonal and diel variability of the underwater noise in the Baltic Sea," J. Acoust. Soc. Am. **139**(4), 1537–1547.

Knudsen, V. O., Alford, R. S., and Emling, J. W. (**1948**). "Underwater ambient noise," J. Mar. Res. **7**, 410–429.

Kuperman, W. A., and Ingenito, F. (**1980**). "Spatial correlation of surface generated noise in a stratified ocean," J. Acoust. Soc. Am. **67**(6), 1988–1996.

McDonald, M. A., Hildebrand, J. A., and Wiggins, S. M. (**2006**). "Increases in deep ocean ambient noise in the Northeast Pacific west of San Nicolas Island, California," J. Acoust. Soc. Am. **120**(2), 711–718.

Menze, S., Zitterbart, D. P., van Opzeeland, I., and Boebel, O. (**2017**). "The influence of sea ice, wind speed and marine mammals on Southern Ocean ambient sound," R. Soc. Open Sci. **4**(1), 160370.

Mustonen, M., Klauson, A., Andersson, M., Clorennec, D., Folegot, T., Koza, R., Pajala, J., Persson, L., Tegowski, J., and Tougaard, J. (**2019**). "Spatial and Temporal Variability of Ambient Underwater Sound in the Baltic Sea," Sci. Rep. **9**(1), 1–13.

Mustonen, M., Klauson, A., Berdnikova, J., and Tommingas, M. (**2017**). "Assessment of the proportion of anthropogenic underwater noise levels in passive acoustic monitoring," in *Proceedings of Meetings on Acoustics 174ASA*, ASA, Vol. 31, p. 070003.

Nichols, T. A., Anderson, T. W., and Širović, A. (**2015**). "Intermittent noise induces physiological stress in a coastal marine fish," PloS One **10**(9), e0139157.

Nystuen, J. A., Moore, S. E., and Stabeno, P. J. (**2010**). "A sound budget for the southeastern Bering Sea: Measuring wind, rainfall, shipping, and other sources of underwater sound," J. Acoust. Soc. Am. **128**(1), 58–65.

Piggott, C. L. (**1964**). "Ambient sea noise at low frequencies in shallow water of the Scotian Shelf," J. Acoust. Soc. Am. **36**(11), 2152–2163.

Pine, M. K., Hannay, D. E., Insley, S. J., Halliday, W. D., and Juanes, F. (**2018**). "Assessing vessel slowdown for reducing auditory masking for marine mammals and fish of the western Canadian Arctic," Mar. Pollut. Bull. **135**, 290–302.

Poikonen, A. (**2012**). "Measurements, analysis and modeling of wind-driven ambient noise in shallow brackish water," Doctoral Dissertation, Aalto University.

Pounder, C. (**1986**). "Sodium chloride and water temperature effects on bubbles," in *Oceanic Whitecaps* (Springer, Berlin), pp. 278–278.

Prosperetti, A. (**1985**). "Bubble-related ambient noise in the ocean," J. Acoust. Soc. Am. **78**(S1), S2–S2.

Putland, R. L., Merchant, N. D., Farcas, A., and Radford, C. A. (**2018**). "Vessel noise cuts down communication space for vocalizing fish and marine mammals," Global Change Biol. **24**(4), 1708–1721.

Scrimger, J. A., Evans, D. J., McBean, G. A., Farmer, D. M., and Kerman, B. R. (**1987**). "Underwater noise due to rain, hail, and snow," J. Acoust. Soc. Am. **81**(1), 79–86.

Simpson, S. D., Radford, A. N., Holles, S., Ferarri, M. C., Chivers, D. P., McCormick, M. I., and Meekan, M. G. (**2016**). "Small-boat noise impacts natural settlement behavior of coral reef fish larvae," in *The Effects of Noise on Aquatic Life II* (Springer, Berlin), pp. 1041–1048.

Urick, R., and Kuperman, W. A. (**1989**). *Ambient Noise in the Sea* (Acoustical Society of America, New York).

Urick, R. J. (**1967**). *Principles of Underwater Sound for Engineers* (Tata McGraw-Hill Education, New York).

Vagle, S., Large, W. G., and Farmer, D. M. (**1990**). "An evaluation of the WOTAN technique of inferring oceanic winds from underwater ambient sound," J. Atmosph. Ocean. Technol. **7**(4), 576–595.

VerfuSS, U. K., Andersson, M., Folegot, T., Laanearu, J., Matuschek, R., Pajala, J., Sigray, P., Tegowski, J., and Tougaard, J. (**2014**). "BIAS Standards for noise measurements," Background information, Guidelines and Quality Assurance.

Wenz, G. M. (**1962**). "Acoustic ambient noise in the ocean: Spectra and sources," J. Acoust. Soc. Am. **34**(12), 1936–1956.

WildlifeAcoustics (**2013**). *User Manual Supplement SM2 M+*, https://www.wildlifeacoustics.com/images/documentation/SM2M-User-Manual.pdf (Last viewed 02/13/2020).

Wright, A. J., Soto, N. A., Baldwin, A. L., Bateson, M., Beale, C. M., Clark, C., Deak, T., Edwards, E. F., Fernández, A., and Godinho, A. (**2007**). "Do marine mammals experience stress related to anthropogenic noise?," Int. J. Compar. Psychol. **20**(2), 274–316.

J. Acoust. Soc. Am. **147** (2), February 2020

Mustonen *et al.*   EL183

Appendix B

MEASUREMENT EQUIPMENT AND DATA PROCESSING

Measurement equipment and data processing

Measurement equipment, its setup and rig design

In the BIAS-project, two different digital autonomous acoustic recorders were used: the DSG Ocean by Loggerhead Instruments [33] and the SM2M by Wildlife Acoustics [34]. The recorders used for the measurement of the data presented in the thesis were the SM2M-s. As with any measurement of a physical quantity it is essential to list the limitations and characteristics of the measurement equipment. The hydrophone of the SM2M is the Standard Acoustic hydrophone option offered which is the HTI-96-Min hydrophone with a preamplifier.

- The free field open circuit sensitivity level of the hydrophones was around -164 dB re 1 V/μPa ($\pm$ 0.2 dB depending on the exact hydrophone). This sensitivity level enables the conversion of the voltage produced by the hydrophone back to sound pressure.

- The directional response of the hydrophone is listed as being omnidirectional with $\pm$ 1 dB up to frequencies of 30 kHz. This means that the response of the hydrophone should be almost independent of the direction of the sound source when the frequency is below 30 kHz.

- In digital autonomous acoustic recorders, as is the SM2M, the voltage values are not saved directly but are digitized and saved as digital audio files. If only the free field open circuit sensitivity level of the hydrophones is given, it is not enough to convert the digital audio data back to sound pressure values. For this the conversion factor between ADC input voltage and corresponding integer valued ADC output known as the ADC sensitivity to voltage has to be specified. The ADC sensitivity to voltage level for the SM2M recorder was -5 dB re 1V/μPa that corresponds to 1.6 V full-scale signal ADC input to the full-scale ADC output.

- The time stability of the rated sensitivity was checked in all the acoustic recorders of the BIAS project. Point calibration at frequencies 100 Hz and 200 Hz with a pistophone was performed before the first deployment and after the last retrieval. Since the end of the BIAS project 250 Hz point calibrations have been continued and within the range of $\pm$ 1 dB, no significant change in sensitivities have been observed.

- According to the manufacturer the stated operating frequency band of the SM2M is 2 Hz to 30 kHz ($\pm$ 2 dB of rated sensitivity). Meaning that the previously noted free field open circuit sensitivity level of the hydrophone should be in the range of 2 dB from the rated sensitivity level within the operating frequency band.

- When measuring lower sound levels, it is crucial to know the levels the system reports in the absence of any actual sound (excluding the ones produced by the equipment itself). This characteristic is referred to as the system's self-noise or sometimes as the "noise floor" [36]. The self-noise is defined as a combination of acoustic self-noise and non-acoustic self-noise [31]. The non-acoustic self-noise is mostly electrical in nature and is generated by the hydrophone itself along with any electronic components in the measuring system such as amplifiers and ADCs. The acoustic self-noise is the noise that would not exist in the measurement location in the absence of the measurement system. Acoustic self-noise can be caused by the vibrations and movements of the measurement rig itself or turbulence induced local pressure fluctuation caused by water flowing around the hydrophone. Table

5 lists the evaluated self-noise one-third octave band sound pressure levels along with the corresponding middle frequency sound pressure spectral density levels of the SM2M recorder.

Table 5: Evaluated self-noise one-third octave band sound pressure levels and mean-square sound pressure spectral density levels of the SM2M recorder. Table taken from [Publication IV].

One-third Octave central freq.	63 Hz	125 Hz	2 kHz
Self-noise level [dB re 1 μPa]	63	65	70
Spectral density [dB re 1 μ^2Pa/Hz]	51	50	43

- Besides the lower bound there also exists upper band values corresponding to the highest levels the equipment can measure. In case of really high amplitude sound pressures *i.e.* loud noises the existence of the upper bound can cause clipping. The appearance of clipping was checked in the data processing and appropriate samples when clipping occurred were flagged.

- Upon digitization of the voltage there are important parameters that define the temporal and amplitude resolution of the audio data. The temporal resolution is given by the sampling frequency of the ADC. The ADC of the SM2M recorder allows measurements with sampling frequencies ranging from 4 kHz to 96 kHz. The sampling frequency chosen in the BIAS project and used afterwards in all Estonian SM2M measurements has been 32 kHz. The amplitude resolution is set by the bit depth which in the SM2M is 16-bits. Altogether the audio data is saved as a set of integer values between 0 - 2^{16} every 1/32 000 seconds.

The SM2M can be programmed to record and switch off according to a predetermined schedule. In the BIAS project duty-cycling was set to record from 20 to 59 minutes per hour. Data exclusion tests with the 59 minute duty cycle recordings did not indicate any significant effect of smaller duty cycles on the long term monitoring statistics. Also the longer rest times save the battery and use less memory allowing for longer deployment periods. The downside of having a longer deployment period is the possibility of larger loss of data in case of system failures. All the presented measurements were performed following the measurement standards developed for the BIAS-project [144]. Fixing the autonomous recorder in place underwater usually requires rigging. The design of the rigging can affect the acousti self-noise level of the system and therefore must be carefully considered. The most extensively used BIAS standard rig design is shown in Figure 23-a. The SM2M recorder has a buoyancy of 1.5-5.5 kg depending on the amount of batteries. The recorder is attached to a weight that was a 20 kg wet weight concrete block in the standard rig. For the retrieval the rigging contains an acoustic release and a float for additional buoyancy.

The rig design shown in Fig. 23-b was used in the BIAS project Polish locations and it was designed to be resistant to trawling. As seen from Fig. 23 the SM2M comes with the hydrophone attached to the body of the recorder. This configuration is known to have different sensitivity at the frequency of the recorder's body resonance [145]. Also, if the hydrophones are calibrated separately from the recorder, the reported sensitivities might not correspond to the sensitivity of the system when hydrophone is attached rigidly to the recorder.
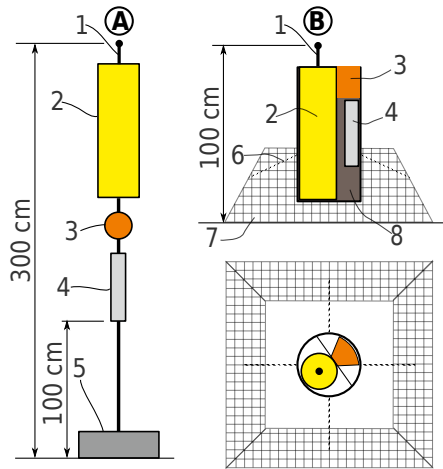
Figure 23: Sketch of the two BIAS standard riggings. The rig design marked with letter A is the main BIAS rig design used with the SM2M recorded. The rigging marked with B ware used in Polish locations due to trawling; 1-hydrophone, 2-SM2M recorder, 3-extra buoyancy, 4-acoustic releaser, 5-ballast (min 20 kg wet weight), 6-rope, 7-steel grid cage, 8-rope container. Figure adapted from [Publication IV].

Data processing

Besides the definition of the one-third octave band the term "average sound level" in the indicator D11 criterion needs to be interpreted and defined. **In the BIAS-project, the average of the sound level in the one-third octave band was determined as the geometric mean of 20 consecutive one-second averaged one-third octave band sound pressure levels, *i.e.* computationally approximately equivalent to RMS-average over the 20 seconds**.

As said in the previous subsection the digital autonomous acoustic recorder SM2M saves the sound data as digital audio in .wav-file format. As an initial step, the discrete 16-bit values are converted to full-scale ADC output values by division. The root-mean-square of discrete values is calculated with the following formula:

$$\widehat{x} = \sqrt{\frac{1}{N} \sum_{n=1}^{N} x^2[n]}. \tag{7}$$

This can be rewritten by applying Parseval's theorem. For a sampled value $x[n] = x[t_n \in 0 \ldots NT]$, where T is the sampling period (equal to the reciprocal of the sampling frequency):

$$\sum_{n=1}^{N} x^2[n] = \frac{1}{N} \sum_{m=1}^{N} |X[m]|^2, \tag{8}$$

where $X[m]$ is the Discrete Fourier Transform (DFT) of $x[n]$, N is the number of samples and DFT coefficients. In practice, the root-mean-square of the discrete samples can be obtained from the sum of the frequency amplitude spectrum. Therefore, the root-mean-square of a discrete valued variable can be expressed in formula form as:

$$\widehat{x} = \sqrt{\frac{1}{N^2} \sum_{m=1}^{N} |X[m]|^2}. \tag{9}$$

No window functions were applied to the data prior to the estimation of the DFT since it did not improve the statistical estimates. If the full scale sensitivity level $|M_{FS}|$ of the measurement system is known (the gain was $G = 1$ and the discrete voltage values $v[n]$ were also known from scaling) the SPL was calculated from full-scale ADC outputs as

$$L_p = |M_{FS}| + 10 \log_{10} \widehat{n_{FS}^2} = |M_{FS}| + 10 \log_{10} \left(\sqrt{\frac{1}{N^2} \sum_{m=1}^{N} |N_{FS}[m]|^2} \right). \tag{10}$$

where n_{FS} is the full-scale ADC output of Nsamples and $N_{SF}[m]$ the DFT of $n[k]$. Additionally the SPL has to be calculated within the aforementioned frequency bands. This makes the choice of using Parseval's theorem more understandable as the calculation of SPL within any frequency band is simplified using this formula. Calculating SPL values for any given frequency band the last expression becomes

$$L_p = |M_{FS}| + 10 \log_{10} \left(\sqrt{\frac{1}{N^2} \sum_{m=k_1}^{k_2} |N_{FS}[m]|^2} \right). \tag{11}$$

where k_1 and k_2 are the indices corresponding to the lower and upper frequencies of the chosen frequency band.

Curriculum Vitae

1. Personal data

Name	Mirko Mustonen
Date and place of birth	2 June 1987 Paide, Estonia
Nationality	Estonian

2. Contact information

Address	Tallinn University of Technology, School of Engineering, Department of Civil Engineering and Architecture, Ehitajate tee 5, 19086 Tallinn, Estonia
Phone	+372 620 2557
E-mail	mirko.mustonen@taltech.ee

3. Education

2014–...	Tallinn University of Technology, School of Engineering, Course Civil and Environmental Engineering, PhD studies
2012–2014	Tallinn University of Technology, Faculty of Science, Engineering physics (applied mechanics), MSc
2006–2012	Tallinn University of Technology, Faculty of Science, Engineering physics, BSc

4. Language competence

Estonian	native
English	fluent
Russian	basic level
Spanish	basic level

5. Professional employment

2016–...	School of Engineering at TalTech, Engineer
2014–2016	Faculty of Civil Engineering at TUT, Department of Mechanics, Engineer
2013–2014	Institute of Cybernetics at TUT, Technician

6. Computer skills

- Operating systems: Linux, Windows

- Document preparation: LaTeX, Inkscape, Zotero

- Programming languages: MATLAB, Python, R

7. Defended theses

- 2014, Magnetic pickup nonlinearity, MSc, supervisor Anatoli Stulov, PhD, Tallinn University of Technology, Institute of Cybernetics, co-supervisor Dmitri Kartofelev, MSc, Tallinn University of Technology, Institute of Cybernetics, co-supervisor Prof. Vesa Välimäki, Aalto University, School of Electrical Engineering, Department of Signal Processing and Acoustics

- 2012, Bass guitar modelling based on experimental data, BSc, supervisor Anatoli Stulov, PhD, Tallinn University of Technology, Institute of Cybernetics, co-supervisor Dmitri Kartofelev, MSc, Tallinn University of Technology, Institute of Cybernetics

8. Field of research

- ETIS CLASSIFICATION: 4. Natural Sciences and Engineering; 4.10. Physics and Technical Physics; CERCS CLASSIFICATION: P190 Mathematical and general theoretical physics, classical mechanics, quantum mechanics, relativity, gravitation, statistical physics, thermodynamics

9. Scientific work
Papers

1. M. Mustonen, D. Kartofelev, A. Stulov, and V. Välimäki, Application of high-speed line scan camera for acoustic measurements of vibrating objects. *In Proceeding of Forum Acusticum, Kraków, Poland* (pp. 7-12), 2014, September

2. M. Mustonen, D. Kartofelev, A. Stulov, and V. Välimäki, Experimental verification of pickup nonlinearity. *In Proceedings International Symposium on Musical Acoustics (ISMA 2014), Le Mans, France* (Vol. 1, No. 6), 2014, July.

3. M. Pàmies-Vilà, I.A. Kubilay, D. Kartofelev, M. Mustonen, A. Stulov, and V. Välimäki, High-speed linecamera measurements of a vibrating string. *In Proceeding of Baltic-Nordic Acoustic Meeting (BNAM), Tallinn, Estonia* (Vol. 1, No. 8), 2014, June.

4. D. Kartofelev, M. Mustonen, A. Stulov, and V. Välimäki, Application of high-speed line scan camera for string vibration measurements. *In Proceedings of International Symposium on Musical Acoustics (ISMA 2014), Le Mans, France* (Vol. 1, No. 6) 2014, July

Conference presentations

1. M. Mustonen, D. Kartofelev, A. Stulov, and Välimäki, V.,*Experimental verification of pickup nonlinearity*, International Symposium on Musical Acoustics (ISMA): 7–12 July 2014, Le Mans, France

2. M. Mustonen, A. Klauson, J. Laanearu, M. Ratassepp, T. Folegot, and D. Clorennec *Passenger ship source level determination in shallow water environment*, Fourth International Conference on the Effects of Noise on Aquatic Life, 10–16 July 2016, Dublin, Ireland

Elulookirjeldus

1. Isikuandmed

Nimi	Mirko Mustonen
Sünniaeg ja -koht	02.06.1987, Paide, Eesti
Kodakondsus	Eesti

2. Kontaktandmed

Aadress	Tallinna Tehnikaülikool, Ehituse ja arhitektuuri instituut, Ehitajate tee 5, 19086 Tallinn, Estonia
Telefon	+372 620 2557
E-post	mirko.mustonen@taltech.ee

3. Haridus

2014–...	Tallinna Tehnikaülikool, Inseneriteaduskond, Ehitus- ja keskkonnatehnika doktoriõpe
2012–2014	Tallinna Tehnikaülikool, Loodusteaduskond, Tehniline füüsika (rakendusmehaanika), MSc *cum laude*
2006–2012	Tallinna Tehnikaülikool, Loodusteaduskond, Tehniline füüsika, BSc

4. Keelteoskus

eesti keel	emakeel
inglise keel	kõrgtase
vene keel	algtase
hispaania keel	algtase

5. Teenistuskäik

2016– ...	TTÜ Inseneriteaduskond, Ehituse ja arhitektuuri instituut, insener
2014–2016	TTÜ Ehitusteaduskond, Mehaanikainstituut, insener
2013–2014	TTÜ Küberneetika instituut, tehnik

6. Arvutioskused

- Operatsioonisüsteemid: Linux, Windows

- Kontoritarkvara: LaTeX, Inkscape, Zotero

- Programmeerimiskeeled: MATLAB, Python, R

7. Kaitstud lõputööd

- 2014, Elektrikitarri helipea mittelineaarsus, MSc, juhendaja Anatoli Stulov Tallinna Tehnikaülikool, Küberneetika instituut, kaasjuhendaja Dmitri Kartofelev, Tallinna Tehnikaülikool, Küberneetika instituut, kaasjuhendaja Prof. Vesa Välimäki, Aalto Ülikool, Elektrotehnika teaduskond, Signaalitöötluse ja akustika instituut

  supervisor Anatoli Stulov, DSc, Tallinna Tehnikaülikool, Küberneetika instituut, kaasjuhendaja Dmitri Kartofelev, MSc, Tallinna Tehnikaülikool, Küberneetika instituut

- 2012, Basskitarri kõla modelleerimine katseandmete põhjal, BSc, juhendaja Anatoli Stulov, Tallinna Tehnikaülikool, Küberneetika instituut, kaasjuhendaja Dmitri Kartofelev, Tallinna Tehnikaülikool, Küberneetika instituut

8. Teadustöö põhisuunad

- ETIS KLASSIFIKAATOR: 4.   Loodusteadused ja tehnika; 4.10.   Füüsika; CERCS KLASSIFIKAATOR: P190 Matemaatiline ja üldine teoreetiline füüsika, klassikaline mehaanika, kvantmehaanika, relatiivsus, gravitatsioon, statistiline füüsika, termodünaamika; TÄPSUSTUS: Rakendusmehaanika

9. Teadustegevus
Teadusartiklite, konverentsiteeside ja konverentsiettekannete loetelu on toodud ingliskeelse elulookirjelduse juures.